Systematic assessment of erosion mitigation in a data poor environment

A case study of Lac Cai, Bonaire

Marijn Groot

August, 2022

UNESCO IHE DELFT

UNIVERSITY OF TWENTE.

Systematic assessment of erosion mitigation in a data poor environment

A case study of Lac Cai, Bonaire

MSc. Thesis

by

Marijn Groot

12th of August 2022

Cover photo by: © We Share Bonaire

Graduation Committee
Dr. Ir. Ali Dastgheib[1]
Prof. Dr. Roshanka Ranasinghe[1,2]
Dr. Ir. Trang Minh Duong[1,2]

In order to obtain the Master of Science degree in Civil Engineering and Management

Department of Civil Engineering and Management (CEM)
Faculty of Engineering Technology
University of Twente

[1] Department of Coastal & Urban Risk & Resilience, IHE Delft Institute for Water Education, P.O. Box 3015, Delft, 2601 DA, Netherlands
[2] Water Engineering and Management, University of Twente, Enschede, 7522 NB, Netherlands

Acknowledgements

This thesis is written in order to complete my Master of Science in River and Coastal Engineering at the University of Twente. This research was carried out in combination with IHE Delft Institute for Water Education which I would like to thank a lot for their facilities and interesting courses in Delft3D modelling.

Writing this thesis during the pandemic has been a very difficult challenge for me and I would like to express my gratitude to all the people who have supported me along the way.

First of all, I would like to thank Rosh Ranasinghe and Trang Duong for their patience and critical reflections. Furthermore I especially would like to thank Ali Dastgheib for all his support. Your positive feedback and analytical insights have helped me to overcome many challenges and I'm very grateful for all the time and effort you put into this project.

Next I would like to thank my mother for her honest criticism and helping me find the motivation. My family and friends for their caring and welcome distractions. And above all my girlfriend for her patience and understanding.

Lastly, I would like to dedicate my graduation to my loving father. He has been a great supporter and inspiration during my studying career. Your enthusiasm and guidance have been missed sincerely.

Abstract

Lac Cai is one of the lagoons in the Dutch Caribbean with a high environmental value which attracts a lot of tourism to the area. Lac Cai is included in the Bonaire National Marine Park (STINAPA) and in order to preserve the ecological variety inside the lagoon, the allowed recreational purposed are delineated in a zonation plan. Cai Beach is one of only two beaches around the lagoon destined for general beach recreational purposes and therefor an attractive location for visitors. Cai is however only accessible over a small road which is endangered by coastal erosion. In an attempt to mitigate the erosion in front of the entrance road, a rock formation parallel to the coast was built in 2019 to serve as breakwater. Unfortunately, this construction did not have the desired effect and erosion continues. The objective of this research is to detect the driving processes causing this erosion and to find a fitting solution by modelling alternative measures in Delft3D and systematically assess these alternatives with the use of a Multi Criteria Analysis.

The availability of actual and accurate data was limited and consisted mainly of outdated or inaccurate data. The coastal evolution was analysed with the use Google Earth images between the years 2002 and 2019 which showed a coastal retreat of approximately 30 meters. With the use of DelftDashboard, a SWAN model was setup with global bathymetry data from the Gebco8 dataset and interpolated with the measured bathymetry data from inside the bay. The wave input is retrieved from the global offshore waveseries of ERA5 which is schematized into a wave climate with the Energy Flux Method. The results of the SWAN model showed that incoming waves enter the shoreline in an oblique angle from the North-East which creates wave-induced longshore sediment transport. Furthermore it was encountered that the adjacent profiles located north of the study area were composed of unerodable reefal limestone terraces which restricts the amount of sediment supply along the coast. Also, the analysis of old aerial photos showed a degradation of the mangrove fringe in front of the entrance road to Cai beach which is considered to have a correlation with the coastal retreat.

Delft3D is used for the setup of a FLOW-model in order to investigate the correlation between mangrove loss and erosion and analyse the long-term morphodynamics. The development of the model is done by a sensitivity analysis and initial simulations are carried out to develop a more realistic bathymetry, starting with an equilibrium coastline profile based on the Dean's method.

The correlation between mangrove deforestation and erosion is analysed by simulating the current mangrove fringe, the historic mangrove fringe and a situation without mangroves. These scenarios are simulated with the use of three different vegetation modelling methods: Vegetation-induced bed roughness, Trachytopes and Digital Point Model (DPM). The impact of the different methods could not clearly be distinguished but the model results did show less coastal erosion in situation with present mangrove fringes. The first method showed the most impact while also, the vegetation-induced bed roughness did not overestimate the impact of the vegetation. Therefore it seemed to be the most appropriate method for the purposes of the subsequent alternative measurement study.

Five different alternatives are investigated by model in order to come up with an alternative measures against the coastal retreat at Lac Cai. The alternative consisted of a reference model without any measure, breakwater, groyne, seagrass implementation and mangroves restoration. Based on the sediment balance and erosive trend over 10 years, the groyne was showing the best results. The implementation of a widespread seagrass meadow with a strongly reduced friction coefficient caused for an overestimation of the vegetation impact. This makes it hard to compare the absolute erosion values but based on the trend this can still be considered as an effective mitigation measure. The mangrove reforestation and expansion towards the sea showed a positive sediment balance with an increasing trend in sedimentation close to the land boundary. The breakwater- and reference model both showed decay in the sediment balance.

The alternatives were assessed by six expert with diverse expertise related to coastal engineering. The multi criteria analysis consisted of five criteria which were weighted and scored by the experts: Impact on hazard reduction, Cost, Environmental impact, Local acceptability and Local feasibility. The experts unanimously weighted the reduction impact criterion as most important after which the cost and local feasibility. Despite the fact that the modelling results showed that the groyne construction was the most effective in hazard reduction, it can be concluded from the feedback that mangrove reforestation is the best mitigation alternative. This alternative received the highest points in each criterion scored by the experts. The mangrove restoration is considered feasible and expected to be received optimistically by the local stakeholders while the lifecycle cost are not expected larger than other alternatives. These scores should be verified as well as the impact on hazard reduction should be further investigated by improving the morphological model with more accurate data.

Table of content

Acknowledgements 3
Abstract 4
List of Figures 8
List of Tables 10
1. Introduction 11
1.1. Background 11
1.2. Problem statement 12
1.3. Research objective 13
1.4. Methodology 13
2. Theoretical background 15
2.1. Beach processes 15
2.1.1. Littoral cell 15
2.1.2. Swash zone 16
2.1.3. Sediment transport 16
2.1.4. Wave refraction 17
2.1.5. Shoaling 17
2.2. Coastal modelling 18
2.2.1. Delft3D 18
2.2.2. Vegetation modelling 19
3. Data Analysis 21
3.1. Study area 21
3.1.1. Geology 22
3.1.2. Vegetation 23
3.1.3. Coastline profiles 24
3.1.4. Hydrology 25
3.2. Wave- and Bathymetry data 25
3.2.1. Bathymetry 26
3.2.2. Wave climate 28
4. Modelling 31
4.1. Model strategy 31
4.2. Model set up 31
4.2.1. FLOW-GUI 31
4.2.2. Grid 32
4.2.3. Bathymetry 32
4.2.4. Waves 33

4.3. Sensitivity analysis 34
4.4. Dean profile 35
4.5. Vegetation modelling 36
5. Mitigation measures 39
5.1. Alternative 1: No measure 40
5.2. Alternative 2: Breakwater 42
5.3. Alternative 3: Groyne 45
5.4. Alternative 4: Mangrove restoration 47
5.5. Alternative 5: Seagrass 50
5.6. Conclusion 52
6. Multi criteria analysis 53
6.1. Criteria 54
6.2. The MCA scoring & weighting grid 55
6.3. Results 56
6.3.1. Expert assessment 56
6.3.2. Alternative scoring 57
6.3.3. Conclusion 60
7. Discussion 61
7.1. Data analysis 61
7.2. Modelling 62
7.3. Mitigation alternatives and MCA 63
8. Conclusion & Recommendations 64
8.1. Conclusions 64
8.2. Recommendation 66
References 67
Appendix A, Delft3D numerical scheme 70
Appendix B, Monthly wave roses 72
Appendix C, Grid properties 75
Appendix D, Alternative description and questionnaire for MCA survey 76
Appendix E, Assessment form 81
Appendix F, Assessed tables 82

List of Figures

Figure 1, Location focus area (figure left), Lac Cai beach (figure right, 2) and the connecting part between the peninsula and the main land (figure right, 1) 12
Figure 2, Historical satellite images of the years 2002, 2012, 2014, 2016, 2018 and 2019 12
Figure 3, Flowchart of research methodology 14
Figure 4, Typical trailing edge coasts and their trailing-littoral cells. Solid arrows show sediment transport paths; broken arrows indicate occasional onshore and offshore transport modes (after Inman, 1994). 15
Figure 5, "Schematic cross-section of the beach and the limits of the swash zone (Elfrink & Baldock, 2002)" 16
Figure 6, Wave refraction 17
Figure 7, Schematized profile of horizontal flow velocity (U_{in}) with depth averaged vegetation (h_{veg}) 19
Figure 8, Location of Lac Cai on Bonaire Island (red square, left), and aerial overview of focus area (right) 21
Figure 9, Zoning plan of Lac Bay (Kalke & Kats, 2011) 21
Figure 10, Geological map Bonaire 22
Figure 11, Mapped mangrove loss between the years 1961 and 1996 in Lac Cai (Erdmann and Scheffers, 2006) 23
Figure 12, Shoreline positions over the years between 2002 and 2019 (GoogleEarth) 24
Figure 13, Water inflow into Lac Cai (Hummelinck & Roos, 1968) 25
Figure 14, Grid on top of the model domain in Delftdashboard with Gebco 08 bathymetry 25
Figure 15, Measured bathymetry points inside Lac Cai 26
Figure 16, Depths map of Lac Bay 1949 (Lott, 2001) 27
Figure 17, Available ERA5wave data sets from ECMWF 28
Figure 18, Wave rose for ERA5 dataset (1979-2017) and monthly averaged wave characteristics 28
Figure 19, Energy flux method for 5 bins over the scatterplot of the ERA5 dataset 29
Figure 20, Significant wave height simulated in SWAN model for 5 wave conditions at 19 stations along the 10m depth contour line 30
Figure 21, Combined bathymetry and unerodable layers 33
Figure 22, Cross sections of sensitivity analysis scenarios with Multiplication (calibration) factors 34
Figure 23, Bedlevel in waterlevel points for initial dean profile at t=1 and after one cycle of wave series at t=130 35
Figure 24, Manually generating a bathymetry by implementing the Dean profile and iteratively approach the morphologic active profile 35
Figure 25, Current- and historic mangrove fringes and cross-sections 36
Figure 26, Cross sections in X- and Y-direction showing the total coastal retreat, simulated with the rigid rod method over 10 years 37
Figure 27, Total cumulative erosion and sedimention volumes for 5 different mangrove models 38
Figure 28, Bed level in water level points for the vegetation-induced historic mangroves after 10 morphological years 39
Figure 29, Map file of the cum. erosion/sedimentation at t=122 for the reference model without any measure 40
Figure 30, Cum. erosion/sedimentation of entire area for the reference model without any measure 41
Figure 31, Cum. erosion/sedimentation of section 2 for the reference model without any measure 41
Figure 32, Aerial overview (Google Earth) (left) and photo on sight (right) of the current situation at Lac Cai were a pile of rocks is deposited perpendicular to the coast in the form of a breakwater 42
Figure 33, Map file of the cum. erosion/sedimentation at t=103 for the modelled breakwater alternative 43
Figure 34, Cum. erosion/sedimentation of entire area for the modelled groyne alternative 44
Figure 35, Cum. erosion/sedimentation of section2 for the modelled breakwater alternative 44
Figure 36, Example of the Royal Hawaiian in Wakatiti, Hawai (Waikīkī Beach Special Improvement District Association, 2020) 45
Figure 37, Schematic overview of a groin at the south side of the beach at Lac Cai (Google Earth) 45
Figure 38, Map file of the cum. erosion/sedimentation at t=122 of the modelled groyne alternative 45
Figure 39, Cum. erosion/sedimentation of entire area for the modelled groyne alternative 46
Figure 40, Cum. erosion/sedimentation of section2 for the modelled groyne alternative 46
Figure 41, Historical areal picture of Lac Cai showing the original state (1961) of the mangrove fringe 47

Figure 42, Map file of the cum. erosion/sedimentation at t=120 of the modelled mangrove restauration to its original state 48
Figure 43, Map file of the cum. erosion/sedimentation at t=120 of the modelled extended mangrove restauration 48
Figure 44, Cum. erosion/sedimentation of section2 for the extended mangrove fringe model 49
Figure 45, Cum. erosion/sedimentation of the entire area for the extended mangrove fringe model 49
Figure 46, Map file of the cum. erosion/sedimentation at t=122 of the modelled seagrass implementation 50
Figure 47, Cum. erosion/sedimentation of section2 for the seagrass model 51
Figure 48, Cum. erosion/sedimentation of section2 for the extended mangrove fringe model 51
Figure 49, Measured data points (L) and triangular interpolated bathymetry (R) with legends showing depths varying between 1 and 26 meters 61
Figure 50, Staggered grid to solve transport equations as used in Delft3D-FLOW (L) and Vertical grid subdivided in σ-layers of equal thickness (R) (Deltares, 2018) 70
Figure 51, Example of suggested open bridge in larger scale 76
Figure 52, Compared to a straight coastline, the hollow area covers width of 200m with coastal retreat of 30m (left) which can be schematized by the parabolic function (right) 77
Figure 53, Historical areal picture of Lac Cai showing the original state of the mangrove fringe 78
Figure 54, Permeable structure to create favourable conditions for mangrove rehabilitation 78
Figure 55, An overview of the current situation at Lac Cai were a pile of rocks is deposited perpendicular to the coast in the form of a breakwater (Google Earth) 79
Figure 56, Current situation at Lac Cai were a pile of rocks is deposited perpendicular to the coast in the form of a breakwater 79
Figure 57, Schematic overview of a groin at the south side of the beach at Lac Cai (Google Earth) 80
Figure 58, Example of the Royal Hawaiian in Wakatiti, Hawai (Waikīkī Beach Special Improvement District Association, 2020) 80

List of Tables

Table 1, Schematized wave climate by EFM 30
Table 2, Wave characteristic at the offshore boundaries 33
Table 3, Sensitivity scenarios 34
Table 4, Vegetation characteristics for Rhizophora mangroves (Horstman, 2015) 37
Table 5, Coastal retreat in m of different vegetation modelling approaches for the cross-sections in current mangrove fringe 38
Table 6, Coastal retreat in m of different vegetation modelling approaches for the cross-sections in historic mangrove fringe 38
Table 7, Trendlines and absolute volumes of cumulative erosion/sedimentation in section 2 (M195:295;N180:190) 52
Table 8, Example of filled assessment form based on fictional scores 55
Table 9, Example of scoring table MCA 55
Table 10, Assessment table with the averaged feedback weights and scores 60

1. Introduction

The research topic is introduced in this chapter, together with the research gap, the scope, the objective.

1.1. Background

The coastal zones, where the land and ocean are linked, are important areas with a high environmental, social and economical value. A large part of these coastal zones are increasingly exposed to coastal hazards as effect of sea level rise and storm events and therefor face the risk of property damage, environmental degradation or loss of life. The impact of climate change will accelerate sea level rise and cause for more frequent and intense extreme events (IPCC, 2022). Current observed impacts and expected future risks of climate change exposes the vulnerability of coastal regions.

One of the common threats to the coastal areas is erosion. Studies show that around 70% of the world's sandy coasts are retreating (Bird, 1985) due to natural causes, like sea level rise and storm impacts, or due to human activities such as the construction of coastal structures or sand mining. The construction of mitigation measures such as sea walls or groyne schemes are commonly applied in disaster risk reduction (DRR). These structures however are effecting the coastal system and cause a shift in the sediment supply in surrounding areas. These shifts can have a negative impact and lead to coastal erosion in down-drift areas or cause for degradation of the biodiversity. The analysis of the long-term shoreline evolution creates a better understanding in the impacts of the mitigation measures and the shift in coastal processes. There are multiple approaches to analyse the shoreline evolution such as physical models, analysing the historical shoreline position or by the use of numerical models.

Furthermore, due to the dense population in coastal areas, the impact of coastal measures generally affects a lot of people. Over 40% of the human population lives in the coastal areas (Shi & Singh, 2003) because of its abundant resources, particularly for the marine trade, fishing industry and cultural activities (Neumann *et al.*, 2015). In order to assess the trade-offs between socio-political, environmental, and economic impacts of (DRR) measures, it is important to involve the divergent stakeholders related to coastal management (Barquet & Cumiskey, 2017).

1.2. Problem statement

The main focus in this study is Lac Cai, which is located at the North-East of the inlet of the lagoon where beach erosion causes narrowing of the recreational area and access route. Figure 1 shows the two locations with coastline changes, where the coastal retreat in area 1 threatens to fade away the only road towards the beach zone. The recreational area 'Cai Beach' is allocated in area 2. The coastal changes in this area are impacted by existing piles of shells, groins and vegetation which protect some parts of the beach and causes for concentrated erosion in other parts. The satellite images between 2002 and 2019 (Figure 2) show that mainly the northern- and southern part of Cai beach are experiencing erosion. The impact of this erosion is visible by the forced removal of a building in the lower left corner of the beach, marked by yellow squares in the years 2002 and 2012.

Figure 1, Location focus area (figure left), Lac Cai beach (figure right, 2) and the connecting part between the peninsula and the main land (figure right, 1)

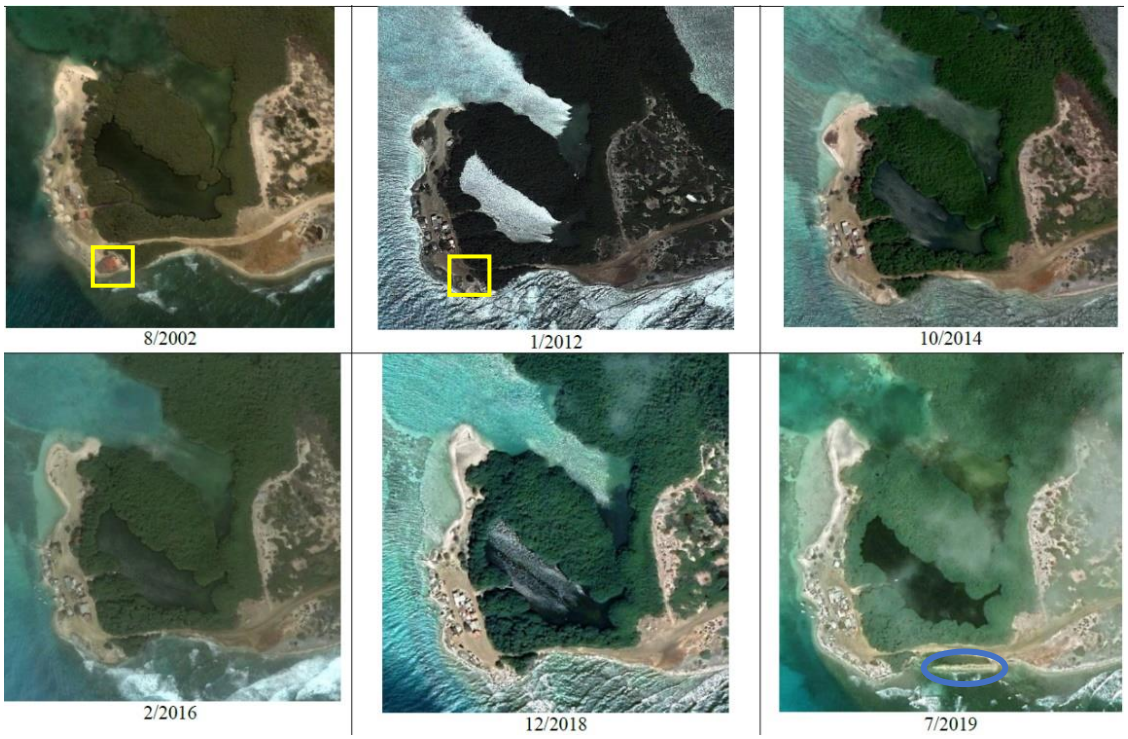

Figure 2, Historical satellite images of the years 2002, 2012, 2014, 2016, 2018 and 2019

Recently a rock structure is deposited in front of the connecting strip of land as can be seen in the satellite image of 2019 (Figure 2, blue circle). The rock structure was deposited to save the strip from further erosion and protect the road from crumbling but this intervention has not produced the desired effect yet.

1.3. Research objective

The main objective of this work is to understand the morphological dynamic of Lac Cai by using data analyses and morphological models, determine the main processes responsible for the erosion and suggest measures to mitigate the erosion if possible. The objective of this thesis is formulated into the following research question:

- What is the main physical process which causes erosion at Lac Cai, Bonaire, and what mitigation measure will help to prevent further erosion in the future?

To achieve the research objective, the structure of this thesis is subdivided into three sub questions:

- What is the main forcing which forms the origin of this coastal erosion?
- How to model the driving hydrodynamic processes causing the coastal erosion at Lac Cai?
- What is the best mitigation measures to serve as a solution for this erosion problem?

1.4. Methodology

This section explains the methodological approaches used in investigation of each of the research questio. The approach and structure of this methodology is schematized in the flowchart in Figure 3.

- What is the main forcing which forms the origin of this coastal erosion?

For the first research question a data analysis is performed on existing data to form an insight in the hydrodynamics forcing the coastal system. Satellite images retrieved from Google earth which are used to manually extract shoreline locations and investigate the coastal retreat. Further data consist of locally measured bathymetry data and waveseries (1979-2017) from the ERA5 dataset. Delftdashboard is used to combine the local bathymetry dataset with the offshore bathymetry retrieved from the Gebco8 dataset. With this combined bathymetry a SWAN model was setup to translate and analyse the nearshore wave conditions. The nearshore waveseries are translated into a wave climate based on the energy flux method. Furthermore, a literature review is used to investigate the ecological, geological and hydrological data in the study area.

- How to model the driving hydrodynamic processes causing the coastal erosion at Lac Cai?

In order to simulate the hydrodynamic and morphological processes at Lac Cai, a morphological model will be constructed within the software of Delft3D. This will consist of a newly generated FLOW model with an online coupling to the WAVE model constructed in DDB. The development of the model will start with a sensitivity analysis to create insights in the impact of various parameters. The second step of modelling is to generate a bathymetry with a gradual transition between the nearshore and offshore data. The bathymetry is iteratively developed with the use of morphological model starting with an equilibrium dean profile as initial condition.

Three different methods for vegetation modelling are used to investigate the correlation between the mangrove loss and coastal erosion and find a fitting solution to schematize the mangroves into the model. The comparison of these models will be made between the erosion rates in the situation with the historic mangrove fringe, the current fringe and in a situation without any mangroves.

- What is the best mitigation measures to serve as a solution for this erosion problem?

In order to counter the erosive trend in front of Lac Cai, five different mitigation measures will be conducted and assessed in a multicriteria analysis. The effectiveness of the five alternatives is analyzed by implementing the mitigation measures into the model and simulate the coastal evolution. The sediment mass balance and erosive trend are compared and the results are taken into account in the MCA. The MCA consists of the following five different criteria:

- Impact on hazard reduction
- Cost
- Environmental impact
- Local acceptance
- Local feasibility

A survey among six expert recipients with diverse range of expertise related to coastal engineering is conducted in order to weigh the criteria and score the alternative measures. The total score of each alternative is the sum of the weight of each criteria times the corresponding score. The scores from the experts and model results will give a favorite mitigation measure.

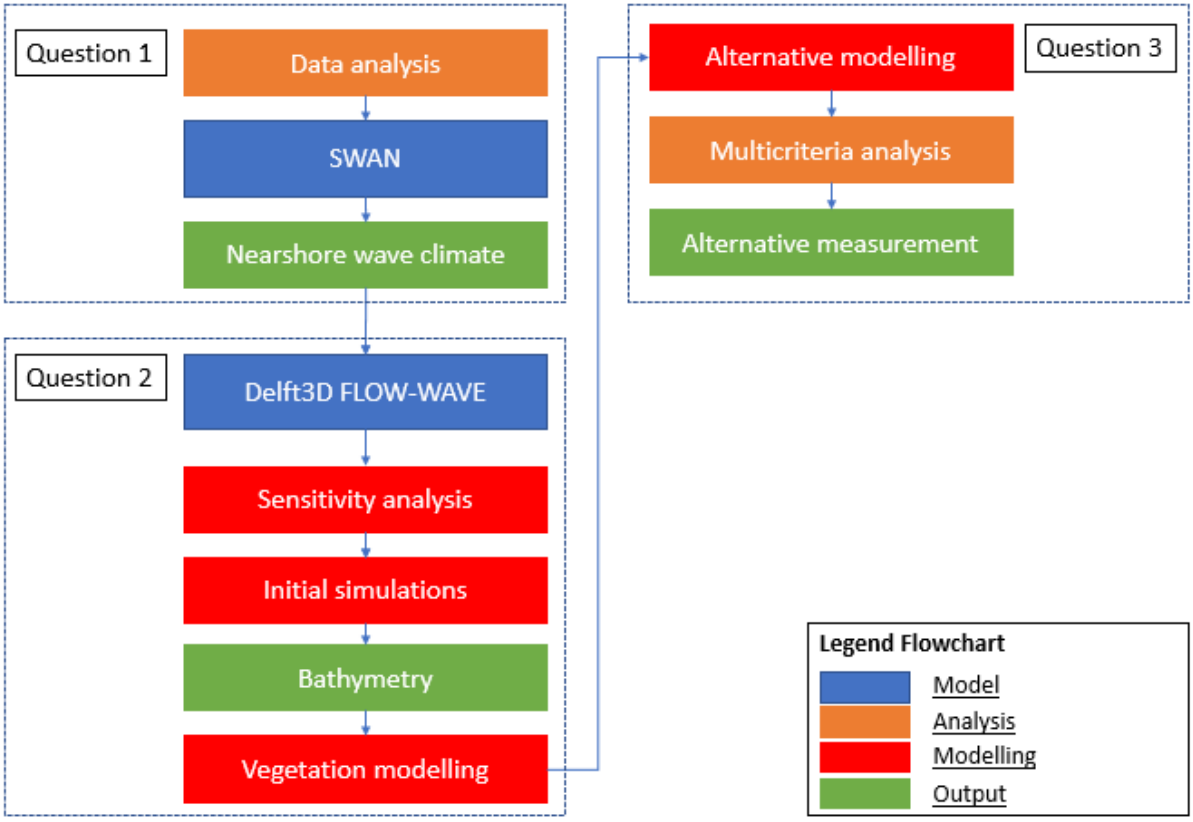

Figure 3, Flowchart of research methodology

2. Theoretical background

This chapter provides theoretical background information which forms the basis of this study. The chapter is divided into a general review about hydro- and morphodynamics in the littoral cell in section 2.1, theoretical background on long term modelling in section 2.2 and the design and assessment of erosion measures in section 2.3.

2.1. Beach processes

The dynamic physical systems of coastal areas are subject to diverse hydrodynamic processes causing for morphological change as results of erosion, sediment transport and deposition. These morphodynamic changes of coastal systems worldwide are of great interest and importance (Deltares, 2014).

2.1.1. Littoral cell

The coastal compartment containing a complete sedimentation cycle in terms of sources, transport paths, and sinks is considered a littoral cell. The geographical area of this cell is delineated by the cell boundaries in which the budget of sediment is balanced. This provides a useful framework to quantitively analyse the coastal erosion and accretion (Inman, 2005).

The sediment sources are commonly streams, sea cliff erosion, onshore migration of sand banks, and material of biological origin such as shells, coral fragments, and skeletons of small marine organisms. The usual transport path is along the coast by waves and currents. Cross-shore (on/offshore) paths may include windblown sand and overtopping. The sediment sinks are usually offshore losses at submarine canyons and shoals or onshore dune migration, rollover, and deposition in bays and estuaries (Figure 4).

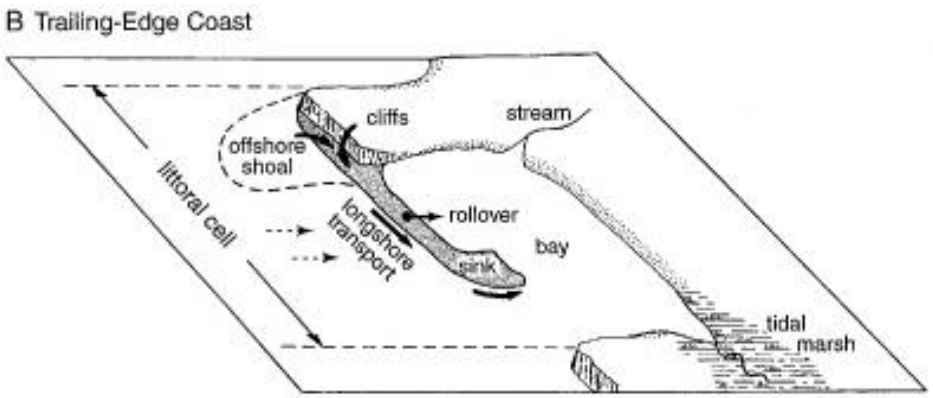

Figure 4, Typical trailing edge coasts and their trailing-littoral cells. Solid arrows show sediment transport paths; broken arrows indicate occasional onshore and offshore transport modes (after Inman, 1994).

The boundary between cells is delineated by a distinct change in the longshore transport rate of sediment. For example, along mountainous coasts with submarine canyons, cell boundaries usually occur at rocky headlands that intercept transport paths. For these coasts, streams and cliff erosion are the sediment sources, the transport path is along the coast and driven by waves and currents, and the sediment sink is generally a submarine canyon adjacent to the rocky headland. In places, waves and currents change locally in response to complex shelf and nearshore bathymetry, giving rise to subcells within littoral cells.

The longshore dimension of a littoral cell may range from one to hundreds of kilometers, whereas the cross-shore dimensions are determined by the landward and seaward extent of the sediment sources and sinks. The seaward limit of significant cross-shore sediment transport on sandy beaches is often referred to as the depth of closure (DoC) (Kraus et al., 1998). DoC is the morhophogical boundary between the landward active region where significant depth change can still be noticed, and the morphological inactive seaward region.

2.1.2. Swash zone

A beach profile can be described in three zones where wave action can be identified; the breaker zone, the surf zone and the swash zone (Figure 5). The dynamic nearshore part of the beach is described as the swash zone. In this zone, the beach face is covered and exposed by uprush and backwash (Bakhtyar et al., 2009). The morphodynamic system in the swash zone consists of hydrodynamics, morphological changes and sediment transport (Masselink & Puleo, 2006) and is characterised by strong and unsteady flows, high turbulence levels, large sediment transport rates and rapid morphological change (Puleo et al., 2000).

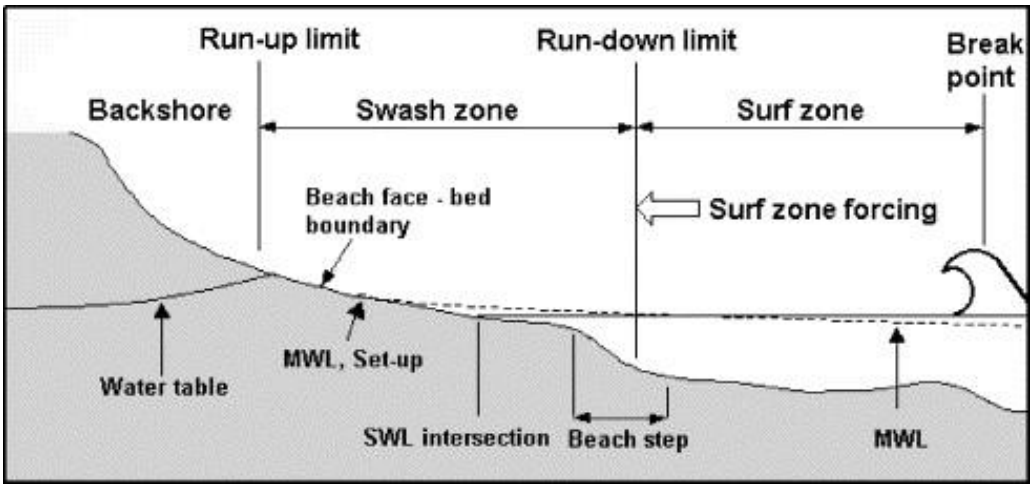

Figure 5, "Schematic cross-section of the beach and the limits of the swash zone (Elfrink & Baldock, 2002)"

2.1.3. Sediment transport

The movement of sediment particles through the water column is described as sediment transport. Insight in the sediment transport can be used to determine whether erosion or deposition will occur, in which magnitude and in what time- and spatial scale. Waves and currents are the primary drivers of sediment transport. Due to the wave impact, the sediment transport is forced along the beach. Under different hydrodynamic conditions the morphology of the beach will change by on- and offshore sediment transport and alongshore sediment transport. Many parameters influence this process, among which bed slope, turbulence, shear stresses and sediment characteristics.

This movement of solid particles (sediment) is typically influenced by the movement of the fluid in combination with the gravity acting on the sediment. Due to an increase of shear stress at a particle, a certain threshold can be exceeded which sets sediment into motion. The Shields parameter determines the initiation of motion of sediment caused by a flow (Shields, 1936):

$$\theta = \frac{\tau_b}{(\rho s - \rho) * gD} \quad (1)$$

Where: τ_b is the dimensional shear stress, ρs is the sediment density, ρ is the fluid density, g the gravitational acceleration and D is the characteristic particle diameter.

As can be seen in equation 1, the critical shear stress is strongly related to the grain size but also the cohesive character of the sediment is an important factor. Sediments can be classified as cohesive and noncohesive, where cohesive sediments are primarly distributed in clay-sized (<2 µm) and silt-sized particles mixed with organic matter or quantities of very fine sand (Shrestha and Blumberg, 2005). Noncohesive sediments consist of sand or gravel-sized material (<75 µm).

Once set in motion, the sediment particles can flow through water in two different forms; bed load sediment transport and suspended sediment transport. The transport and deposition of sediments is largely dependent on the grainsize. Bedload transport consists of larger particles for which the transport of sediment particles travel through a thin layer of the water column close to the bed (van Rijn, 2007a). In this form, the general part of the moving particles is in continuous contact with the bottom (Rooijen, 2011). The suspended sediment transport consists of fine particles which are mainly floating through the water column and are rarely in contact with the bed. The suspended sediment concentration (SSC) is influenced by the flow velocity, the turbulence and gravity.

Under different hydrodynamic conditions, the morphology of the beach will change by onshore and offshore sediment transport and/or longshore sediment transport. The net on- and offshore sediment transport is relatively low and will eventually reach a equilibrium state for each set of wave conditions (The Open University, 1999). This equilibrium is however often disturbed by the occasional extreme events such as storm surges. Longshore sediment transport (LST) is the movement of sediment particles along (parallel to) the coastline. This process arises when waves approach the shore in an oblique angle which generates a longshore current with speeds between about 0.3 and 1 m/s^{-1} (The Open University, 1999). An increase in these currents will lead to higher shear stresses and can result in coastal erosion.

2.1.4. Wave refraction

When waves are travelling into shallow water, their speed becomes depth-determined (c=√gd). Assuming a uniform cross shore beach profile, the landward side of the wave will slow down faster in the shallow water when these waves approach the shore in a oblique angle. This causes the wave to turn towards the coast, a phenomenon called refraction. Figure 6, illustrates the phenomenon refraction for an idealized wave crest.

Refraction of waves in progressively shallowing water can be described by Snell's law, where the angles (θ) of approach are related to the wave speed (c):

$$\frac{sin\theta_1}{sin\theta_2} = \frac{c_1}{c_2} \quad (2)$$

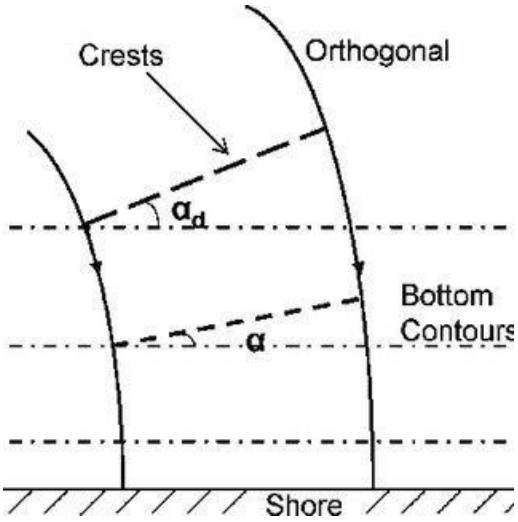

Figure 6, Wave refraction

2.1.5. Shoaling

As waves move into shallower water, the waves increase in height. This process is called shoaling and leads to an increase in the orbital velocity of the wave and thereby increase the shear stress at the bed. An increased shear stress also causes for an increase in potential sediment movement. However, the oscillating wave motion will stir up the sediment but will not result in a net transport.

2.2. Coastal modelling

For the modelling of coastal morphodynamics, the use of three types of models is used in practice: coastal area-, coastline- and cross-shore profile models. These models types are based on different modelling approach and therefor have deviating purposes. Coastal profile models focusses on cross shore dynamics and coastline models on longshore sediment transport. Coastal area models can be applied in cases where both processes need to be combined and are able to simulate more complex systems, for example when modelling complex bathymetric changes around tidal inlets (e.g., migrating channels and shoals) (Roelvink & Reniers, 2011). The downside of these coastal models is that the computational time and knowledge for this models is much higher which makes that these models are less suitable to preform for long term simulations.

Prior to this study, the applicability of the coastline model ShorelineS (Roelvink, 2017) was investigated for the purpose of the erosion problem at Lac Cai (Groot, 2021). From this study it is considered that the ShorelineS model was inadequate for simulating the complex hydrodynamics with the little available data. For the continuation of this study, the hydrodynamic- and morphodynamic processes are simulated with the use of the process-based numerical model Delft3D.

2.2.1. Delft3D

The Delft3D modelling framework is a widely applied software for the modelling of hydrodynamics, sediment transport and morphological processes (Horstman, 2015) and is applicable to predict non-steady flow and transport phenomena in e.g. shallow seas, coastal areas and lagoons (Deltares, 2014). The framework consist of multiple, independent modules of which the FLOW-module forms the core of the system. Within this module the hydrodynamic processes are computed, providing the basis for other modules such as waves (WAVE) and morphology (MOR).

The hydrodynamics in the FLOW module are generated by solving the Navier Stokes equations for an incompressible fluid under the shallow water and the Boussinesq assumptions (Deltares, 2014). The system of equations can be solved in depth averaged two-dimensional (2DH) or three-dimensional (3D) simulations and consists of the horizontal momentum equations, the continuity equation, the transport equation and a turbulence closure model (Lesser et al., 2004a). 2DH computations solving depth-averaged equations and are based on assumptions regarding the vertical velocity profile and turbulent mixing profile (Lesser et al., 2004b). These 2DH flow equations are useful and applicable in simulations with for instance tidal waves, storm surges or tsunamis in vertically well-mixed flow regimes (Deltares 2014). In case of transport problems where significant vertical variations in the horizontal flow fields occur, for instance due to bed stress or bed topography, 3D modelling could lead to more accurate results. The numerical solution methods in Delft3d are based on finite differences and therefor the partial differential equations are transformed onto a curvilinear grid. The equations are formulated in orthogonal curvilinear co-ordinates or in spherical co-ordinates on the globe. The vertical flow domain in the 3D shallow water model is subdivided into a number of σ-layers between the surface and bottom. The system of equations and schematization of the grid are given in Appendix A.

The WAVE module is used to simulate the evolution of waves in the coastal area by the use of the third generation of SWAN, Simulating Waves Near Shore (Booij, Ris &Holthuijsen, 1999). The waves are computed with the wave action balance equation (Deltares, 2018) and includes the wave propagation, wave interaction and dissipation based on the topography, wind direction and the water level.

The morphodynamics in the model are simulated by updating the control volumes in each computational cell for every half time step. The suspended- and bedload sediment transport for noncohesive sediment fractions are based on the approach of Van Rijn (2007) which considers a reference height between the bedload and the suspended transport. The settling velocity and the sediment exchange with the bed, in terms of sediment sink and source, are exchanged between the layers above the reference height and calculated by the advection-diffusion (mass-balance) equation.

2.2.2. Vegetation modelling

Within the modelling system of Delft3d, there are multiple methods to include vegetation into the model. For the purpose of this modelling study a distinction between three renowned methods is made: Vegetation induced bed roughness, trachytopes and a directional point model (DPM).

2.2.2.1. Vegetation-induced bed roughness

The most basic representation of vegetation can be implemented by reducing the hydraulic roughness of the bed. The reduction of the Chézy friction coefficient can be calculated by the White-Colebrook formula which includes the Nikuradse equivalent roughness height (k_s) and the hydraulic radius (R):

$$C = 18log\frac{12R}{k_s} \tag{3}$$

Another commonly used method to conduct the Chézy friction coefficient over a vegetation-induced body is by the use of Manning formulation:

$$C = \frac{H^{1/6}}{n} \tag{4}$$

For the Chézy formulation in the Delft3D FLOW-module, the roughness is specified by means of bottom roughness coefficients in the U- and V-direction. Within a roughness file (*.rgh) a distinction can be made for the different areas in the model. The *.rgh-file is generated within Quickin.

2.2.2.2. Trachytopes

The next method enables the simulation of vegetation roughness in a depth averaged (2DH) mode (Figure 7). The trachytopes functionality within Delft3D allows for user defined roughness formulations in different layers of the model domain in which the vegetation density can be specified for each layer. The function is activated with additional parameters in the Flow-GUI and formatted in a trachytope-definition file. This file exists of the trachytope number, formula number and corresponding parameters. For vegetation based areas there are four different methods implemented in Delft3D. In this study, the formulation according to Baptist (2005) is used:

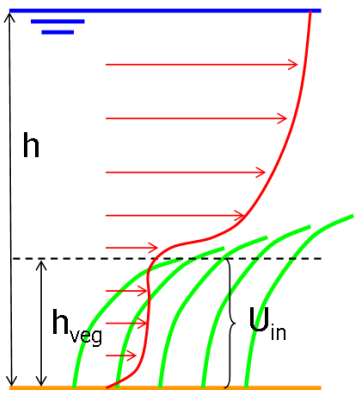

Figure 7, Schematized profile of horizontal flow velocity (U_{in}) with depth averaged vegetation (h_{veg})

$$C_R = C_b + \frac{\sqrt{g}}{\kappa}\ln\frac{h}{h_{veg}} + \sqrt{\frac{1}{1+\frac{C_D n h_{veg} C_b^2}{2g}}} \tag{5}$$

With the representative Chézy value (C_R), the vegetation height (h_{veg}) , the vegetation density (n), drag coefficient (C_D) and the bed roughness (C_b), the water depth (h), the gravitational constant (g) and the Von Kármán's constant (κ =0.41).

2.2.2.3. Directional point model (DPM)

In the directional point model (DPM) the vegetation is represented as rigid vertical cylinders to account for the contribution of vegetation on flow and turbulence. This method enables the possibility to implement a vertical variation. The impact of vegetation is included into the momentum equation and a turbulence closure model.

The cylindrical vegetation elements create flow drag which is implemented into the momentum equation by the depth-dependent vegetation-induced the friction force $F(z)$:

$$F(z) = \frac{1}{2}\rho_w C_D n(z) D(z) |u(z)| u(z)$$

where ρ_w is the water density (kg/m3), C_D the drag coefficient, $n(z)$ the depth-dependent number of cylindrical elements [n/m^2], $D(z)$ the depth-dependent diameter (m) and $u(z)$ the horizontal velocity [m/s] at elevation z [m].

The obstruction of momentum and turbulence is included through the eddy viscosity (v) which accounts for the vegetation-induced turbulence generation, dissipation and diffusion. The eddy viscosity is resolved by the $k - \varepsilon$ turbulence closure model which includes the vegetation porosity ($1 - A_z(z)$) obtained from the cross-sectional area of the vegetation:

$$A_p(z) = \frac{1}{4}\pi D^2(z) n(z)$$

The input parameters for this model are defined in the *.pla-file and consist of the vegetation height, stem diameter, the number of stems and drag coefficient (C_D).

3. Data Analysis

3.1. Study area

Bonaire is one of the three islands in the Old Dutch Caribbean region clustered in the leeward Antilles, also know as the ABC-islands, and is situated the most easterly. It is crescent shaped and oriented NW-SE, approximately 40 km long by 11 km at its widest point. The island has a total land area of 294 km² and a coastline of 120 km long. At present, cruise, beach and dive tourism are the most important economic activities of the island, and the capacity for growth is rapidly increasing. Coastal development have experienced enormous increases to accommodate the large influx of visitors and residents to the island in the last years.

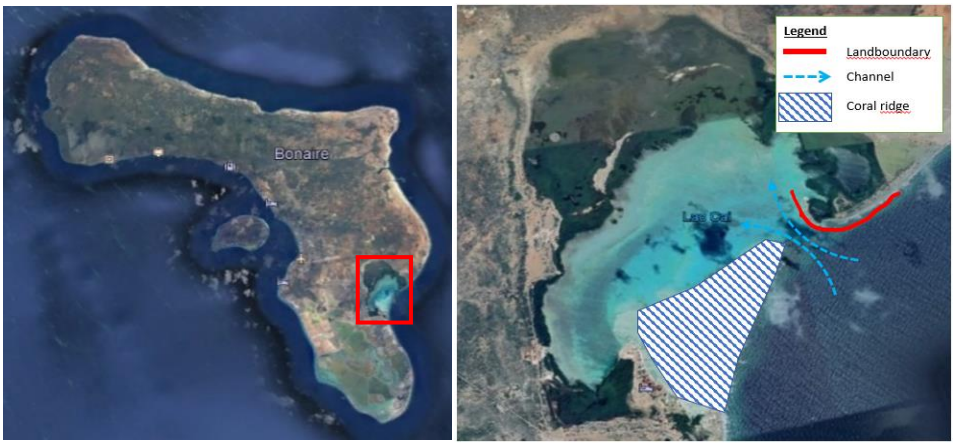

Figure 8, Location of Lac Cai on Bonaire Island (red square, left), and aerial overview of focus

Bonaire's seabed environment is primarily made up of fringing coral reefs that surround the island and is protected as part of the Bonaire National Marine Park (BNMP). The Bonaire National Marine Park (BNMP) was established in 1979 and is managed by Stichting Nationale Parken Bonaire (STINAPA Bonaire). The park starts at the high water mark and extends to a depth of 60 meters, covering an area of 27 km2 that includes fringing reefs, seagrass beds and mangroves.

Lac Bay is a shallow lagoon of about 700 hectares and is situated at the south-West side of the island (Figure 8). The lagoon is mostly separated from the open sea by a shallow coral dam except for a small channel at the north side of the inlet, in front of Cai Beach. The sheltered area create a great environment for settlement of coral and seagrass on the lagoon bed and therefor forms a habitat to a great variety of sea life. A further contribution to the ecological value are the surrounding mangroves which serve as an important breeding area.

The high ecological value is one of the reasons why the lagoon is a very attractive location for tourism. To protect and preserve the lagoon for future generations, a zoning plan is made which divided the area into zones of six different purposes. Figure 9, shows the zoning plan of Lac Bay (Kalke & Kats, 2011) in which the red areas are conceived as general recreational beach zones. This means the beach at Lac Cai is one of only two beaches in the surroundings of Lac Bay and therefor has a high economical and social value.

Figure 9, Zoning plan of Lac Bay (Kalke & Kats, 2011)

3.1.1. Geology

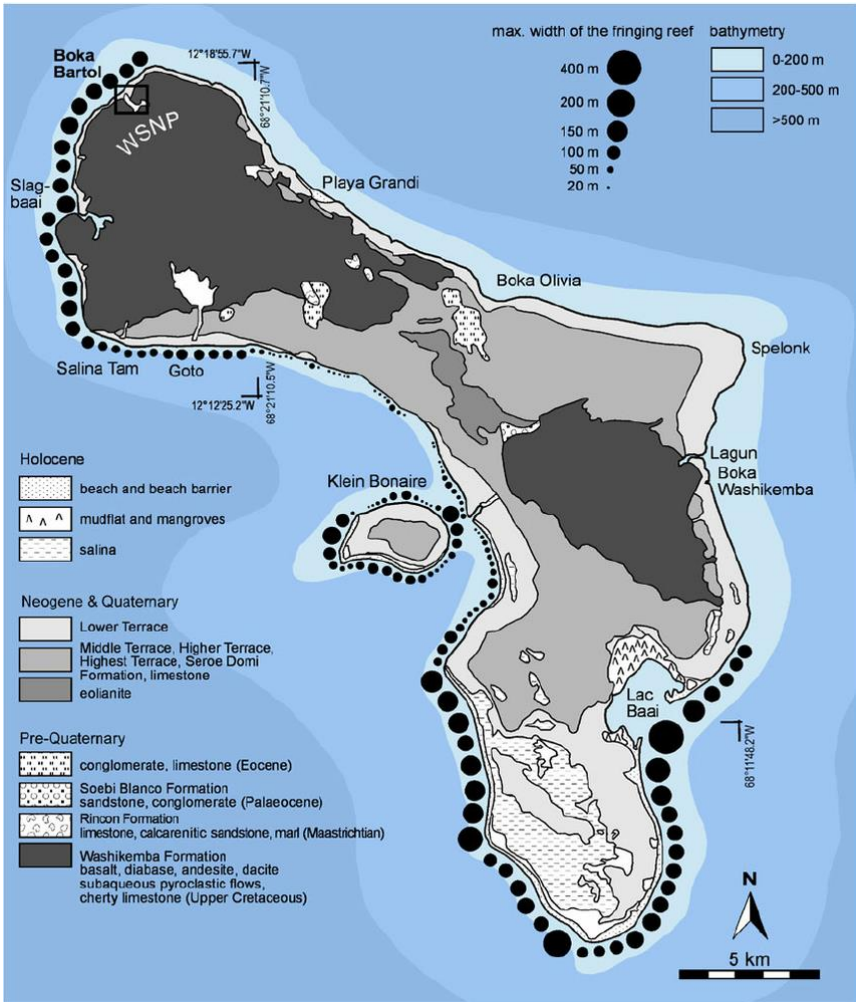

Figure 10, Geological map Bonaire

Figure 10 shows the geological map of Bonaire retrieved from the paper of Engel et al. (2012). The map gives insight in the different geological characteristics and compositions in and around Lac Bay. In this map it is visible that the Northern part of the bay is surrounded with mangroves and mudflat. Furthermore, there are fringing coral reefs is located in front of the coast. The spit of the Lac Cai beach is considered corresponding as 'beach and beach barrier' and is adjacent to the lower terrace composed of reefal limestone (Engel et al. 2012). The non-cohesive sandy composition of the sediment fraction at Cai is confirmed in the study executed by Lott (2001).

3.1.2. Vegetation

The environmental landscape of Lac Cai is a dynamic natural ecosystem (Lott, 2001) consisting of mangroves forest, coral reefs and seagrass meadows which provides important ecosystem service by creating a stable erosion-resistant seabed that contributes to effective coastal protection (James, 2020). Changes in vegetation cover of the lagoon impact the hydro- and morphodynamics in the coastal system and degradation could be correlated with the increase in erosion rates due to the loss in flow- and wave attenuating characteristics and their ability to trap and stabilize sediments.

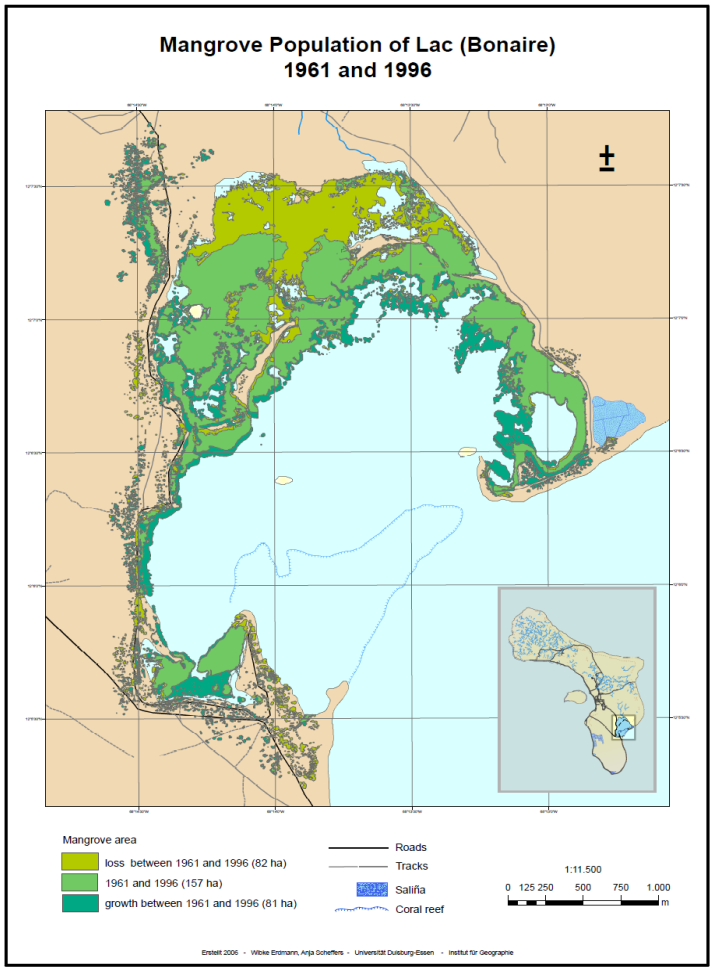

Figure 11, Mapped mangrove loss between the years 1961 and 1996 in Lac Cai (Erdmann and Scheffers, 2006)

Multiple studies have been conducted on mangrove deforestation around Lac Cai. Figure 11 shows the mangrove deforestation between the years 1961-1996 as manifested in the research conducted by Erdmann & Scheffers (2006). The map mainly shows the decay in the interior mangrove sub-basin but analyzing satellite images in section 1.1 (Figure 2) also show deforestation of the mangrove fringe in front of the entrance road to Cai Beach.

Furthermore, the native seagrass species *Thalassia testudinum,* occurring in and around Lac Cai, is threatened due to intensive grazing of megaherbivores and the rapid spread of the invasive opportunistic seagrass specie *H. stipulacea.* The native specie benefits long-leaved, dense meadows which provide the high sediment stabilization and wave attenuating functions whereas the invasive species is a low below-ground biomass susceptible to uprooting (James, 2020).

Lastly, coral mortality due to rising sea temperatures could also contribute to a coastal vulnerability as healthy coral reefs significantly contribute to reducing wave energy (Reguero, 2018).

3.1.3. Coastline profiles

The historical satellite images from the Google Earth Engine were used to manually extract shoreline locations in World Geodetic System (WGS) 84 latitude and longitude coordinates. The coordinates are exported in a Keyhole Markup Language (KML) file and converted to Universal Transverse Mercator (UTM) coordinates.

In Figure 12, the historical shoreline profiles for the years: 2002, 2012, 2014, 2016, 2018 and 2019, are drawn over the 2002 satellite image retrieved from Google Earth Pro. Comparing the profiles from 2002 and 2019 show a gradual coastline retreat of approximately 30 metres in front of the entrance road to Cai Beach. The profile of Lac beach is fluctuating over the years but also shows coastal retreat in the upper corner.

Figure 12, Shoreline positions over the years between 2002 and 2019 (GoogleEarth)

Based on the gradual coastal retreat, it can be assumed that the cause of the coastal erosion does not originates in the effect of short hazardous events but rather by an ongoing coastal process. This is substantiated by the fact that there occurred only 6 tropical storm event in the Bonaire region between the years 1944 and 2010 (James, 2020).

The cause of the coastal erosion of Cai beach, inside the bay, is presumable due to wave diffraction as shown in Figure 12. The lagoon is mostly sheltered from incoming waves by a coral reef dam except for the small channel in front of Cai beach where the waves refract around the beach and flow sediments into the interior mangrove sub-basin.

The small channel could also lead to accelerating flow in front Cai Beach and therefor higher erosion rates but this effect could not be retrieved from the coastal evolution of the beach. The fact that the erosion in front of the beach is limited could be explained by shelter provided by the piles of conch shell or due to the inflow of sediments from adjacent eroded areas.

3.1.4. Hydrology

The hydrological cycle in the Lac Bay area comprehends both offshore and coastal currents, tidal action, wind-driven surface currents, and evaporative processes (Lott, 2001). The inflow into the bay is concentrated at the narrow channel between the coral ridge and Cai beach and disperse into the interior mangrove sub-basins. The water inflow is schematized in Figure 13.

The tidal range is limited (<0,3m) and rainfall is low (<560 mm/year). Also, extreme storm events are infrequent at the windward side of Bonaire (James, 2020)

Figure 13, Water inflow into Lac Cai (Hummelinck & Roos, 1968)

3.2. Wave- and Bathymetry data

In the wave module of Delft3D, a SWAN model was set up to translate and analyse the bathymetry and wave data. The Graphical User Interface (GUI) 'Delftdashboard' (DDB), is used for setting up the model and is coupled with the Delft3D WAVE module. The bathymetry for the offshore wave transformation will be based on the Gebco data and can be retrieved in the DDB GUI. The offshore bathymetry will be combined with measured data off the bathymetry inside the bay. These two data sets will be combined by the help of the RGF grid and Quickin modules in Delft3D.

The wave time-series of the ERA5 reanalysis with 0.25°× 0.25° resolution, produced by the European Centre for Medium-Range Weather Forecasts (ECMWF) were used to extract a wave climate. The model domain in DDB, as depicted in Figure 14, contains the entire bay and will cover a size of approximately 5 km x 15 km to include the data point from which the wave data is extracted. The point where the wave data is available (12.125ºN, 68.125ºW) is situated about 10 km outside the coast at a depth of approximately 500 m.

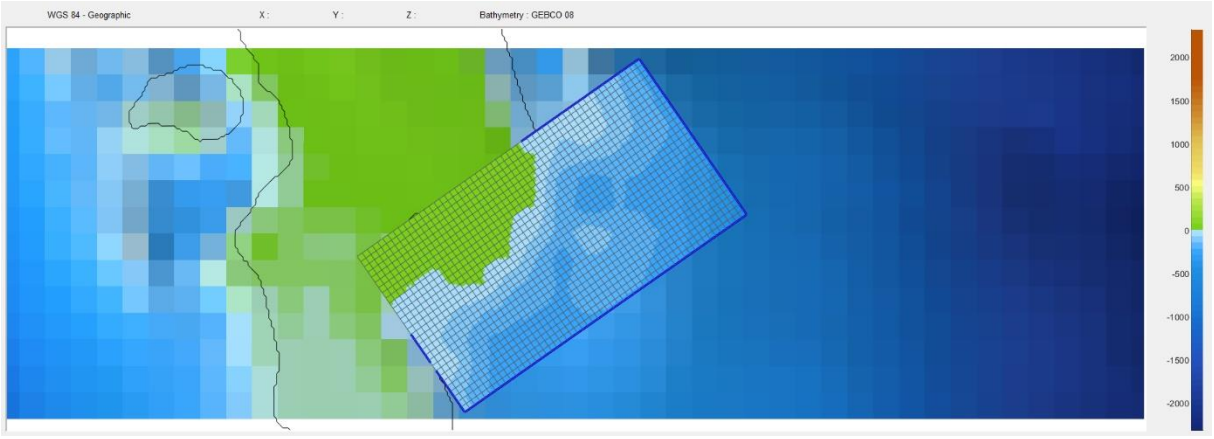

Figure 14, Grid on top of the model domain in Delftdashboard with Gebco 08 bathymetry

3.2.1. Bathymetry

The topography inside the bay is measured on June 2017 with the use of depth soundings done with a Lowrance HDS7Gen3. As can be seen in Figure 15, the measured data is not consistent and therefor considered as inadequate material for the interpolation of a bathymetry. The measured points fluctuate between depths of 1 till 45 meters which is considered unrealistic for a shallow lagoon such as Lac Cai. Furthermore, there are large differences between adjacent points. For instance there are measured points within a distance of 1 meters from each other, which show fluctuations in depth of over 10 meters. Also, there are depths measured right in front of the coastline reaching over 16 meters, this is considered unrealistic in the area.

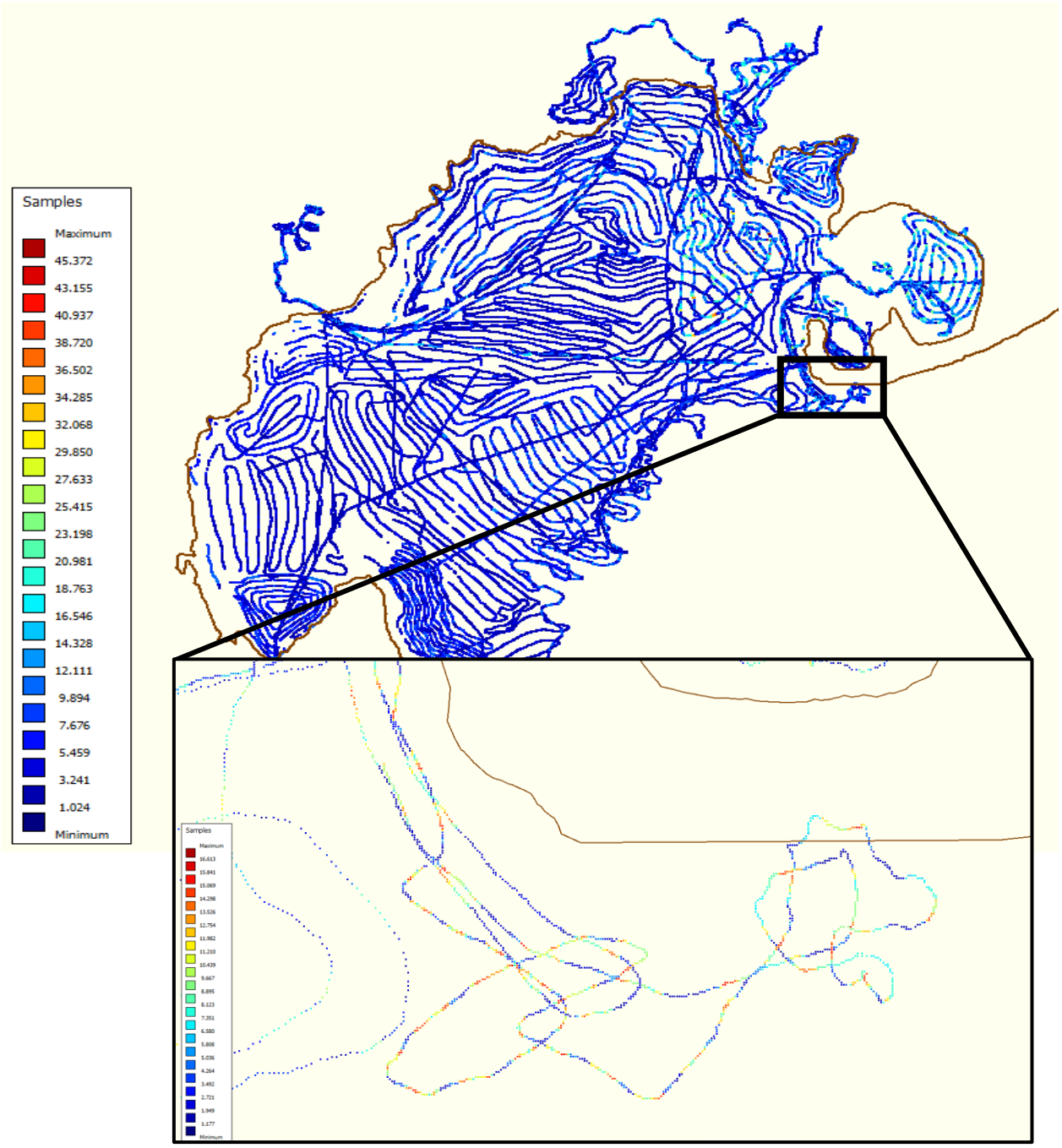

Figure 15, Measured bathymetry points inside Lac Cai

Figure 16 shows the depth map inside the lagoon based on the paper from Wagenaar, Hummelinck and Roos (1969). This map shows depths within the lagoon are given between half a meter and 5 meters. In order to approach a realistic translation of the model bathymetry, a uniform depth of 5 meters is inserted inside the bay.

Figure 16, Depths map of Lac Bay 1949 (Lott, 2001)

The earlier mentioned, coral dam which separates the lagoon from the open ocean, is reconstructed as an unerodable layer with a depth of 1 meter. In contrast with the bathymetry inside the bay, the channel between the coral dam and the main land at Cai, is interpolated from the measured data points. The measured data in the channel consists of 4 strings which is relatively concentrated. The fact that the depths are larger in comparison with the bathymetry inside the bay is in agreement with the depth map from 1949 (Figure 16). The narrow strip causes for an acceleration of the inflow into Lac Cai which results in the deepening of this channel. It is likely that this process continued over the years and therefor the higher depths from the measured data are considered more realistic and are used for interpolation of the model bathymetry.

3.2.2. Wave climate

The offshore wave data is retrieved from the ERA5 wind-wave data (1979–2017) produced by the ECMWF. This study used 41 years of wave information including significant wave heights, periods and direction with the temporal resolution of 1 hour. Figure 17, shows the grid points for the available data. The data set measured closest to Lac Cai (P6) is used as input wave data in this study. The distance between the beach and the ERA5 measurement point is approximately 10 km.

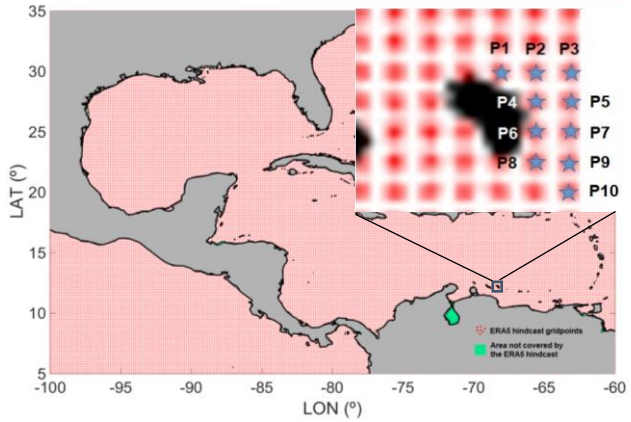

Figure 17, Available ERA5wave data sets from ECMWF

The wave-time series are analysed to asses daily, monthly and seasonal patterns in wave heights (Hs), wave period (Tp) and direction (Dir). The wave rose in Figure 18 gives an overview on wave direction and distribution of the wave heights of the entire dataset. This is further specified into a monthly averaged height and direction. From this averaged monthly wave characteristics in Figure 18 it can be seen that the range in both height as direction is limited distributed. The monthly averaged wave heights fluctuate between 1.2 and 1.8 meters and the direction is dominated from the North-Northeast (NNE).

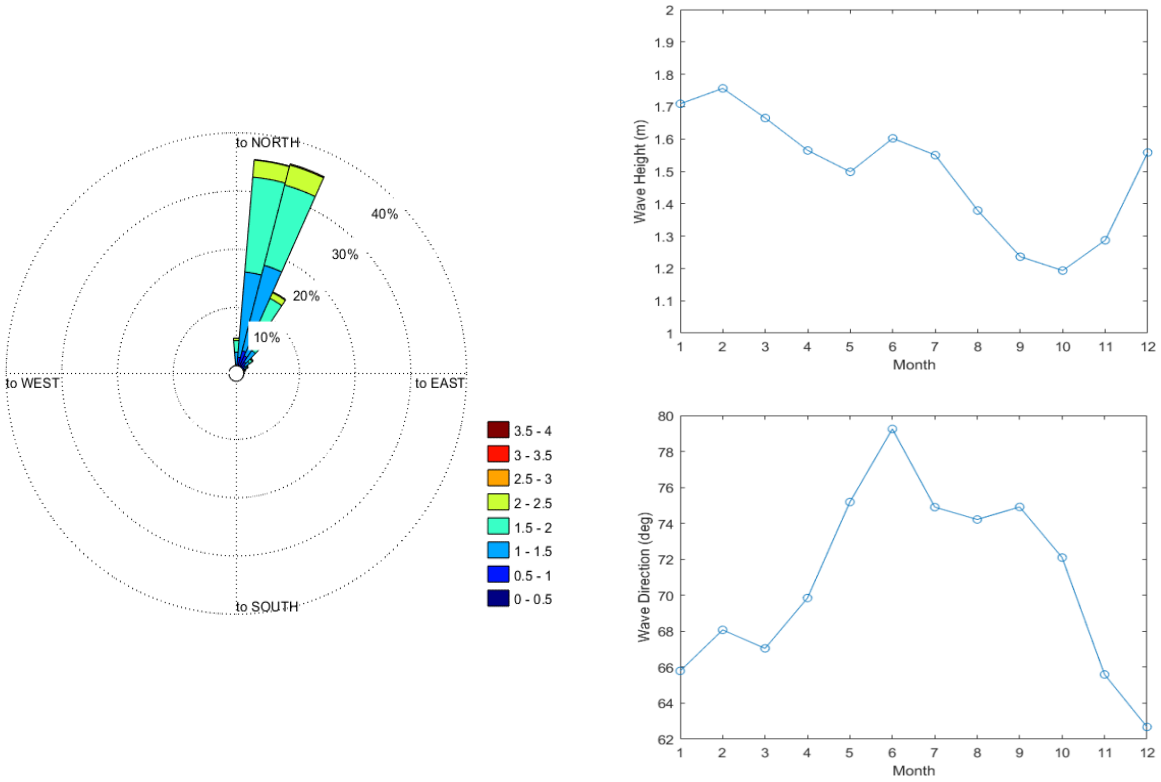

Figure 18, Wave rose for ERA5 dataset (1979-2017) and monthly averaged wave characteristics

To bring down the computational time of a morphological model, the specific input wave conditions prescribed at the boundaries of the SWAN model, are reduced to a schematized wave climate. For the wave climate schematization there are four different methods directly based on the wave climate characteristics (Benedet et al, 2016): 'Fixed Bins Method' (FBM), 'Energy Flux Method' (EFM), 'Energy Flux with Extreme Wave Conditions Method' (EFEM) and the 'CERC Method' (CERC). These methods divides the wave time-series into representative wave height- and direction classes. The number of representative wave classes influences the accuracy and computational time of the model. This study will make use of the EFM in order to translate the wave time-series.

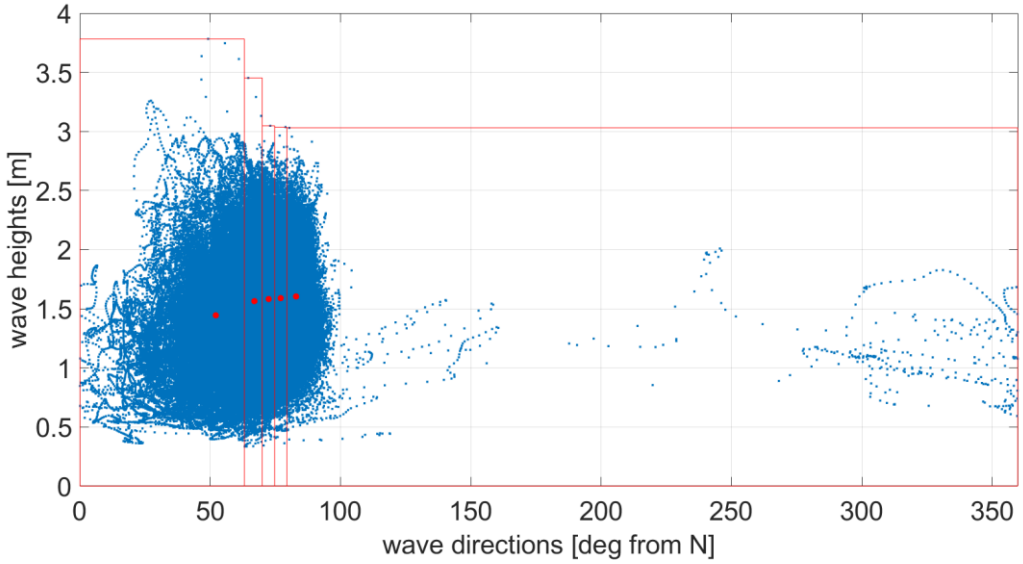

Figure 19, Energy flux method for 5 bins over the scatterplot of the ERA5 dataset

The energy flux method separates wave conditions according to the concept of equal energy. The energy flux of each wave record from the time-series is calculated and the total energy is distributed over an user specified number of wave conditions. This means that each derived wave condition is holding an equal amount of energy. The energy flux of the individual wave records are calculated by:

$$E_F = (\frac{1}{8}\,\rho\, g\, {H_s}^2)\, C_g$$

where ρ is the water density, g is the gravity acceleration, H_s is the significant wave height and C_g is the deep water wave group celerity.

The development of a wave climate utilizing the EFM schematization is established in a couple of steps (Benedet, 2016). First a scatter plot is made wherein wave height is plotted against the wave direction. Next, the wave time-series is divided into a number of wave directional bins which hold $1/n^{th}$ of the total energy of the wave set. The directional bins are subdivided into in a number of wave height bins so each wave height class holds $1/m^{th}$ of the total energy in that particular directional bin. Each bin is then re-derived into a representative wave height.

The number of bins for the EFM schematization for this study are retrieved iteratively. Figure 19 shows the scatter plot of the entire wave time-series divided into 5 directional bins. The data is relatively clustered and with a few exceptions, the variation in height and direction of the individual wave records are limited. Increasing the number barely adds to the variation of wave conditions and only complicates the modelling process with redundant wave conditions.

Table 1, Schematized wave climate by EFM

Wave condition	Height [m]	Period [s]	Direction [◦]
1	1.445	8.4504	52.2126
2	1.565	7.4856	67.0047
3	1.582	7.0787	72.4995
4	1.590	6.7627	77.0839
5	1.604	6.4954	83.0052

The wave climate derived by the EFM is given in Table 1. The deviation in height and period is small but the wave conditions distinguishes in direction. The waves will approach the island with an oblique wave angle and wave refraction will occur because the orientation of the shoreline position in front of the connecting road is approximately 90^0. Based on the direction of the waves it is likely that the erosion is caused by the longshore sediment transport for which the critical angle of entering waves lays between the 42-44 degrees.

The offshore wave climate was translated by the SWAN model and the near shore wave conditions are analysed at 19 stations along the 10 meter depth contour line. Figure 20 shows the significant wave height and mean direction for wave condition 4 and gives the locations of the 19 stations along the 10 meter depth contour line, where station 1 is located at the lower right, and station 19 at the upper left. Figure 20 also gives the wave heights for the 5 different wave conditions. From this figure it is visible that the waves refract towards the coastline and attenuate while entering into lagoon.

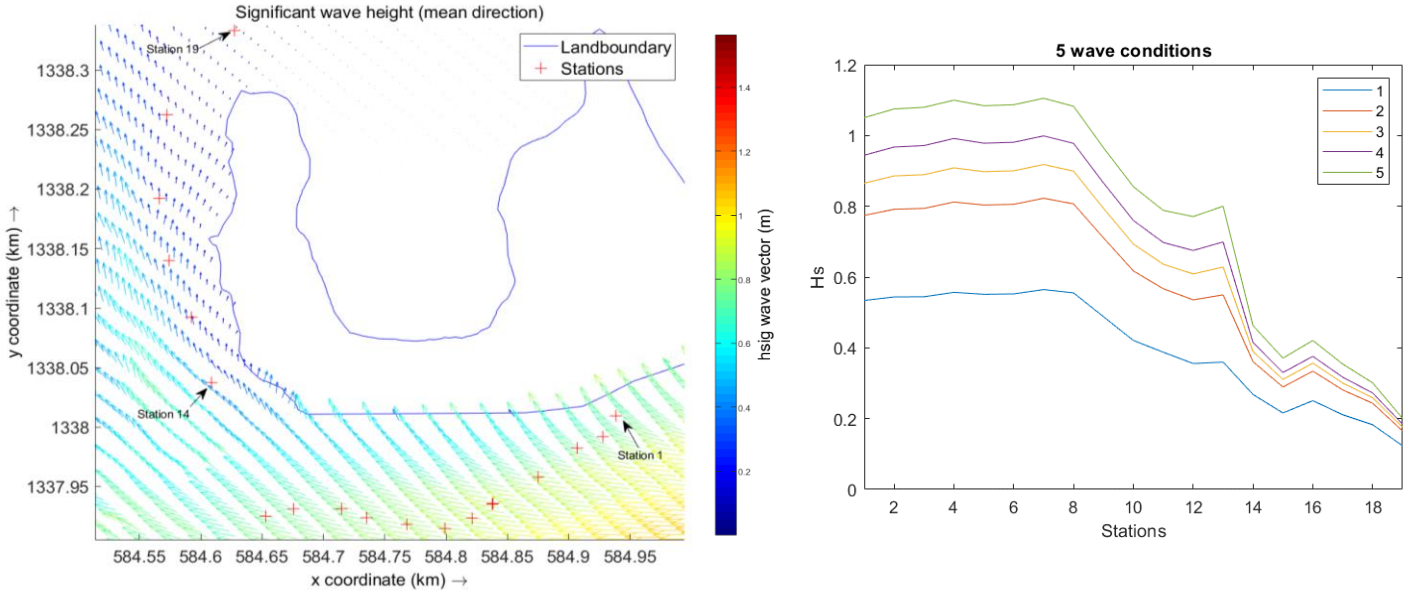

Figure 20, Significant wave height simulated in SWAN model for 5 wave conditions at 19 stations along the 10m depth contour line

4. Modelling

This chapter starts with the modelling strategy in section 4.1 and model setup in section 4.2. The model results for the sensitivity analysis, dean profile and vegetation models will be presented in respectively the sections 4.2. 4.3 and 4.4. The modelling of the alternative mitigation measures will follow in Chapter 5.

4.1. Model strategy

In order to simulate the hydrological and morphological processes at Lac Cai, a morphological model will be constructed within the software of Delft3D. A FLOW model will be generated and coupled online with the SWAN model from the previous section (3.2). Several modelling steps will be taken before the assessment of the measurement alternatives can be properly executed.

The development of the model will start with a sensitivity analysis to create insights in the impact of various parameters. The parameters included into this analysis are the wave-related transport factors, the bed gradient factors and the factor for erosion of adjacent dry cells. The preferred values for these parameters will be used over the course of the remaining modelling.

Since the data analysis showed the bathymetry data is incorrect or inaccurate, the second step of modelling is to generate a more realistic bathymetry with a gradual transition between the coastline and offshore.

Next, the proposed correlation between the mangrove loss and coastal erosion will be investigated by modelling the effect of the vegetation in three different, commonly used modelling methods: vegetation-induced roughness, trachytopes and rigid rods. The comparison of these models will be made between the erosion rates in the historic situation, the current situation and in a situation without any mangroves.

From the vegetation models, a subsequent model will be created to quantify the impact of the different alternative measures against the beach erosion at Lac Cai. The final bathymetry of the vegetation model will be exported and used as initial bathymetry for the models including the alternatives.

4.2. Model set up

4.2.1. FLOW-GUI

The input parameters for the hydrodynamic simulation are defined in the Master Definition Flow file (MDF) which is created in the FLOW Graphical User Interface. This GUI consist of multiple data groups which are coherent sets of input parameters that together define a certain type of input data (Delft3d, 2018). The different data groups are: Description, Domain, Time frame, Processes, Initial conditions, Boundaries, Physical parameters, Numerical parameters, Operations, Monitoring, Additional parameters and Output. The most important input parameters are elaborated below.

The open sea boundary is a water-level boundary with the option for harmonic forcing of a representative morphological tide. The tidal influences are excluded in this study due to the small tidal range so the model will be only forced by the online coupling with the WAVE module. The other open boundary is perpendicular to the North side of the coast and therefor here is chosen for a Neumann boundary. The uncertainties at the boundary are solved by imposing the alongshore water level gradient (Deltares, 2018).

Sediments can be added by including a sediment in the data group 'processes', which enables the sediment transport and morphology features into the model. The sediment characteristics can be further specified in the sediment input file (*.sed) and the necessary morphology information is collaborated in the morphology input file (*.mor). Based on the geology analysis the sediment is considered a non-cohesive sandy sediment composition. Sediment characteristics are taken from common, frequently used sand composition. This comes down to a specific density of 2650kg/m^3, dry bed density of 1600 kg/m^3 and a D50 of 350 μm. The formulations of Van Rijn (2007) are used as default setting for the calculation of suspended and bed-load transport for non-cohesive sediments.

The parameter 'Equilibrium sand concentration profile at inflow boundaries' is selected to maintain the initial bathymetry along your boundaries and minimize the accretion or erosion near the model boundaries. The parameter is activated to limit the influence of bathymetry changes at the edges of the model.

To speed up morphological processes and safe on computation time, a morphological acceleration factor (MorFac) is used. The output map and communication files of the online coupling between FLOW and WAVE are stored every 360 minutes. These output files show the hydrodynamic changes for every 6 hours and morphological changes for approximately one month due to a MorFac of 120. This MorFac can be justified by the fact that the tidal influences are excluded in this study and the model will be only forced by the online coupling with the WAVE module.

4.2.2. Grid

A curvilinear grid will be set up to be able to create a high grid concentration in the areas of interest and at the same time limit the computational time as much as possible, by coarsen the grid in areas of less importance. The aim is to create grid cell sizes below 5 meters in both the X and Y direction, in the surrounding areas of Lac Cai. This resolution is implemented in order to create sufficient accuracy in the surf zone processes. The grid is created by the use of Splines following the contours of the coastline of Lac Cai and perpendicular lines. The coarse grid is smoothened and refined to minimize the errors in the finite difference approximation. Furthermore, the orthogonalization module is used to create a more efficient model. Increasing the orthogonality of a grid saves computationally expensive transformation terms (Delft3d, RGFmanual). The grid is created in an iterative procedure by starting with a coarse version of the grid and improve and refine the grid until the required resolution is achieved. Trial and error in combination with expert knowledge has led to the generation of the grid as seen in Appendix C.

4.2.3. Bathymetry

The model bathymetry is created by combining the Gebco data with the interpolated data from the field measurements. Because both data sets differ from each other and the measured points also show inconsistency/irregularities between adjacent points, the bathymetry is manually adjusted to create a smooth transition between the two data sets. The cells covering the main land are set at a height of one meter above sea level and the bathymetry inside the bay at a homogeneous depth of 5m. The transition between the two data sets is linearly interpolated and the coastline profile will be further developed by the use of the Dean equation in section 4.4.

In contrast with the other data, the measured data within the channel is used to interpolate a bathymetry. There are three strings of measured points which is considered sufficient for grid cell averaging combined with the manual modification to a linear transition between the land boundary, the coral dam and the bathymetry inside the bay. The channel is considered important because it is likely that this narrow stroke experiences more erosion due to accelerated currents and functions as a passage for waves and sediment entering lagoon.

Non-erodible areas are translated into an sdb-file. This file will include non-uniform values for the initial sediment layer thickness at each cell centre. A distinction between erodible and non-erodible layers will be set by inserting a thickness of respectively five and zero. There are two areas specified as non-erodable layer. First of all, the literature study conducted on the study area, given in section 3.1.1., shows the lower terrace adjacent to the beach is composed of reefal limestone ridges (Engel et al. 2012). Based on the stony characteristics of this geology, this area is computed as unerodable layer in the model. Secondly, the coral dam, separating the lagoon from the ocean, is also considered as non-erodible (Figure 21, right).

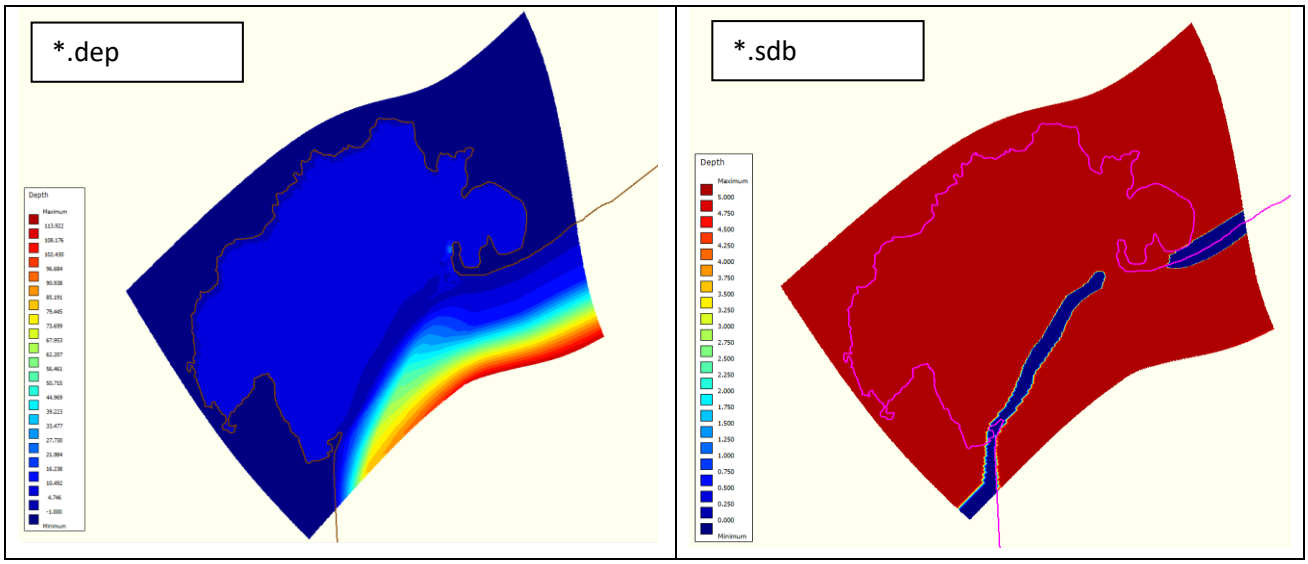

Figure 21, Combined bathymetry and unerodable layers

4.2.4. Waves

The online coupling with the Delft3D WAVE module was activated. The grid is more extensive and coarse compared to the FLOW module. The wave condition at the boundary are based on the offshore wave climate. The characteristics of the wave conditions are elaborated in a wavecon-file (Deltares, 2018b). The time point for each condition is set at 720 minutes. With a MorFac of 120, the model forcing is changing between the five wave conditions every other month in a fixed order.

The significant wave height, peak period, mean wave direction and directional standard deviation (ms) are specified as given in Table 2. The additional waterlevel and wind characteristic are excluded in this study.

Table 2, Wave characteristic at the offshore boundaries

Wave condition	Timestep [min]	Height [m]	Period [s]	Direction [◦]	ms [◦]
1	1-2,11-12,…,71-72	1.445	8.4504	52.2126	4
2	3-4,13-14,…,73-122	1.565	7.4856	67.0047	4
3	5-6,15-16,…,65-66	1.582	7.0787	72.4995	4
4	7-8,16-17,…,67-68	1.590	6.7627	77.0839	4
5	9-10,19-20,…,69-70	1.604	6.4954	83.0052	4

4.3. Sensitivity analysis

A sensitivity analysis is conducted on five significant parameters of the morphological input file in order to analyse the impact of the different parameters to the morphological dynamics of the model. Four scenarios are simulated in order to review the impact of the following Multiplication (calibration) factors:

- the wave-related suspended sediment factor (SusW)
- the wave-related bed-load transport factor (BedW)
- Streamwise bed gradient factor for bed load transport (α_{Bn})
- Transverse bed gradient factor for bed load transport (α_{Bs})
- Factor for erosion of adjacent dry cells (ThetSD)

The scenarios are given in Table 3. In order to identify the interaction between the parameters, the range of the parameters is alternated independently. The erosion factor is disabled in the first three scenarios to be able to analyse the interdependencies of the other parameters. The wave related sediment transport factors are ranged between 0 and 0.2 and the bed gradient factors between 0 and 1.

Table 3, Sensitivity scenarios

Scenario	A	B	C	D
SusW	0	0	0.2	0.2
BedW	0	0	0.2	0.2
α_{Bn}	0	1	1	1
α_{Bs}	0	1	1	1
ThetSD	0	0	0	1

The model results of the different scenarios are visualized in Figure 22. The cross sections are taken from the landboundary in the middle of the entrance road and reach towards the sea. The morphological timescale is 1.5 years. The model for scenario B are not shown Since the variation in the bed gradient factors did not show any difference.

The wave related factors did show a more smooth nearshore profile because of the tempered wave intensity but this did not effect the DoC. For the purpose of this study, it will be sufficient to use wave-related transport factors of 0.2 and has the advantage that vegetation modelling will not be effected by high intensive transport rates. The factor for erosion of adjacent dry cells will be activated since the goal of this research is to investigate the erosion and coastal retreat at Lac Cai.

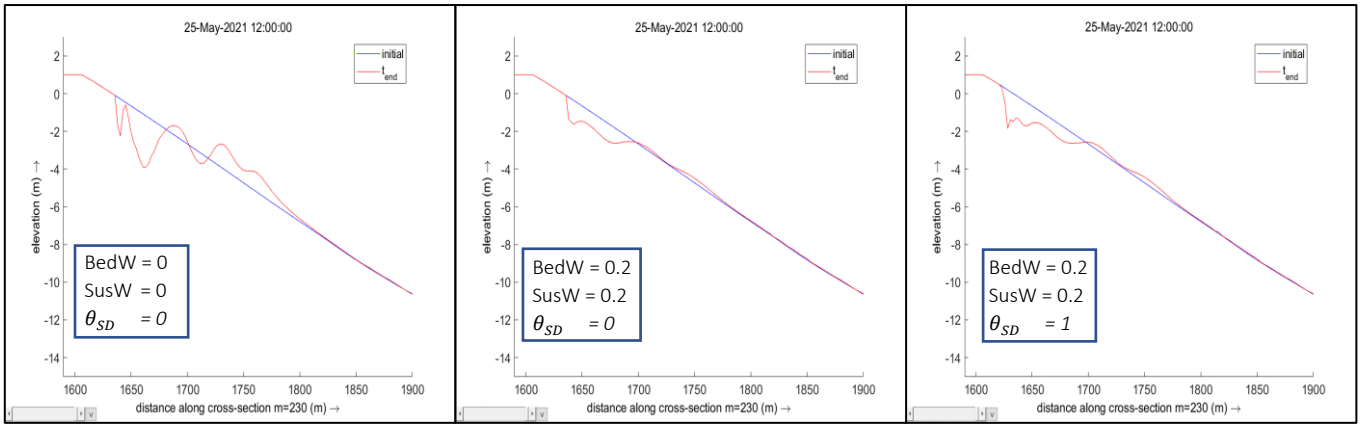

Figure 22, Cross sections of sensitivity analysis scenarios with Multiplication (calibration) factors

4.4. Dean profile

The bathymetry is iteratively developed in a 1.5 years morphological model starting with an equilibrium dean profile as initial condition. The equilibrium depth profile is encountered with the use of Dean's method (Dean, 1991). This relative simple approach approximates a depth profile for the morphologically active part of the coastline profile which is considered between the range from the shoreline till the depth of closure.

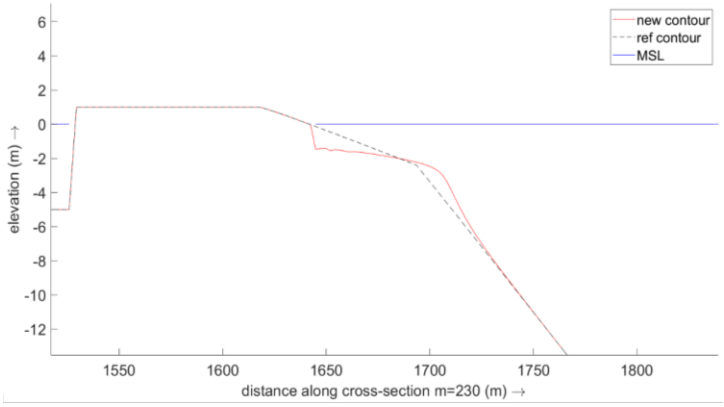

Figure 23, Bedlevel in waterlevel points for initial dean profile at t=1 and after one cycle of wave series at t=130

The dean profile generates a general coastline profile and a DoC based on the specific wave height, wave period and the average grainsize (D50) of the sediment. The sediment composition at Lac Beach is considered non-cohesive with an D50 of 350μm. The wave conditions are based on the wave climate: $H_s = 1{,}5m$ and $T_p = 7s$. This results in an active profile of approximately 80 meters with a depth of closure of 2.2 meters. Figure 23 shows a cross profile of the equilibrium depth based on Dean's equations and the newly generated profile after a morphological period of 1.5 years.

The profile is linearly interpolated between the land boundary and the DoC with the use of Quickin. The newly generated profile in Figure 23 shows to be morphologically active till a depth of 6 meters. Based on this knowledge, the equilibrium profile is extended and the slope is continued to a depth of approximately 6 meters. This profile is manually approached by deleting the bathymetry inside the rectangular polygon in Figure 24, and inserting the new profile. The newly generated bathymetry is used as input for a subsequent simulation with morphological timescale of 1.5 years.

This process is repeated iteratively until the depth differences between the reference profile and the output equilibrium profile is reduced with less than 5% of the total depth. This resulted in an equilibrium profile of approximately 450 m wide with a DoC of -14m below MSL. The newly generated bathymetry serves as input for the vegetation modelling in the following section (4.5).

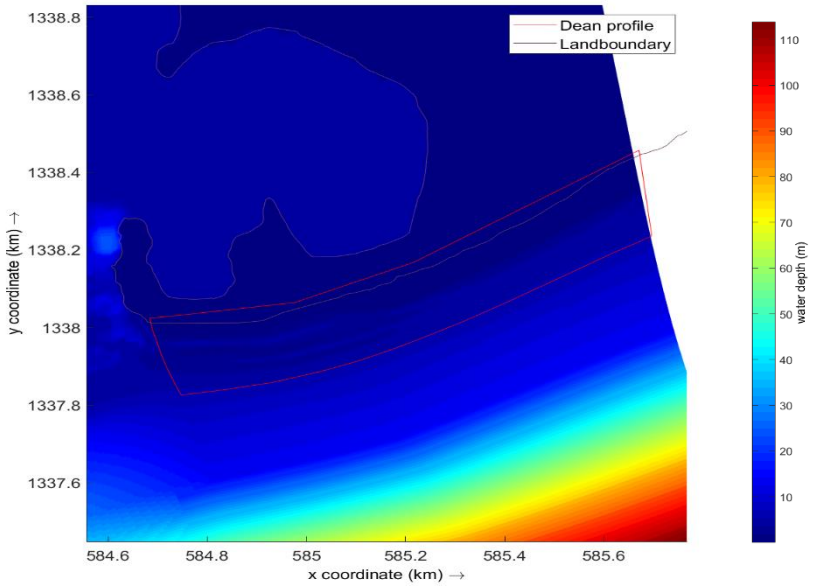

Figure 24, Manually generating a bathymetry by implementing the Dean profile and iteratively approach the morphologic active profile

4.5. Vegetation modelling

Historical aerial pictures of the area show that the mangrove fringe along the entrance road between the main land and the beach of Lac Cai was more extensive. In order to analyze the correlation between the mortality of the mangrove fringe and the beach erosion, a comparison is made between the erosion rates in the historic situation, the current situation and in a situation without any mangroves.

The different mangrove fringe scenarios are added to the model by the three different types of vegetation modelling as described in section 2.2.2. The first method is increasing the bed shear stress, the second method is making use of trachytopes and the third method is introducing the mangroves as rigid rods into the model.

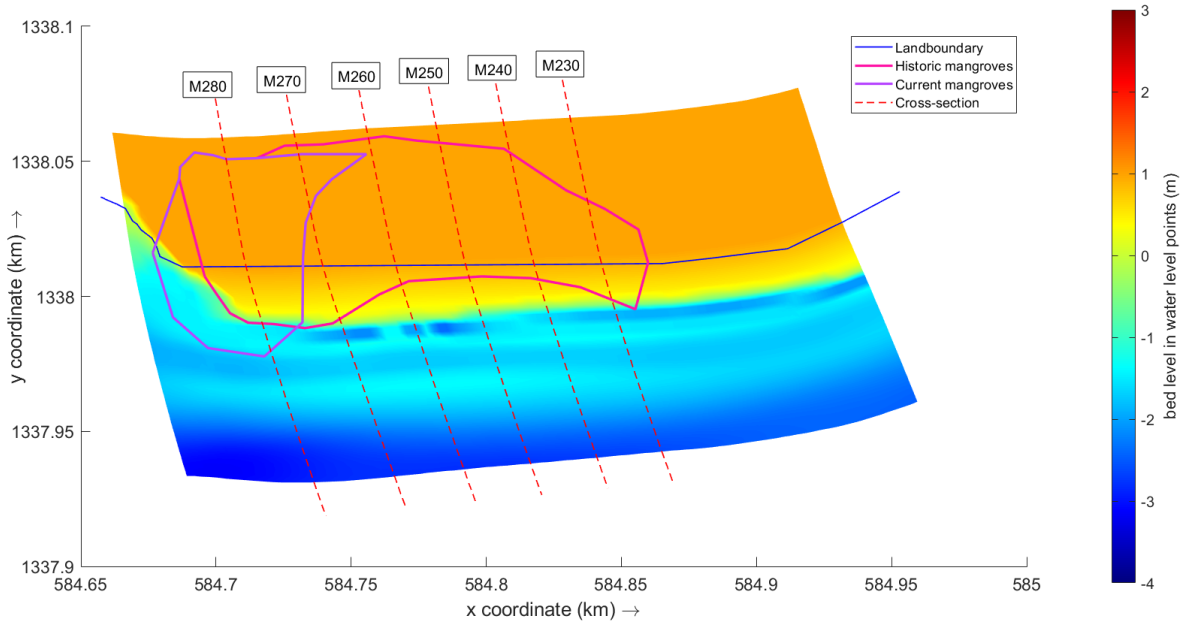

Figure 25, Current- and historic mangrove fringes and cross-sections

The three different scenarios are introduced to modelling outcomes of the sensitivity analysis from the previous chapter. In Figure 25, the contours of historic and current fringes are shown on top of the output bathymetry of prior simulations, which served as input for the new model. From this figure it is visible that the coastline still follows the straight perpendicular shape of the ldb-line but the profiles already show some deviations. The analyses will compare the impact of the different vegetation-modelling methods and the different shapes of the mangrove fringes on the erosion progress. In order to perform these analyses, five cross-sections are added to the model. The cross-sections cover the gridlines 230, 240, 250, 260, 270 and 280 as plotted in Figure 25.

For the first method, the Chézy friction coefficient reduction due to the vegetation-induced bed roughness is derived from the Manning formula. The representative Manning's roughness coefficient for mangroves was retrieved from the modelling data of Horstman (2015) and set at 0.030 ($s/m^{1/3}$) and the averaged depth at the 1m. For the mangrove vegetation within this model, the bottom roughness coefficients are reduced from 65 to 40 in the area of the mangrove fringes.

The parameters for the trachytopes method and the DPM are also retrieved from the paper of Horstman (2015) and based on the mangrove species *Rhizophora,* which appears to be the species at Cai beach (Hummelinck and Roos, 1963). The retrieved vegetation characteristics are presented in Table 4. The mangrove is considered unsaturated and therefor the vegetation height is set equal to the water depth for the trachytopes method. The remaining input parameters for this method are based on the averaged characteristics from Table 4 together with the reference Chézy friction coefficient of 65.

Table 4, Vegetation characteristics for Rhizophora mangroves (Horstman, 2015)

Height	Stem diameter (D)	Vegetation density (n)	Drag coefficient (C_D)
0.00	0.026	342	2.0
0.10	0.026	342	2.0
0.50	0.031	100	2.0
1.00	0.045	21	2.0
2.00	0.155	2	2.0

Analyzing the cross sectional coastal profiles creates insights in the effect of the various vegetation modelling types. Quantifying the coastal retreat in both X- and Y-direction can be translated into the total retreat per cross-section. Figure 25 visualizes the simulated coastal retreat in both directions for the rigid rod model where both plots show the cross-section along the M280 gridline, which is the cross-section intersecting the current mangrove fringe. The comparison between the both plots show the main retreat is occurring in the Y-direction. This makes sense since the grid is formed curvilinear along the coast.

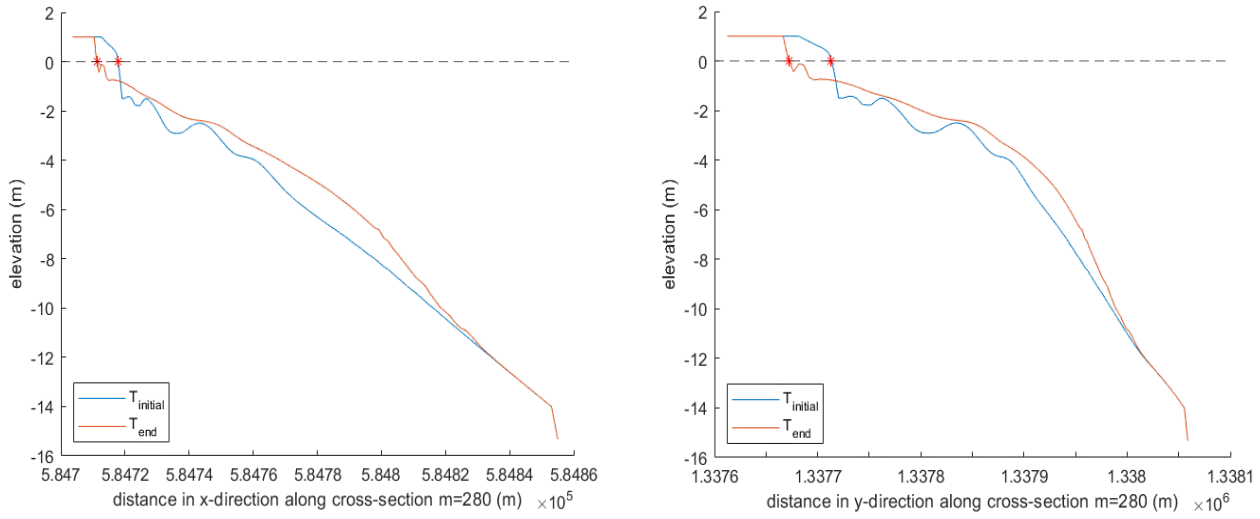

Figure 26, Cross sections in X- and Y-direction showing the total coastal retreat, simulated with the rigid rod method over 10 years

The coastal retreat at the different cross-sections are given in Table 5 and Table 6. The results are taken at timestep t=97 because some models were interrupted preliminary. This still covers a morphological running time of 8 years which is considered sufficient. In the first table, the model results of the current mangrove fringe are given.

Table 5, Coastal retreat in m of different vegetation modelling approaches for the cross-sections in current mangrove fringe

Vegetation model	M230	M240	M250	M260	M270	M280
Bed shear stress	28.743	28.855	25.509	33.504	36.535	30.377
Trachytopes	28.741	28.889	25.575	31.238	34.891	37.581
3D	28.751	29.049	25.561	33.453	34.345	38.771
No mangroves	28.739	28.879	25.586	33.486	39.162	39.976

Table 6, Coastal retreat in m of different vegetation modelling approaches for the cross-sections in historic mangrove fringe

Vegetation model	M230	M240	M250	M260	M270	M280
Bed shear stress	17.052	24.377	25.532	28.840	25.211	30.374
Trachytopes	28.746	28.975	25.540	29.688	34.699	39.927
3D	25.761	28.623	25.548	33.745	35.622	39.892
No mangroves	28.739	28.879	25.586	33.486	39.161	39.976

The effect of the different methods is clearly reflected in Table 6 by the deviations in coastal retreat at cross-section M270. This cross section intersects the historic mangrove fringe at a point where the fringe is stretched towards the sea. The coastal retreat along this cross-section has decreased from 39.2m in the model without mangroves to a 25.2m retreat in the model with an increased bed shear stress. This implies that the implementation of the mangrove fringe results in the desired effect but this is barely substantiated by the coastal retreat in of the other cross-section.

Looking at the sediment balance creates better insights into the effect of the different models by showing the amount of sediment volumes flowing in and out of the model area. The total cumulative volume and separate erosion/sedimentation volumes for the different vegetation modelling approaches of the historic fringe are schematized in Figure 27. From this figure it can be seen that the sedimentation rates in the different models stay quite similar while the erosion rates show more variation between the models. The highest erosion rates are occurring in the model without any vegetation representation. Logically, an unerodable fringe show the lowest erosion rates. The three vegetation models show a gradual difference in erosion rates where the bed shear stress simulates the less-, and the rigid rod model show the most erosion.

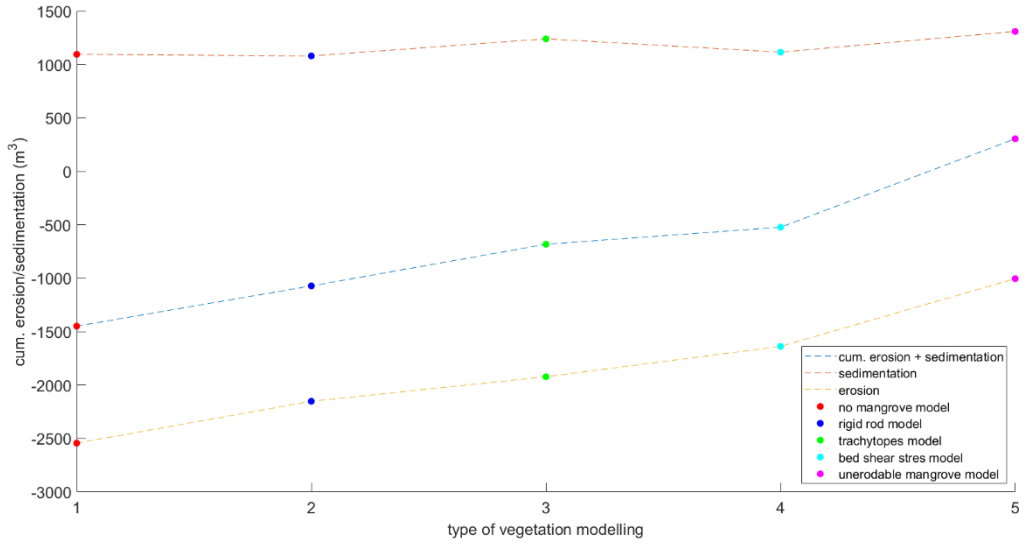

Figure 27, Total cumulative erosion and sedimention volumes for 5 different mangrove models

The sediment balance shows that modelling method 1, where an increased bed roughness was applied to the mangrove area, retains the most sediment in the system. Therefor it is considered the most effective method to simulate the vegetation-induced reduction of coastal erosion. Since this method is not overestimating the impact of the vegetation, it will be applied in for the modelling of the mitigation alternatives.

Nevertheless, the reduction of the Chézy friction factor to 40 instead of 65 still results in significant erosion and coastal retreat. The erosion rates might still be the result of the model adjusting towards an equilibrium profile. In Figure 28 the modelling results of the vegetation-induced bed roughness are given which shows that the coastal profile is transforming. The bathymetry will be used as input for the modelling of the mitigation alternatives.

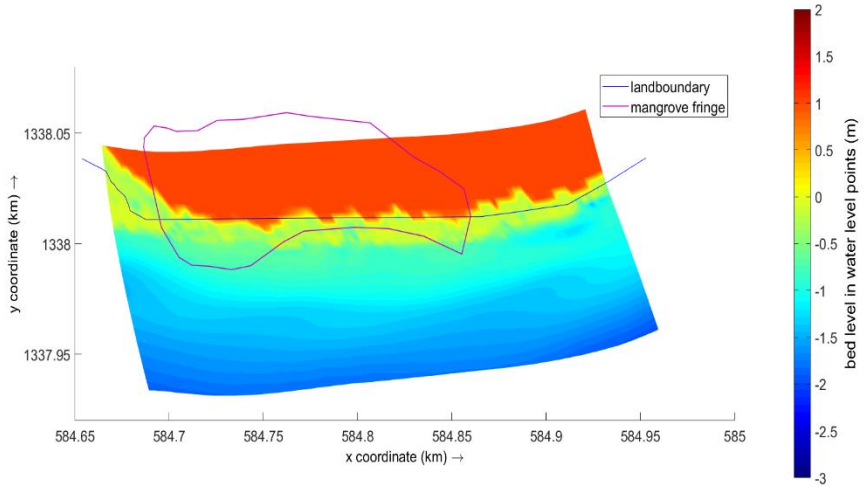

Figure 28, Bed level in water level points for the vegetation-induced historic mangroves after 10 morphological years

5. Mitigation measures

In order to counter the erosive trend in front of Lac Cai, an assessment on five different mitigation measures will be conducted. The effectiveness of the five alternative measures are checked by the model simulating 10 years of coastal evolution. The result is then used as input for the assessment of the MCA in chapter 7.

First of all, an analysis is conducted on the sediment balance (cumulative erosion / sedimentation) within the area in front of the entrance road. The grid is set to limit the results in the area along the LDB of the entrance road to Cai Beach and stretch a few kilometers into the sea. The map files of the cumulative erosion and/or sedimentation, at the last timestep of simulation, are given for each alternative in the following sections (e.g. Figure 29, Figure 33 and Figure 38).

The area is further specified into a narrow stroke along the LDB in order to concentrate more on the coastline and compare the cross-shore and long-shore sediment movement. The narrowed area is specified as section 2 in the map files. Also, the alternative structures are indicated as well as the land boundary. Since the initial erosion is zero for all the different models, the comparison between these map files indicate the locations where erosive behavior plays a role and what areas show sedimentation.

Furthermore, the sediment balance is visualized over time in order to analyze the erosive patterns at the end of every wave condition. This gives insights in the correlation between wave conditions and erosion rates as well as an overall trend in erosion/sedimentation over the duration of 10 years.

5.1. Alternative 1: No measure

The first alternative which will be introduced into the MCA will be the 'zero' situation scenario, the scenario which serves as reference point to value the impact of the other mitigation measures. No measurements will be implemented and the erosion will continue to cause for coastal retreat. In this alternative it is likely that, over time, Lac Cai is being separated from the mainland.

The cumulative erosion/sedimentation after a morphological simulation of 10 years is shown in Figure 29. The area is zoomed in on the area of interest, the coastline in front of the entrance road to Lac Cai beach. Figure 29 shows that the erosion is particularly occurring in the western part of the coast. The occurrence of erosion rates in this part corresponds with the data analysis of the coastline retreat from the historical satellite images (see section 3.1.3.). These historical images, see Figure 2, showed the forced deconstruction of one of the building at Lac Cai between the years 2002 and 2007 due to this erosion.

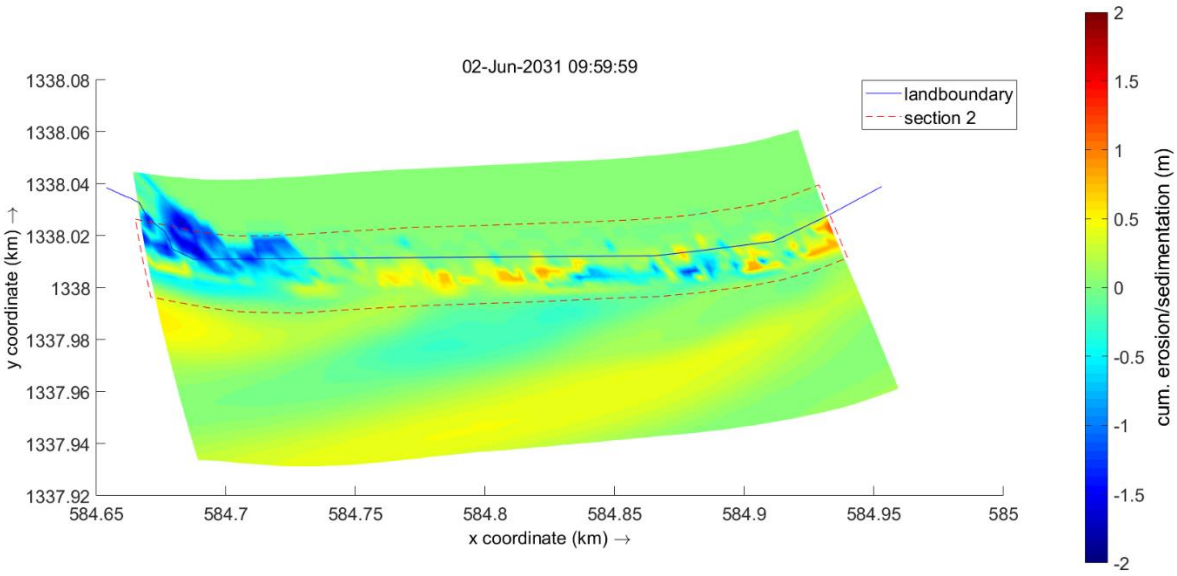

Figure 29, Map file of the cum. erosion/sedimentation at t=122 for the reference model without any measure

However, the model is build as an analogue to reality in order see if the erosive patterns correspond to the observed coastal retreat. This means that the actual coastline of 2002 was adjusted into a straight coastline with the goal to hindcast the origin of the cove in front of the coast. The results of the vegetation models in the previous chapter, showed erosive activity in front of the coast but this trend has diminished in the current model and erosion is hardly present in this area. In an attempt to shift the perceived erosion from the western corner more towards the center of the coastline, the available sediment thickness is reduced to 2 m from 5 m in the corner of the coast. This adjustment can be substantiated by the current presence of a small mangrove fringe in this area and also taken into the subsequent models of the other alternatives.

As the map file in Figure 29 shows, the result of these adjustments did not have the desired effect. The eroded sediment from the end of the spit is moving through the channel between the coral dam and the coast into Lac Bay. This happens outside of the domain displayed in Figure 29, on the left side domain.

However, the cumulative erosion/sedimentation over time shows the erosive trend in the zone in front of the coast. Figure 31 shows the total sediment volumes of the entire grid whereas Figure 30 only shows the volumes within section 2. This distinction makes it possible to compare the cross-shore and long-shore sediment movement within the area. Although the area of Figure 30 is more than three times the size of section 2, the volumes in the graph are not significantly larger than the volumes in Figure 31. This shows that most of the sediment activity is occurring around the coastline and LST rates having more impact than cross shore movement.

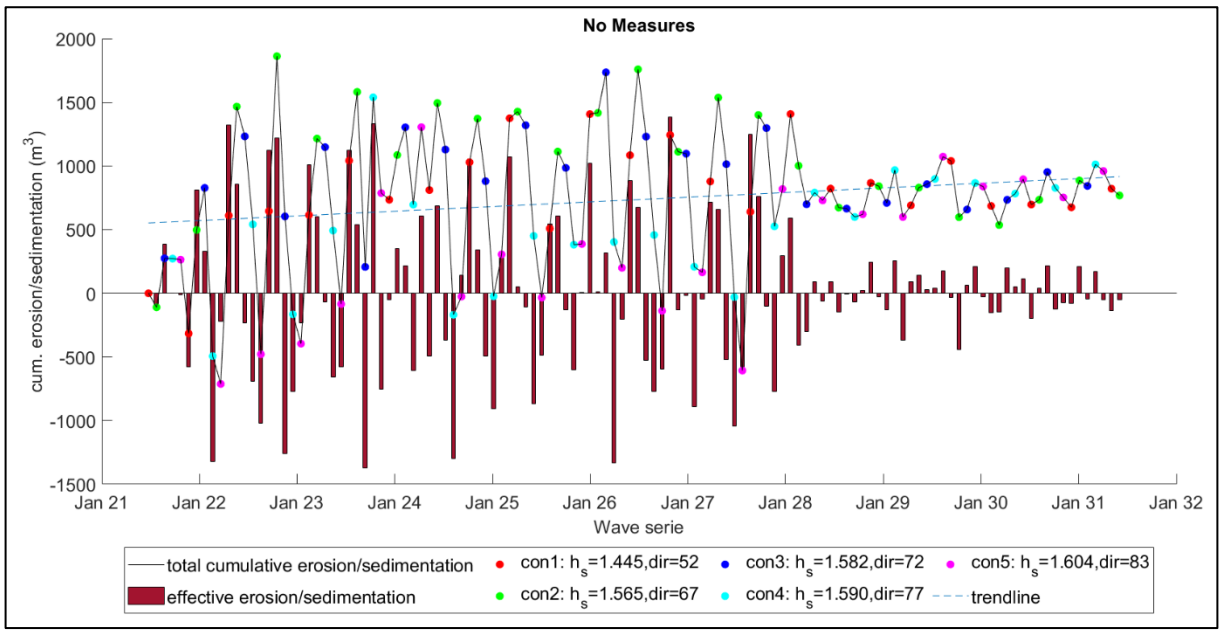

Figure 30, Cum. erosion/sedimentation of entire area for the reference model without any measure

Nevertheless, the trend in both graphs is showing a different pattern. Where the cumulative sediment volumes in the entire area are slightly increasing over time, the graph of section 2 is showing an erosive trend. This observed erosive trend along the coast corresponds with the expectations. Only the location of this erosion is shifted towards the corner of Cai Beach instead of in front of the entrance road (Figure 28).

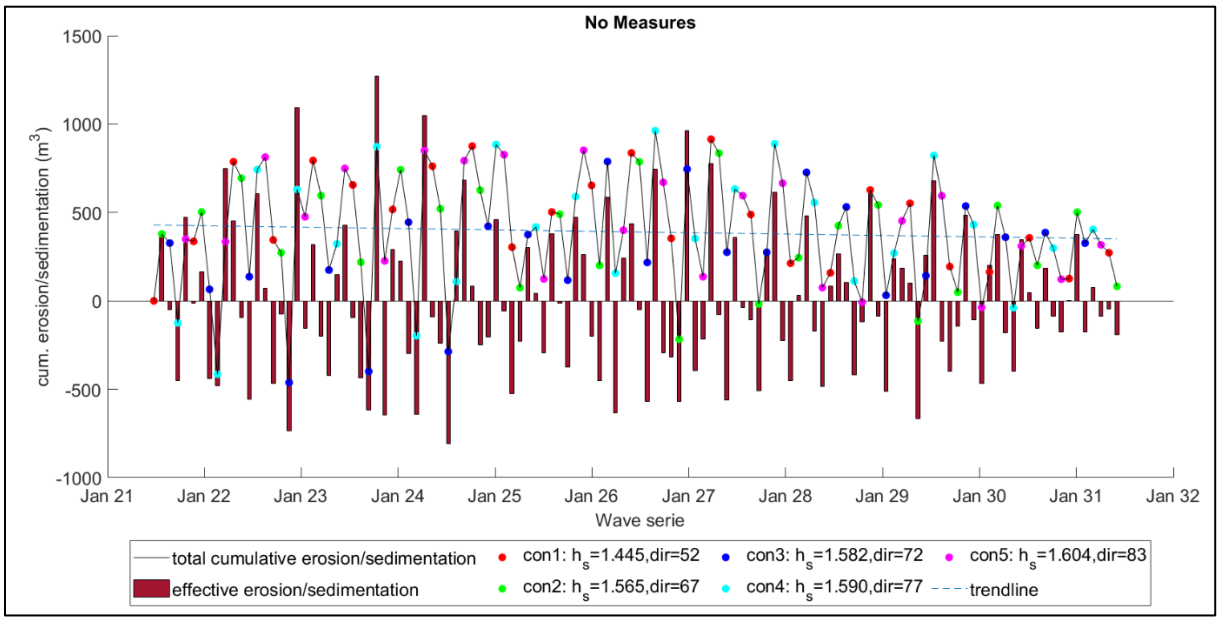

Figure 31, Cum. erosion/sedimentation of section 2 for the reference model without any measure

5.2. Alternative 2: Breakwater

The next alternative design which will be investigated is the construction of a breakwater at the North side of the beach and parallel to the coast. This alternative is based on the measure completed in June 2019, where a rock formation was dumped in front of the coast.

The breakwater was constructed to act as wave barrier, allowing the beach to grow while preventing further erosion. As waves hit the breakwater, they deposit their load of sediment along it. In practice, the erosion in front of the entrance road continued. Another aspect of the breakwater is the continuation of erosion in the areas of the coast which are not protected by the breakwater. This leaves the Western part of the coast unprotected.

The constructed rock-structure which should serve as breakwater is evaluated in terms of effectivity because the ought purpose of minimizing further erosion was not observed. The result of the model could show opportunities for improvement of the current construction, such as expending in length or width. Figure 32 shows the areal overview and an sight impression of the current situation.

Figure 32, Aerial overview (Google Earth) (left) and photo on sight (right) of the current situation at Lac Cai were a pile of rocks is deposited perpendicular to the coast in the form of a breakwater

In order to analyze this problem, the breakwater was included into the model. The breakwater is modelled as a non erodible layer by applying a spatial varying sediment layer thickness. The breakwater is modelled with a height of 1 meter above MSL which allows the waves to flow over the structure, resulting in an overtopping volume. The simulation continued for approximately 8.5 years (8 years and 153 days). The results however are considered sufficient since the patterns concerning the erosion rates already give enough insights to draw adequate conclusions.

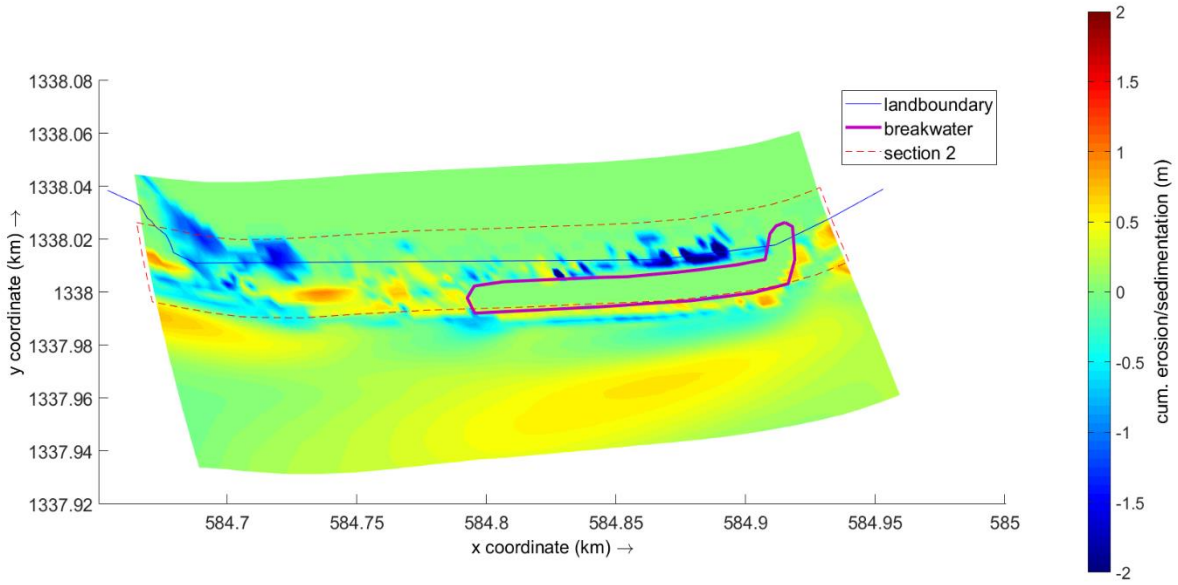

Figure 33, Map file of the cum. erosion/sedimentation at t=103 for the modelled breakwater alternative

Figure 33 shows the location of the breakwater and the cumulative erosion in meters after 8.5 years. The blue areas behind the breakwater and in the western corner of the beach are the two locations where erosion is occurring. The erosion in the corner was already present in the model without any erosive counter measure but improvement of this area is barely noticeable. The erosion behind the breakwater could not be observed in the reference model which means it has arisen due to the construction. This can be explained due to blocking of the bed load transport induced by the breakwater. Therefor the sediment supply is diminished whereas erosion rates could still be caused due to overtopping or high water levels behind the breakwater.

The cumulative inflow- and outflow volume of sediment in the entire area, as well as the specified section 2 area, is visualized over the period of 8.5 years in the Figure 34 and Figure 35. In Figure 34, the erosion patterns over the entire area creates insights in the sediment balance in front of the coast. This includes the depths up to six meters. The trendline in Figure 34 shows no decrease in sediment volume over the entire period. There even is a slight sedimentation trend. The bigger part of these volumes however, settle in the more deeper parts. This correspond with the cumulative sedimentation parts as can be seen in Figure 33.

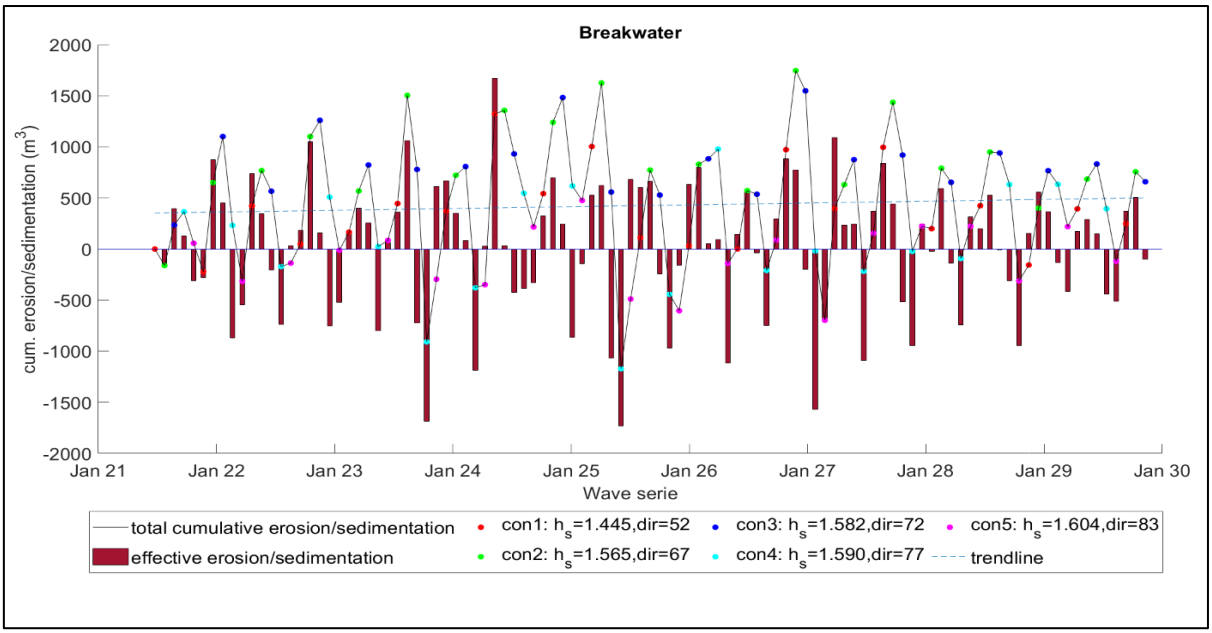

Figure 34, Cum. erosion/sedimentation of entire area for the modelled groyne alternative

In Figure 35, the erosion patterns are focussed on the area around the land boundary. Looking more closely at the sediment volumes around the beach, the trend is erosive. The comparrison between both Figure 34 and Figure 35 shows that the sedimentation is mainly occuring in the deeper parts in front of the coast and the erosion is still occuring at coastline.

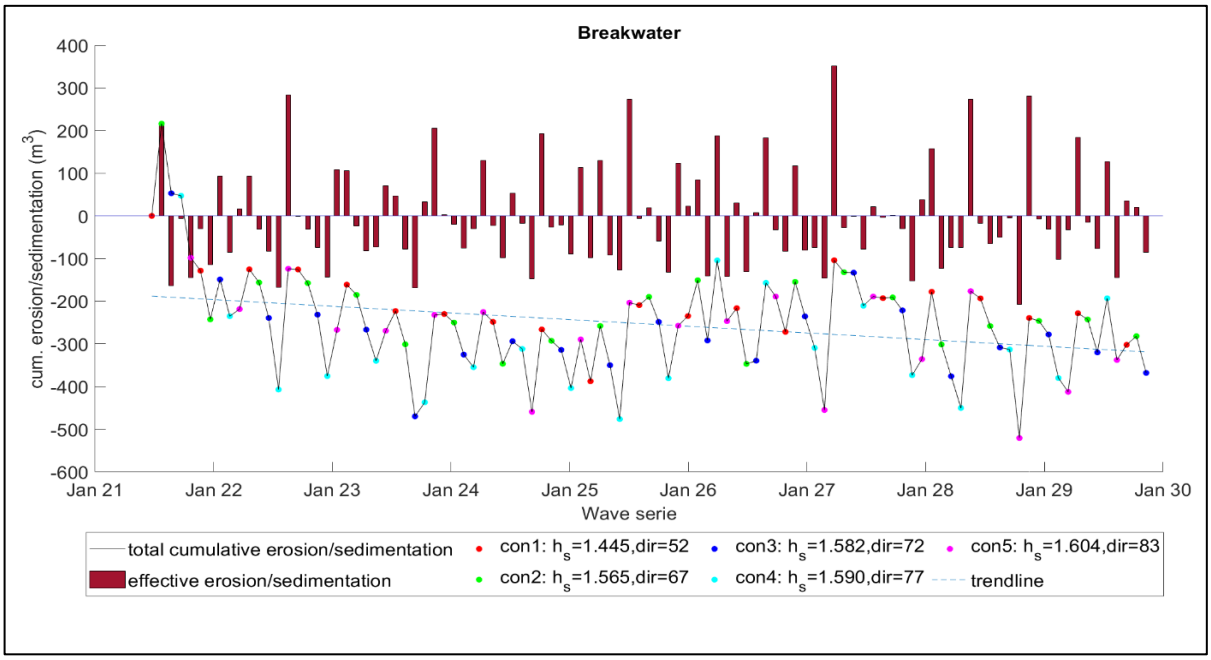

Figure 35, Cum. erosion/sedimentation of section2 for the modelled breakwater alternative

5.3. Alternative 3: Groyne

Another hard solution which is studied in this MCA is the construction of a groin at the southside of the beach perpendicular to the coast. Because the channel between the coral ridge and Lac Cai functions as a sediment sink, the eroded sediment is moving inside the bay. This groin will prevent the sand for flushing away and lead to accumulation of sand in front of the coast. Figure 36 shows an example of such a measure taken in Wakatiti, Hawai. Dimensions are approximately 50 meters long with a width of 10 meters.

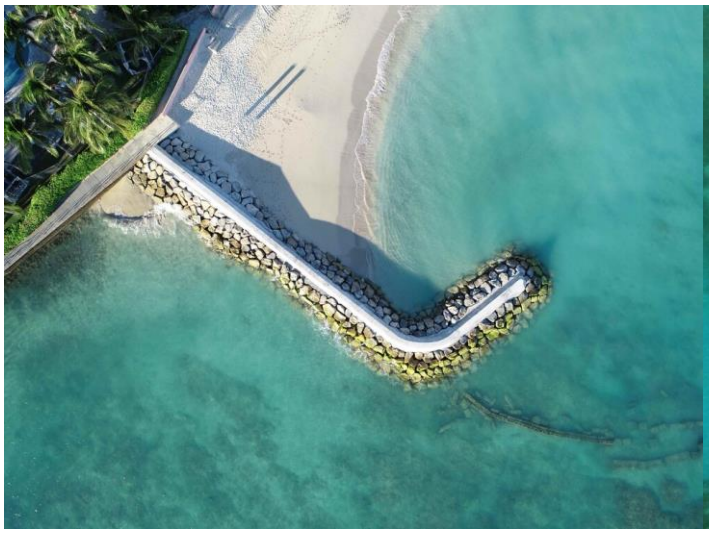

Figure 36, Example of the Royal Hawaiian in Wakatiti, Hawai (Waikīkī Beach Special Improvement District Association, 2020)

Figure 37, Schematic overview of a groin at the south side of the beach at Lac Cai (Google Earth)

The groyne is added to the model in the same way as the previous breakwater. The structure has a height of 1 meter above MSL and is made unerodable. Also the sediment thickness at the location of the current mangrove fringe is decreased to 2m. The groyne is built 40 meters in to the sea with a small widening at the top and reaches till a water depth of 1.3 meters.

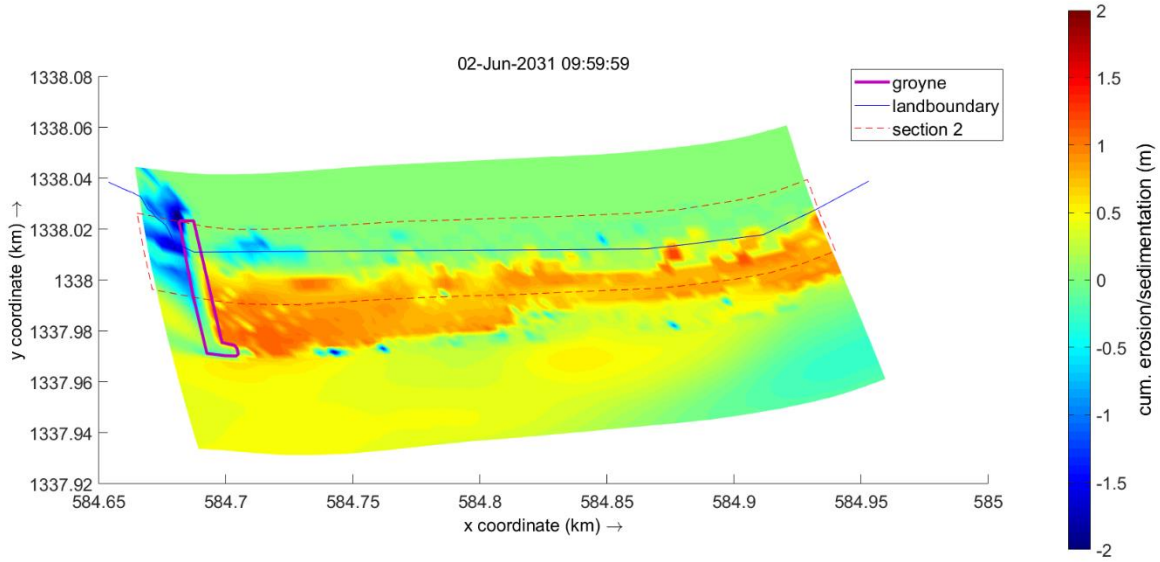

Figure 38, Map file of the cum. erosion/sedimentation at t=122 of the modelled groyne alternative

The erosion patterns of the entire area in front of the coast and the area around the coastline, section 2, are given in Figure 39 and Figure 40. Both graphs show a sedimentation trend. In other words, there is more sediment settling in front of the coast than eroding. From the map shown in Figure 38 it becomes visible that sediment is depositing along the entire coast except for the area straight behind the groyne. Here the erosion has intensified. Despite this erosion, the overall trend in the area is sedimentative.

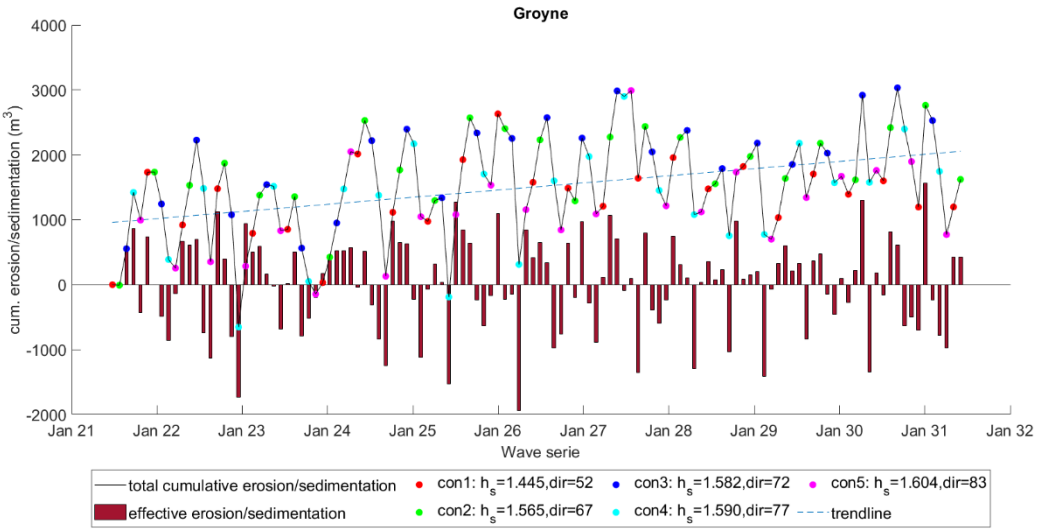

Figure 39, Cum. erosion/sedimentation of entire area for the modelled groyne alternative

The trendline over the cumulative sedimentation in section 2 shows less sediment deposition but still has a positive slope. The flattening of the trendline can be explained by the strongly increased erosion behind the groyne. The impact of this erosion has bigger influence on the total cumulative volume in section 2.

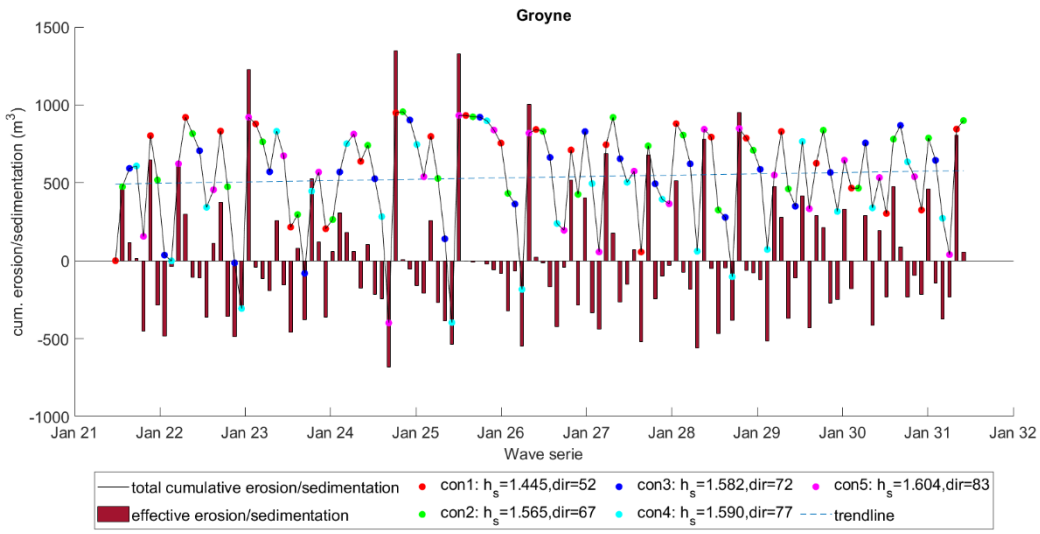

Figure 40, Cum. erosion/sedimentation of section2 for the modelled groyne alternative

5.4. Alternative 4: Mangrove restoration

The impact of the loss of mangrove fringes was already investigated earlier in this thesis project (section 4.5) and prove was given for the correlation between mangrove loss and the erosion. The research conducted by Erdmann & Scheffers (2006) manifested mangrove deforestation between the years 1961-1996. This can be confirmed by analyzing the aerial pictures from these years and compare them with the current situation of the mangrove fringe, see Figure 41. In this alternative, the possibility and effectiveness of the restoration of this mangrove fringe towards its original state (1961) is investigated.

Figure 41, Historical areal picture of Lac Cai showing the original state (1961) of the mangrove fringe

The mangroves are introduced as increased bed shear stress into the model. The methods of introducing vegetation to the model are discussed in chapter 5. Since the different methods did not have an significant effect to the outcome concerning the erosion rates, the most simple method of introducing vegetation is used. The bottom roughness is adjusted by reducing the Chézy friction coefficient from 65 to 40 in the area of the mangrove fringes.

Due to the uncertainty of the bathymetry and the lack of actual bathymetry data, the bathymetry of the alternative measures models was retrieved from the model results of the previous chapters. This alternative is based on the restoration of mangrove fringe to its original state. However, the restoration of the original mangrove fringe is not reaching deep into the sea in this model. Therefor the results on impact of the measure could be indistinct. To clearly see the impact of the wave attenuating- and sediment trapping values of the mangrove restoration, a second model with a wider fringe is simulated as well. Both fringes are shown in the map files in Figure 42 and Figure 43.

Figure 42 and Figure 43 give an overview of the cumulative erosion/sedimentation after a morphological running time of 10 years for both mangrove restoration scenarios. In these figures it can be seen that the introduction of both mangrove fringes causes for sedimentation along the coast. Furthermore, by comparing the cumulative erosion/sedimentation volumes of the two different mangrove fringes it becomes clear that the wave damping effect of a wider fringe is higher. Inside the curved land boundary in Western corner of the beach, both the figures show erosion after 10 years of simulation. With the smaller stroke of plants, the intensity of erosion is comparable to the reference model while the erosion rates in Figure 43 are considerable less extensive.

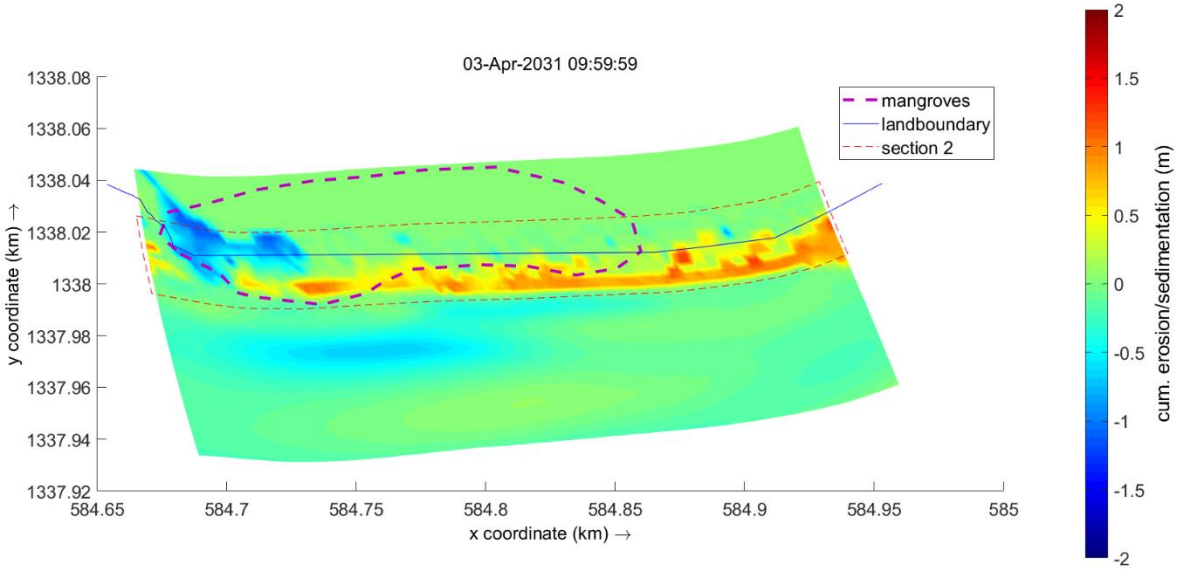

Figure 42, Map file of the cum. erosion/sedimentation at t=120 of the modelled mangrove restauration to its original state

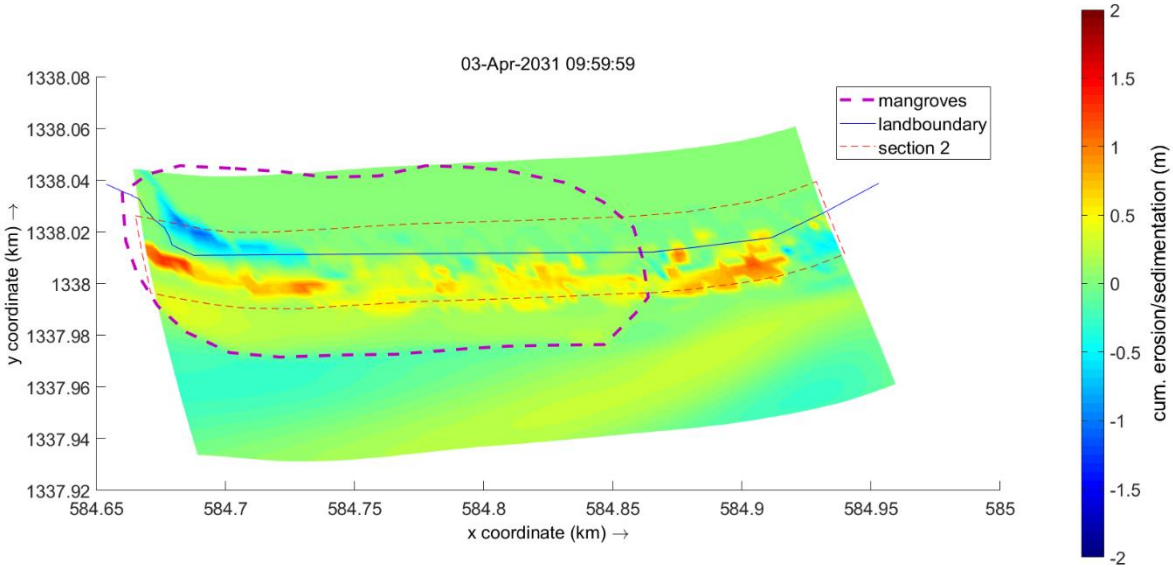

Figure 43, Map file of the cum. erosion/sedimentation at t=120 of the modelled extended mangrove restauration

Based on the comparison between the cumulative erosion map files of both models, it can be concluded that a more extensive mangrove restauration towards the sea has a positive effect on the erosion in the area. The wider mangrove fringe shows a decrease in erosion while sediment is settling along the coast. However, in total cumulative volumes, the both models do not differ significantly because the model with a smaller fringe shows slightly higher sedimentation rates along the coast. In this case, the erosion reduction is considered of more importance and therefor the model results of the wider mangrove fringe is further elaborated.

The cumulative erosion/sedimentation charts in Figure 45 and Figure 46 show similar trends and also the total volumes do not differ much from each other. This confirms that most of the sediment activity occurs around the coastline. The trendlines show an overall increase of sediment supply.

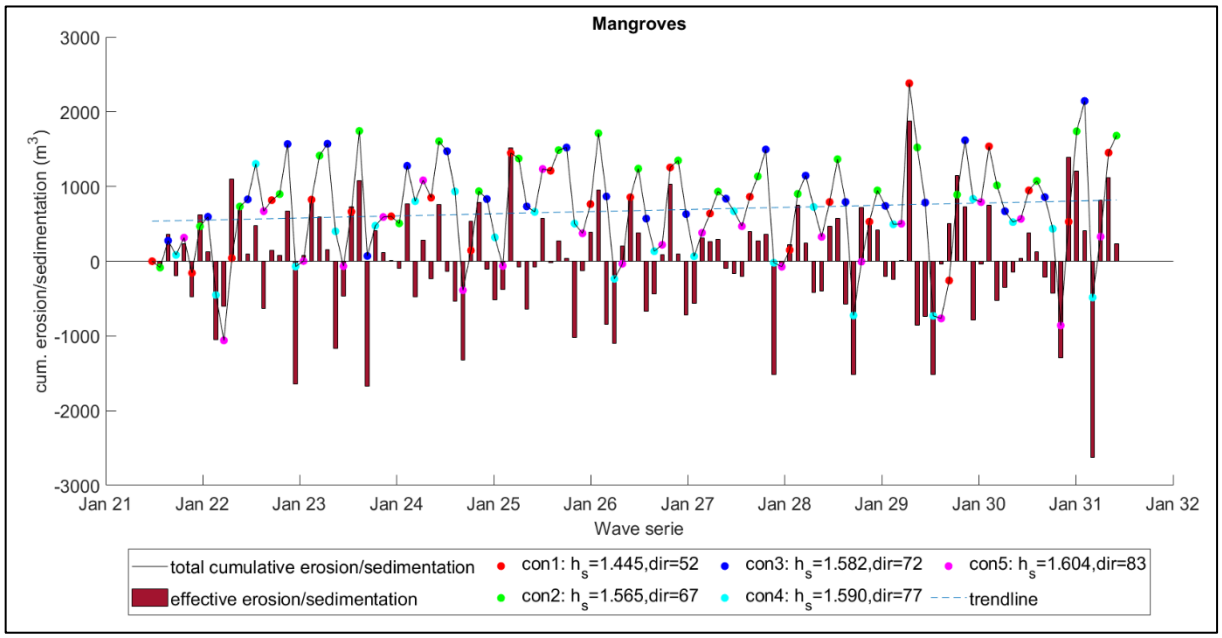

Figure 45, Cum. erosion/sedimentation of the entire area for the extended mangrove fringe model

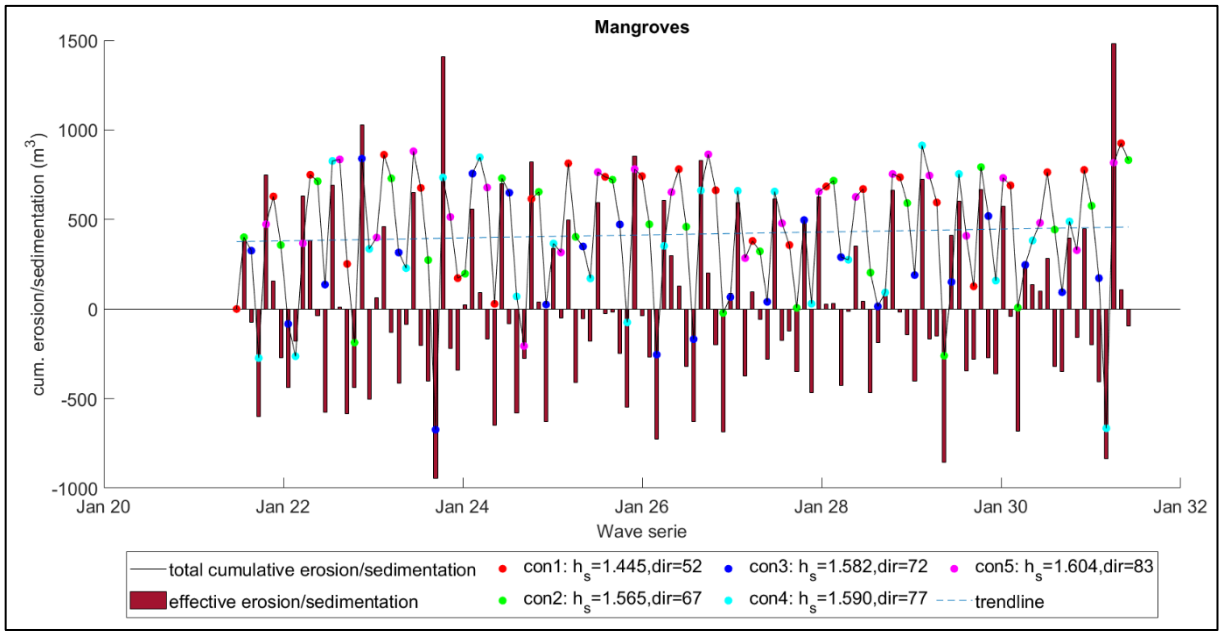

Figure 44, Cum. erosion/sedimentation of section2 for the extended mangrove fringe model

5.5. Alternative 5: Seagrass

The last alternative measure to mitigate the coastal retreat at Lac Cai is the introduction of a seagrass meadow. This 'Building with Nature' solution using the establishment of sea grass in front of the coast will have wave attenuating function and cause for vegetation induced drag forces (James et al., 2020). A suitable native species which also occurs inside of the bay is *Thalassia testudinum* (turtle grass) which has good wave damping characteristics due to its species large leaves.

The seagrass is introduced to the model in the same way as the mangroves in the previous section, by increasing the bed shear stress. The reduction of the Chézy friction coefficient is retrieved from the Stickler-Mannings formula (4) with a Manning's roughness coefficient of 0.03 (Chow, 1959) and an averaged depth of 1m. This results in a reduction of the Chézy friction coefficient from 65 to 33 $m^{½}/s$:

$$\frac{1^{1/6}}{0.03} = 33.3\, m^{\frac{1}{2}}/s$$

This reduction accounts for the flow- and wave attenuating characteristics of seagrass in combination with their ability to trap and stabilize sediments. This value is however equivalent to a fully grown, healthy seagrass meadow. The implemented seagrass meadow has a width of approximately 60 meters along the entire coastline and reaches until a depth of 1.5m.

The reduction of the Chézy friction coefficient creates an increase in bed shear stress which surpasses the bed shear stress of the modelled mangroves in the previous section. Besides, the seagrass meadow is simulated as large patch in front of the coast.

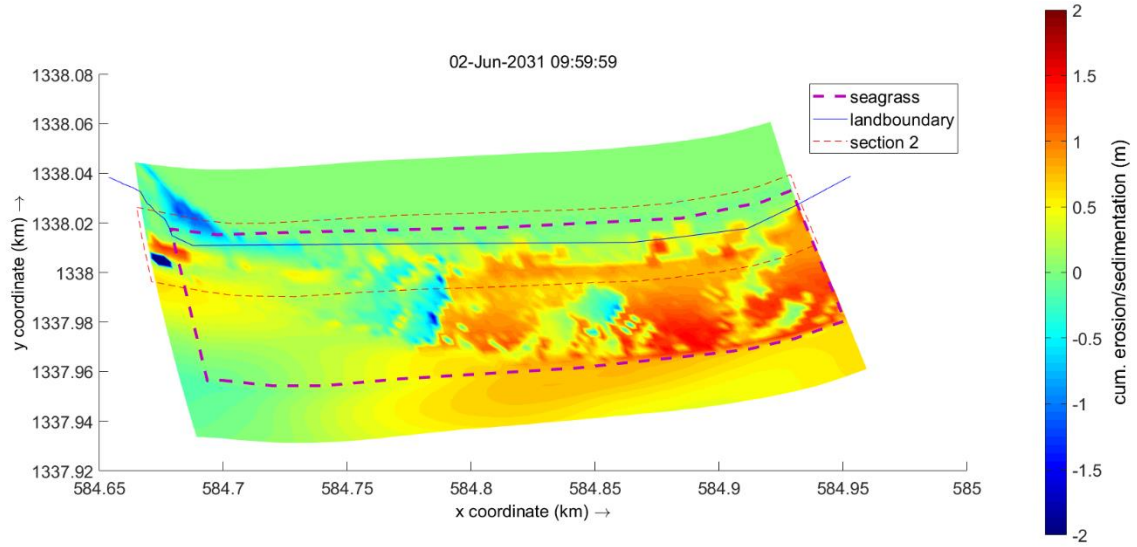

Figure 46, Map file of the cum. erosion/sedimentation at t=122 of the modelled seagrass implementation

The cumulative erosion and sedimentation zones due to the implementation of the seagrass are depicted in Figure 46. From this figure the it is clearly visible that the implementation of seagrass has a positive effect on the sedimentation in front of the coast. This effect is both occurring close to the coastline as well as in the deeper parts but is mainly observed at the right side of the grid. The high withdrawal of sediment in the right part of the seagrass meadow is sheltering the remaining part. Also because of this block in sediment supply, there is still erosion occurring in the Western corner.

In Figure 47 and Figure 48 the cumulative erosion and sedimentation volumes are given over the morphological time period of 10 years. The large increase in bed shear stress to schematize an adult seagrass meadow, creates an instant peak value in the sediment balance after the first wave conditions. The reason for this peak could be the overestimation of the Mannings roughness coefficient which consequently leads in a too low Chézy-coefficient. Furthermore, the expansion of the seagrass meadow is stretched along the entire length of the coast and is multiple km wide. The model needs to adjust to this instant sediment sink of this large patch. After this initial deposition, the sediment volumes continue to increase over the entire area but along the coast the trend shows decay.

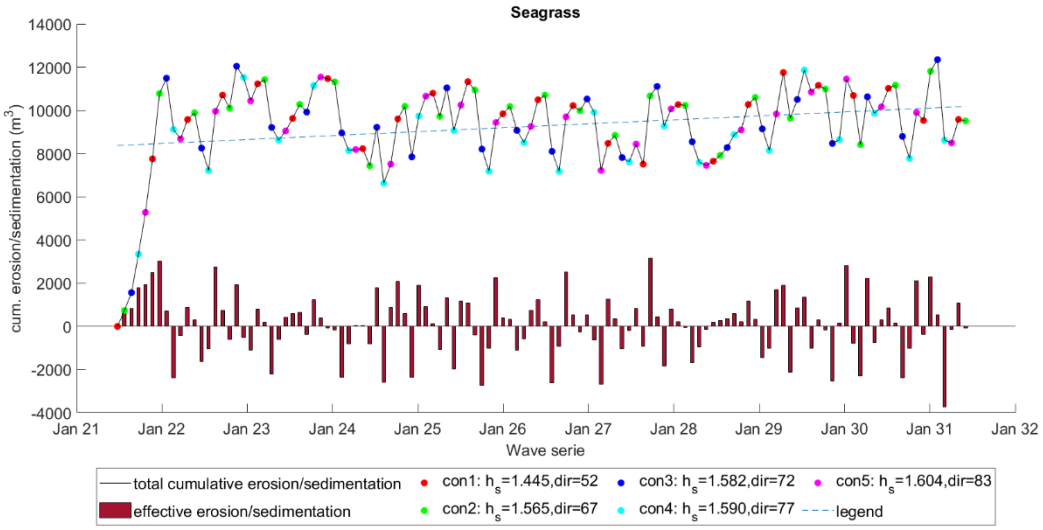

Figure 47, Cum. erosion/sedimentation of section2 for the seagrass model

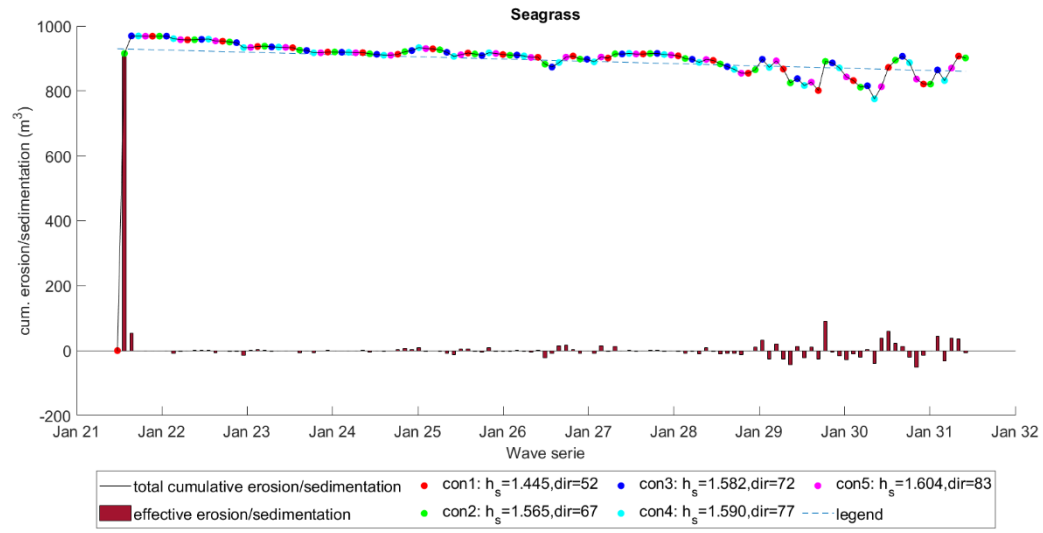

Figure 48, Cum. erosion/sedimentation of section2 for the extended mangrove fringe model

5.6. Conclusion

Five different alternatives are investigated by model in order to come up with an alternative measures against the coastal retreat at Lac Cai. The first alternative serves as reference model and shows that the erosion is mainly occurring at the Western corner of the coastline. This erosion is in a certain degree also visible in the results of the simulation of the other alternatives. From the comparison between the reference model and the breakwater from the second alternative, the decrease in erosion is hardly notable. Remarkable to notice is the erosion direct behind the breakwater. This erosion has arisen due to the construction and in contrast to the situation without any measure. The cumulative sediment volumes over time show an erosive trend along the coast. This could be explained due to the fact that the supply in sediment is blocked by the breakwater while high water levels behind the breakwater still flush away sand towards the lagoon.

The construction of a groyne at the Western corner of the coast results in the increase in sedimentation in front of the coast. However, the coast behind the groyne is still experiencing a continuation of erosion. Overall, the general trend of the cumulative volumes is showing sedimentation into the area as well as along the coast.

In order to create a better insight into the effect of mangrove restauration, a distinction between two models is made. The first model is based on the restoration of mangrove fringe to its original state and the second model includes a wider mangrove fringe which is expanded more towards the sea. The impact of the small mangrove fringe becomes already visible by the sedimentation in the adjacent areas along the coast. The erosion at the Western corner is still occurring. This is diminished in the model with a wider fringe.

The last alternative measure is the implementation of a seagrass meadow in front of the coast. This meadow is implemented by increasing the bed shear stress. The Chézy friction coefficient is decreased from 65 to 33 which is based on healthy, fully grown seagrass. The abrupt increase of the bed shear stress causes for an instant peak of sedimentation after the first wave condition. After this peak, the cumulative volumes show a slight erosive trend. Despite the slight decline in sediment volume, the cumulative sedimentation in the area remains more than twice as big as the volumes in the reference situation without any measure. This applies in smaller extent also to the reference alternative which explains the contradictions in trendline and sediment balance in Table 7.

Table 7, Trendlines and absolute volumes of cumulative erosion/sedimentation in section 2 (M195:295;N180:190)

	No measure	**Breakwater**	**Groyne**	**Mangroves**	**Seagrass**
Trendline (m3/y)	**-0.639**	**-1.072**	**0.705**	**0.672**	**-0.572**
Cum. volume at the end of simulation (m3)	**351**	**-319**	**578**	**458**	**860**

Table 7 shows the absolute cumulative volumes in section 2 after a morphological running time of 10 years as well as the overall trend during the simulation. The analyses of the model results show the positive impact of the construction of a groyne which is in absolute numbers the most effective measure. The sedimentation in front of the coast is constantly growing over the years and the total cumulative erosion is positive. Only seagrass has a larger volume after 10 years simulation but the trend shows decay. Mangrove restoration also has a positive effect on the erosion at Lac Cai.

Both the breakwater construction as the reference model without any measure show an erosive trend over time which is in agreement with the expectations. However, for the reference model the erosion is less and at a different location than expected which impacts the reliability of the model. The comparison between the different alternatives create insights in the effect of the measurements but does not forecast the exact coastal evolution after implementation.

6. Multi criteria analysis

In order to find a fitting solution against the beach erosion at Lac Cai, a multicriteria analysis is conducted in which the five alternative measures are scored against five different criteria. The purpose of the participatory MCA is to involve the different stakeholders, investigate the different visions and combine the knowledge of varying disciplines to evaluate strategic alternative on criteria as feasibility, acceptability and sustainability (Barquet & Cumiskey, 2018). For the sake of this study, the number of recipients was limited to 6 experts with diverse expertise related to coastal engineering.

The following criteria will be used to assess and prioritize the proposed alternatives in a comprehensive way:

- Impact on hazard reduction
- Cost
- Environmental impact
- Local acceptability
- Local feasibility

The criteria will be further specified by clear sub-criteria or indicators. Each criterion is weighted by the experts with a value ranging from 1 to 5 to indicate the importance and priorities for all criteria. The criterion which is considered the most important will be weighted with 5 points and the least with 1 point. The weight of all independent stakeholders will be collected and averaged.

To assess each alternative, every alternative is scored by the experts with the symbols plus or minus (--,-,+-,+,++) which score is respectively between 1 and 5. The scoring of the criteria 'Impact on hazard reduction' will be based on the model outcome and therefor will be given. The recipients will have to judge critically and score alternatives based their own interpretation and knowledge.

6.1. Criteria

Criteria 1: Impact on hazard reduction

The effectiveness of the alternatives is compared by simulating the long-term effect of proposed mitigation measures by the use of a computational model in Delft3D. The mitigation measures will be implemented into the model and the effectiveness will be assesses by comparing the resulting erosion simulated by model with and without the measure. The timescale on which the alternatives will be tested are 5, 10, 25 and 50 years.

Criteria 2: Cost

The cost criterion is based on a rough estimation of the life cycle cost. The alternatives will be weighted on the cost of the construction materials, the maintenance cost and the lifetime of the structure.

Criteria 3: Environmental impact

For the environmental impact, the alternatives will be judged on the contribution to the local environment, the impact of the location of the structure and the effect on sediment supply in down-drift areas. Sediment aggregation can have a negative impact on surrounding coral reefs if it exceeds a certain threshold.

Criteria 4: Local acceptability

The local acceptability will be scored by the stakeholders based on experience and intuition. The acceptability takes the preferences of the local inhabitants into consideration such as the added or reduced value for landscape, tourism and fishing activities.

Criteria 5: Local feasibility

The local feasibility will also be scored completely by the stakeholders because of the local knowledge. The feasibility focusses on the implementation and maintenance of the alternatives. The scoring of this criterion can be influenced by the availability of local construction materials and/or expertise of contractors.

6.2. The MCA scoring & weighting grid

As an example for weighing of the criteria and the scoring of the alternatives, Table 8 is filled with fictional scores. These scores are used to calculate the final scores of the alternatives in Table 9, based on a single response rate. In practice the weighing and scoring will be averaged over the number of responses.

Table 8, Example of filled assessment form based on fictional scores

Main criteria	Weight (pnt)	Specific sub-criteria / indicators	Scores of Alternative				
			A	B	C	D	E
1. Impact on hazard reduction	5	Meters coastline retreat reduction	--	+-	+-	-	+
2. Cost	2	Investment-, maintenance- and life cycle cost	+-	+-	+	-	--
3. Environmental impact	3	Positive or negative impact on existing nature	+-	+	++	-	-
4. Local acceptance	4	landscape, tourism and fishing activities	--	+-	+	-	+-
5. Local feasibility	1	Implementation and maintaince	--	++	+	+-	+-

The total score of each alternative is the sum of the weight of each criteria times the corresponding score. In the example in Table 9, the two alternatives based on a Building with Nature approach both get a higher score because of the positive score on the criteria 3, the environmental impact, which is weighted as second most important criteria next to the effectiveness of the measures. The alternative including sea grass + sand nourishment scores higher in the end because the sand deposition in front of the coast will contribute to beach restoration on short notice, what favors the alternative for criteria 1, which is weighted as the most important criteria in this example.

Table 9, Example of scoring table MCA

Alternative	1. Reduction impact in m	2. Cost in €	3: Environ. impact	4: Local Acceptability	5. Local Feasibility	**Scoring**
	5 pnt	2 pnt	4 pnt	3 pnt	1 pnt	
A. No measure	1 (--)	3 (+-)	3 (+-)	1 (--)	1 (--)	5*1+2*3+4*3+3*1+1*1 = 23 points
B. Sea grass + nourishment	3 (+-)	3 (+-)	4 (+)	3 (+-)	5 (++)	5*3+2*3+4*4+3*3+1*5 = 51 points
C. Mangrove restoration	3 (+-)	4 (+)	5 (++)	4 (+)	4 (+)	5*3+2*4+4*5+3*4+1*4 = 59 points
D. Breakwater	2 (-)	2 (-)	2 (-)	2 (-)	3 (+-)	5*2+2*2+4*2+3*2+1*3 = 37 points
E. Groyne	4 (+)	1 (--)	2 (-)	3 (+-)	3 (+-)	5*4+2*1+4*2+3*3+1*3 = 42 points

6.3. Results

A survey among six expert recipients with diverse range of expertise related to coastal engineering is conducted in order to assess the alternative measures of the MCA. The survey included the introduction of the MCA in section 6, the criteria descriptions in section 6.1, the MCA scoring and weighing grid of section 6.2, a brief description of the alternative measures and an assessment form as given in Appendix E. The expertise and experience of each recipient is given in section 6.3.1, together with an analysis of their feedback. In section 6.3.2, the model results of previous chapter are added to score the effectiveness criteria and complete MCA score for each individual alternative. Section 6.3.3. concludes the MCA and gives the best alternative measure.

6.3.1. Expert assessment

Among the experts were varying disciplines related to coastal engineering; three coastal engineers, a marine ecologist, a coastal ecologist and a coastal zone manager. The complete, returned assessment forms together with from the survey can be found in Appendix F.

The first table in Appendix F is the feedback from a senior coastal engineer with 18 years of experience. From the weight given to the criteria, the cost of the alternative is considered the most important next to the effectiveness of the measure. Leaving out the scores for the effectiveness criteria, results to a preference for the reference alternative without measure. The second best option is the mangrove restoration which receives high scores on the other three criteria but is considered expensive according to this expert.

In the assessed table of the second senior coastal engineer, with 25 years of experience, the alternative with no measure also receives high rates due to the importance given to the cost criteria. However, the value of local feasibility is weighted higher what gives that the mangrove scores slightly higher than the reference alternative. Mangrove restoration is preferred in all the criteria except for the cost. Both hard measures score more than twice as low as the reference and mangrove alternatives. The seagrass implementation is ranked as third option by both senior coastal engineers because this is considered expensive and the local feasibility is questioned. Also, the coastal ecologist, who has 8 years of experience and have worked on Bonaire, gives only 1 point for the local feasibility of implementing a seagrass meadow in front of the coast and sees it as expensive solution. Still this alternative scores better than hard structure alternatives because of the high weight given for the environmental impact. The breakwater and groyne are both considered to have a negative impact on the surrounding environment and therefor given a score of 1 point. The mangrove restoration is clearly the best alternative according to the coastal ecologist and scores the most on all criteria.

This opinion is shared with the expert in marine ecology. This expert has 25 years of experience and also have worked on Bonaire. According to this assessment, the most important criteria for a mitigation measure are also the environmental impact and hazard reduction. The weight of the environmental criterion make both BwN alternatives favourable with preference for the mangrove alternative. The mangrove restoration alternative scores the higher because of the scores on local acceptability and -feasibility. This assessment is extra valuable due to the local working experience of both experts.

The coastal engineer with 5 years of experience weighted the local feasibility as semi-important with a score of 3 points but considered this not in his area of expertise and therefor left out the scores for this criterion. This led to a smaller variation in the total scores of the alternatives but still it becomes clear from this assessment that the hard structures are least preferable. The last expert from this survey is a coastal zone manager with 25 years of experience. The alternatives are also scoring quite similar in this assessment and the hazard reduction must show the best solution.

6.3.2. Alternative scoring

The scores for the criterion of the impact on hazard reduction are based on the modelling results of Chapter 6. The groyne is scored as most effective counter measure for the current erosion problem (++). The model results of the seagrass alternative give the highest cumulative volumes of sediment deposition in front of the coast but also show an erosive trend over the ten years of simulation. Besides, the value for the bed shear stress is based on a fully grown seagrass meadow for which a time-scale of establishment is uncertain. Nevertheless, the implementation of seagrass is considered to have a positive impact on the hazard reduction (+). The reforestation and expansion of the mangrove fringes is also scored as positive impact on the erosion (+) because of the positive trend and cumulative volumes. The construction of a breakwater shows to increase the erosion rates behind the structure, presumably by blocking the supply of sediment, and therefor scores negative (--) on this criteria. The impact of the 'no measure' alternative obviously also scores negative but the model results did not show the same areas and intensity of erosion as observed in the reality and the impact of hazard is less than with the constructed breakwater. Therefor the alternative with no measure is scored less negative than the breakwater alternative (-).

The average score from the different expert assessments for alternative 1 are combined and given in the table below. This results in a total average score of 55.5 points. Compared to the other measures, this score indicates that this alternative is still a better solution than implementing one of the hard structure alternatives. This is mainly because of the high scores on the cost criteria and the relative high scores on the environmental impact.

Alternative A: No measure	1. Reduction impact in m	2. Cost in €	3: Environ. impact	4: Local Acceptability	5. Local Feasibility
Averaged weight	*5.0 pnt*	*3.8 pnt*	*3.0 pnt*	*3.3 pnt*	*3.8 pnt*
Sr. Coastal Engineer	2	5	3	1	5
Sr. Coastal Engineer	2	5	3	2	4
Coastal Engineer	2	5	3	3	-
Marine Ecologist	2	5	3	1	3
Coastal Ecologist	2	4	3	2	2
Coastal Zone Manager	2	4	3	1	3
					Total: 55.5 points

The seagrass implementation is assessed as second best alternative in this MCA, next to the mangrove reforestation. The scores of the cost and environmental impact are comparable with the scores of alternative C but the scores of local acceptability and feasibility are considerably lower. The feasibility criteria in particular is important to notice because the two ecologist experts with local experience on Bonaire see this alternative as less promising.

Alternative B: Seagrass	1. Reduction impact in m	2. Cost in €	3: Environ. impact	4: Local Acceptability	5. Local Feasibility
Averaged weight	*5.0 pnt*	*3.8 pnt*	*3.0 pnt*	*3.3 pnt*	*3.8 pnt*
Sr. Coastal Engineer	4	2	5	1	3
Sr. Coastal Engineer	4	1	4	3	4
Coastal Engineer	4	2	5	4	-
Marine Ecologist	4	2	5	4	2
Coastal Ecologist	4	1	4	4	1
Coastal Zone Manager	4	1	4	4	1
					Total: 58.8 points

The mangrove reforestation alternative has scored the most points in every individual assessment and obviously scores the highest total average score of the five alternatives. The experts agree on the persuasion that the investment and maintenance cost of this operation will be expensive but this is also the case for the other three active measures. Only the alternative without the implementation of a mitigation measure scored more points for the cost criteria than the mangrove alternative. The local feasibility for mangrove reforestation and establishment receive a high average score regardless of the critical opinion of by the coastal zone manager. This score is balanced by the positive feedback of the two ecologist experts. This is comforting note considering the ecological background and local experience of these two experts.

Alternative C: Mangrove restoration	1. Reduction impact in m	2. Cost in €	3: Environ. impact	4: Local Acceptability	5. Local Feasibility
Averaged weight	*5.0 pnt*	*3.8 pnt*	*3.0 pnt*	*3.3 pnt*	*3.8 pnt*
Sr. Coastal Engineer	4	2	5	4	4
Sr. Coastal Engineer	4	2	5	5	5
Coastal Engineer	4	2	5	5	-
Marine Ecologist	4	1	4	5	5
Coastal Ecologist	4	2	5	5	4
Coastal Zone Manager	4	1	5	4	1
					Total: 71.0 points

The impact on hazard reduction by the breakwater construction was already proven incompetent in practice which is confirmed by the modelling results. Since this criterion is considered as most important factor in the MCA, the score of this alternative is not competing with the other alternatives. Moreover, the construction of a breakwater scores considerably lower on both the cost and the environmental impact criteria.

Alternative D: Breakwater	1. Reduction impact in m	2. Cost in €	3: Environ. impact	4: Local Acceptability	5. Local Feasibility
Averaged weight	*5.0 pnt*	*3.8 pnt*	*3.0 pnt*	*3.3 pnt*	*3.8 pnt*
Sr. Coastal Engineer	1	1	1	3	4
Sr. Coastal Engineer	1	1	1	4	2
Coastal Engineer	1	1	2	4	-
Marine Ecologist	1	1	1	3	5
Coastal Ecologist	1	1	1	2	2
Coastal Zone Manager	1	2	2	4	4
					Total: 37.6 points

The effectiveness of the impact reduction of a groyne construction does not weigh up to the negative assessment from the experts. Based on the survey, this is the least favoured alternative and however the model results did show the most impact on hazard reduction in the area, the overall averaged score of this alternative is of the same order as no measure. From the expert opinions it becomes clear that they agree on the conception of local acceptance for this alternative. This local acceptability could be high due to a visible and direct solution to the problem but the creditability might be lower since the earlier construction of the breakwater did not result in the desired effect. For the local feasibility it might be an option to replace the current rock structure but based on the expert input this is not a reliable solution.

Alternative E: Groyne	1. Reduction impact in m	2. Cost in €	3: Environ. impact	4: Local Acceptability	5. Local Feasibility
Averaged weight	*5.0 pnt*	*3.8 pnt*	*3.0 pnt*	*3.3 pnt*	*3.8 pnt*
Sr. Coastal Engineer	5	1	1	3	3
Sr. Coastal Engineer	5	1	1	4	2
Coastal Engineer	5	1	2	4	-
Marine Ecologist b	5	1	1	3	3
Coastal Ecologist b	5	1	1	2	2
Coastal Zone Manager	5	1	2	4	4
					Total: 54.7 points

6.3.3. Conclusion

The experts unanimously weighted the reduction impact criterion as most important with a rating of 5. Second most important were the criteria for cost and local feasibility which gained an average weight of 3.8. The local acceptability was given a 3.3 average weight and at last the environmental impact ended up with a 3.0 weight. This is despite the fact that both the marine ecologist as the coastal ecologist have weighted the environmental criteria as important as the reduction of coastal erosion. Furthermore, it is interesting to notice that the other experts weighted the cost criterion heavily while both experts with local experience see this criterion as least important.

Table 10, Assessment table with the averaged feedback weights and scores

Alternative	1. Reduction impact in m	2. Cost in €	3: Environ. impact	4: Local Acceptability	5. Local Feasibility	**Scoring**
Averaged weight	*5.0 pnt*	*3.8 pnt*	*3.0 pnt*	*3.3 pnt*	*3.8 pnt*	
A. No measure	2	4.7	3.0	1.7	3.4	55.5
B. Sea grass + nourishment	4	1.5	4.5	3.3	2.2	58.8
C. Mangrove restoration	4	1.7	4.8	4.7	3.8	71.0
D. Breakwater	1	1.2	1.7	3.3	3.4	38.6
E. Groyne	5	1.0	1.3	3.3	2.8	54.7

From the modelling results, the groyne shows the most effect in hazard reduction but this alternative received negative assessments on both the cost and environmental impact criteria. The same goes for the breakwater alternative but this alternative also does not contribute to the reduction of the erosion and is therefor scored as least favorable option. Alternative A and B both score higher than the groyne construction. The relative high score for alternative A is due to the fact that this alternative is the least expensive and has no direct negative impact on the environment. This alternative however would not be supported by local acceptability and can not be considered as serious alternative since the breakwater is already built in 2019. The seagrass alternative is the second best measure according to the experts assessment. The feasibility of seagrass establishment is questioned by the ecologist experts and the acceptability also scores lower than the mangrove alternative.

Altogether, the mangrove restoration scores considerably higher than the other alternatives and is the best alternative measure according to this MCA. The cost for mangrove reforestation is considered substantial but even in this criterion it assessed high in respect to the other alternatives. Besides there is a lot of knowledge and an active community on Bonaire who is committed to the reforestation and preservation of the mangrove fringes around Lac Cai. This creates opportunities to limit the cost and to increase the local acceptance of this alternative.

7. Discussion

Discussion on the lack of data, assumptions and uncertainties in the modelling process, interpretations of the modelling results and the MCA.

7.1. Data analysis

One of the main challenges in this thesis was the lack of actual and accurate data. Lac Cai is widely studied but these researches mainly focus on the ecological value and recreational purposes inside the bay. Data on, for instance, historical coastlines, bathymetry and waves for the area around Cai beach are scarce, outdated or inaccurate.

First of all, the measured bathymetry data was inaccurate and inconsistent. The bathymetry data is deemed inadequate because of the large fluctuations between two adjacent measured points. For example, while at one point the depth is be measured one meter, the next point which is less than a meter off, can show a depth of more than 15 meters. Also, the measured data shows depths of over 15 meters in front of the entrance road to Lac Cai. Despite the erosion rates in this area it seems unrealistic that depths of this magnitude could be measured here. Most probably the data has been stored with wrong coordinates and the original measurements are not available anymore. Figure 49 shows the inaccuracy of available bathymetry data.

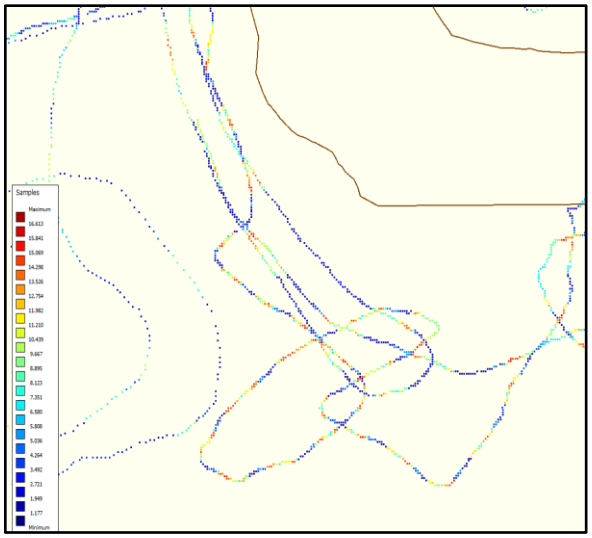

Figure 49, Measured data points (L) and triangular interpolated bathymetry (R) with legends showing depths varying between 1 and 26 meters

Secondly, the wave data was retrieved from the ERA5 dataset. This global data is very complete (1979-2017) but is for offshore points. For the aim of this study, the closest data point was located 10 km outside the study area. The setup of a SWAN model was used for the translation of this data set to a nearshore wave climate, but this model was again built with the global bathymetry data from Gebco. The accuracy of this SWAN model is questionable because of the combination of two coarse data sets.

Also coastline profiles were only available from Google Earth images and old aerial photos. This resulted in an information gap which led to assumptions. The available images in Google earth only showed a couple of years in which the coastal retreat seemed to evolve gradually but this could still be the effect of intermediate storm events.

Furthermore, the information on tidal amplitudes, sediment characteristics and mangrove loss along the coast at Cai were outdated (Hummelinck & Roos 1968, Lott 2001). This created insights into the structure of the system but leaves plenty for interpretation. Assumptions for the sediment characteristics were made based on the description of the bed composition at Cai as 'sandy beach'. Moreover, the mangrove loss was only investigated between the years 1961 and 1996 and the exact dimensions of the historical fringes could only be approximated from aerial pictures.

The estimated tidal range inside the bay was approximately a maximum of 30cm and therefor considered negligible in this thesis. This range however, was measured inside the bay and could therefore be different than the coast area.

7.2. Modelling

Due to the limited available data, the Delft3D model was constructed as an analogue of reality rather than a virtual reality (Roelvink & Reiniers, 2011). The goal in this modelling strategy is to assess the processes and effects instead of replicating the exact situation. This approach however, is unsuitable for proper calibration of the model and therefor modelling forecasts contain uncertainties in the morphodynamics and in timescale. In early phase of the modelling process, the outcome of the model was considered sufficiently accurate in modelling the hydrodynamic processes and simulating the erosion in front of the coast. Also, the wave and flow phenomena into the bay were consistent and showed agreement with flow charts of the prior investigations (Hummelink & Roos, 1968). Unfortunately, the development of the model in order to result in a more realistic bathymetry to hindcast the exact cove in front of the entrance road to Cai was not succesful. The erosion is not located in the area where the impact is observed and the coastal retreat was more concentrated at the corner of the beach near the inlet channel into the bay. The robustness of the conclusions derived from these modelling results could therefor be questioned.

The first step in the modelling strategy was the conduction of a sensitivity analysis based on very limited parameter selection in a small range. This analysis focused on the sediment transport and erosion in front of the entrance road to Cai. The difficulty in executing this analysis in a sensible way was again the lack of data. Because of the limited available data, it was hard to carry out a calibration or validation of the model. The simulation of erosion rates and coastal retreat in the right areas was therefor considered as most feasible approximation to reality.

The bathymetry was further developed by the use of a Dean profile (Dean, 1991). Only, this profile is based on wave- and sediment characteristics for which the sophisticated data was also not found. The sediment composition is based on the average sandy beach in the Caribbean and the wave heights and period came from the SWAN simulation. With this profile the model was iteratively created based on the approximation of the DoC. Furthermore, the manual implementation of this profile gives a uniform coastline profile along the beach which is different to the actual coastal system around Lac Cai.

The effect of mangrove deforestation was investigated by the use of three different methods on vegetation modelling. The vegetation-induced bed shear stress showed the most effect in erosion reduction and was therefore the most evident to analyze. For the implementation of the seagrass alternative this resulted in a peak increase of sedimentation in front of the coast. Although the value for the vegetation-induced bed shear stress was retrieved from Manning's roughness coefficient substantiated in literature (Chow, 1959), the extent of the seagrass patch and the uniform shear stress resulted in unrealistic sedimentation. This effect could be prevented by the use of a different method in which more detail of the vegetation, like height and diameters, can be included.

7.3. Mitigation alternatives and MCA

The scope of this investigation was for five mitigation alternatives as described in Chapter 6 of this report. The variation in the designs of these alternatives were based on conventional, innovative and nature based methods. Furthermore, the local feasibility was one of the criteria for the composition of these mitigation measures and therefor the fitting of possible scenarios into the current system at Lac Cai were considered. The feasibility of the designed alternatives was scored by experts with varying disciplines related to coastal engineering but these experts had no influence on the design of the alternatives. The possibility exists that there are other possible mitigation alternatives or the combination between two of the suggested alternatives could be even more effective in reducing the erosion. Also, the multi-disciplined insights are only based on the feedback of six respondents. This is a low attendance which should be expanded.

Another note on the seagrass alternative is that the description of this alternative in the MCA survey differs from the modelled alternative. The alternative was described as a combination between sand nourishment and seagrass implementation in order to restore the beach to its original state but for simplicity the modelled alternative only included an increased bed shear stress to represent wave attenuating and sediment trapping functions of the seagrass meadow. This appears as a sufficient measure and the additional sand nourishment could thus be omitted. Due to the description of this alternative towards the experts, it is possible that the scores on the cost criterion, the environmental impact and local acceptance has been negatively affected. Still the local feasibility for this alternative is considered to be difficult. This score is weighed heavily in the conclusion since the two experts with an ecological background and local experience do not recommended the implementation of seagrass for this case.

Lastly, the reduction impact of the mangrove reforestation is scoring high in the MCA. This score is based on the model results for the reforestation of mangroves in an area bigger than the original fringe of 1962. The feasibility of reforestation in this area and the circumstances for establishment are uncertain. The origin of the mangrove deforestation between the years 1961 and 1996 is unknown and should be further investigated. The implementation of braided walls is proven valuable in these kind of reforestation projects but the effectiveness, with the hydrodynamic processes playing a role around Lac Cai, is not investigated.

8. Conclusion & Recommendations

8.1. Conclusions

The implementation and reforestation of a mangrove fringe in front of the coast of Lac Cai is considered as the most fitting solution for the erosion problem at Lac Cai. This conclusion is derived based on the model results and multicriteria analysis in this thesis. The structure of this research was built around the research question which consisted of three sub questions. The findings of this investigation and elaboration of the conclusions are given per question.

- Research question 1: What is the main forcing which forms the origin of this coastal erosion?

The analysis of the ERA5 wave data shows a dominant wave direction from the north. This data was converted into 5 wave conditions with the energy flux method and translated to near-shore waves with a SWAN model. From this translation it became clear that the waves approach the coastline at Lac Cai in an oblique angle which approximates the critical wave angle for which the longshore sediment transport accelerates. In addition, the adjacent unerodable part towards the north of the coast cause for a lack of sediment supply. These two observations, together with the gradual coastal retreat shown in the coastline analysis, have led to the hypothesis that the LST is the main hydrodynamic force causing the erosion. This hypothesis is confirmed by the modelling results which showed erosive activity could be simulated with a realistic analogue approach. Analysing the cumulative sediment volumes show more sediment activity around the coastline which indicates that the LST rates have more impact in the system than cross-shore sediment transport.

Furthermore, the data analysis showed the loss of mangrove fringes along the coast. The loss of these fringes could be correlated with the increase of erosion rates over the years. The data was inadequate to confirm this theory and therefor the impact of mangrove loss was investigated with the use of the model. The erosion rates were compared in three different scenarios: the current mangrove, the historical fringe, based on old arial pictures, and a scenario without any mangroves. The vegetation in these scenarios is integrated in three different, renowned modelling theories. The modelling results were analysed by the coastal retreat in various cross-sections and showed less retreat in the sections through the fringes. However, the model still showed plenty of erosion for all three methods and so it is difficult to conclude that this draw back

- Research question 2: How to model the driving hydrodynamic processes causing the coastal erosion at Lac Cai?

The erosion problem at Lac Cai is modelled with the use of Delft3D. This model was chosen after the abortive attempt to model the system with the coastline evolution model ShorelineS (Groot, 2022). This investigation showed that the available coastline data was inadequate for calibrating and validating the model and moreover, the bathymetry was too complex for this type of modelling. Within the Delft3D software there are more options to construct and adjust the bathymetry and also to analyse the flow and wave data. The bathymetry was constructed by combining the offshore data from Gebco with the data from the field measurements. Because of the inconsistencies in the measured data, the coastal profile was adjusted manually based on the Dean profile theory and linearly interpolated with the offshore data.

Furthermore, the options for modelling vegetation are more competent and various within Delft3D. This created the opportunity to analyse the correlation between the mangrove loss and the erosion. The three methods to include vegetation into the model consisted of a vegetation-induced bed shear stress, trachytopes and rigid rods. From these three methods, the bed shear stress showed the most effect and was the most straightforward to implement. Therefor, this method was considered most suitable for the scope of this research.

- Research question 3: What is the best mitigation measures to serve as a solution for this erosion problem?

Based on the valuation of the alternative measures for the different criteria assessed in the MCA, the mangrove reforestation in front of the entrance road to Lac Cai is considered the most effective and sustainable solution to the erosion problem. The MCA was conducted among six multi-disciplinary experts related to coastal engineering and included the following five criteria:

- Impact on hazard reduction
- Cost
- Environmental impact
- Local acceptability
- Local feasibility

The impact on hazard reduction was weighed unanimously as most important criterion and was scored based on the model results. These results showed that the groyne was the most effective measure against the erosion and cumulative volumes over time show sedimentation in front of the entrance road to Cai. This was also the case for mangrove implementation but on a slightly smaller scale. The seagrass alternative had an instant peak value in the cumulative sediment volumes but showed decay over time around the coastline. This could be explained due to the fact that the bed shear stress increased over the extension of large area and functions as sediment trap in the model. This is disproportionate to reality but the seagrass alternative is still considered as effective measure against the erosion. The breakwater was not effective in the mitigation of the hazard impact because the construction blocks the supply of sediment while erosion behind the breakwater is still occurring.

Besides the small advantage of the groyne alternative for the reduction impact criterion, the mangrove reforestation scored better in the other criterions. The expansion of the mangroves fringes was considered as addition to the environment and scored relatively high on the local feasibility criterion. However, the actual implementation and establishment still needs further investigation. All of the experts believed the local acceptability for this alternative was high and would receive positive feedback from stakeholders. This should be verified by the use of a stakeholder analysis. The cost was still considered substantial but this could be limited by local knowledge and willingness for the reforestation of the mangroves at Lac Cai.

8.2. Recommendation

Recommendations concerning the different gaps and sequent studies based on the results, discussion and conclusion of this thesis.

Data collection and model improvement

The model did not simulate a perfect representable reflection of the coastal system. This is due to the limited available data what complicates calibration and validation options. Recommended is to preform further research on the local circumstances to improve the model input. This investigation should include new bathymetry measurements, data collection of nearshore wave heights and waterlevels and also sediment samples to improve the validity of the model.

Furthermore, it is recommended to review the wave data, waterlevels and coastline profiles in order to check the origin of the erosion. With the given data, the hydrodynamic processes were investigated and the LST was reckoned as most probable cause based on the gradual coastal retreat and the nearshore wave data. However, the coastline data and translation to nearshore wave climate consist of assumptions and therefor new data could also show other plausible reasons for the erosion at Lac Cai.

Mangroves reforestation

Furthermore, it is interesting to investigate the cause of the mangrove deforestation. Since the recommended mitigation measure from this research is replanting the mangrove fringe to its original state and expand this more towards the sea, it is important to investigate the cause of mangrove loss in this area. This could be human intervention or it could be related to the hydrodynamics or environmental circumstances as high salinity values. Also, the different mangrove species on the island should be further investigated in order to conclude on the mangroves with the best wave damping characteristics and establishment features in the hydrodynamic environment at Lac Cai.

Stakeholder analysis

The stakeholders at Lac Cai should be included into the decision making process concerning the mitigation measures. In order to map the different stakeholders it would be recommended that a stakeholder analysis is performed. Among these stakeholders, an MCA could be conducted to investigate the local support and preference.

References

Bakhyar, R., Ghaheri, A., Yeganeh-Bakhtiary, A., & Barry, D. (2009). Process-based model for nearshore hydrodynamics, sediment transport and morphological evolution in the surf and swash zones. *Applied Ocean Research*, 44-56. doi:https://doi.org/10.1016/j.apor.2009.05.002

Baptist, M. (2005). *Modelling floodplain biogeomorphology.*

Barquet, K., & Cumiskey, L. (2018). Using participatory Multi-Criteria Assessments for assessing disaster risk reduction measures. *Coastal Engineering*, 93-102. doi:https://doi.org/10.1016/j.coastaleng.2017.08.006

Benedet, L., Dobrochinski, J., Walstra, D., Klein, A., & Ranasinghe, R. (2016). A morphological modeling study to compare different methods of wave climate schematization and evaluate strategies to reduce erosion losses from a beach nourshment project. *Coastal Engineering*, 69-86. doi:https://doi.org/10.1016/j.coastaleng.2016.02.005

Bird, E. C. (1985). Coastline changes: A global review. *Geological Journal*, 215-216. doi:https://doi.org/10.1002/gj.3350210215

Booij, N., Ris, R. C., & Holthuijsen, L. H. (1999). A third-generation wave model for coastal regions 1. Model description and validation. In *Journal of Geophysical Research: Oceans 104 (C4)* (pp. 7649-7666).

Chow, V. (1959). *Open channel hydraulics.* New York: McGraw-Hill.

Dean, R. (1991). Equilibrium Beach Profiles: Characteristics and Applications. *Journal of Coastal Research*, 53-54.

Deltares. (2014). *Delft3D-Wave User manual.*

Deltares. (2018). *Delft3D-Flow user manual.*

Elfrink, B., & Baldock, T. (2002). Hydrodynamics and sediment transport in the swash zone: A review of perspectives. *Coastal Engineering*, 149-167. doi:https://doi.org/10.1016/S0378-3839(02)00032-7

Engel, M., Brückner, H., Fürstenberg, S., Frenzel, P., Konopczak, A., Scheffers, A., . . . Daut, G. (2012). A prehistoric tsunami induced long-lasting ecosystem changes on a semi-arid tropical island - The case of Boka Bartol (Bonaire, Leeward Antilles). *Naturwissenschaften*, 51-67.

Erdmann, W., & Scheffers, A. (2006). *Mangrove Population of Lac Bay (Bonaire) 1961-1996.* University Duisberg-Essen.

Google Earth Pro. (2020). *Google Earth Pro*.

Horstman, E., Dohmen-Janssen, C., Bouma, T., & Hulscher, S. (2015). Tidal-scale flow routing and sedimentation in mangrove forests: Combining field data and numerical modelling. *Geomorphology*, 244-262.

Horstman, E., Dohmen-Janssen, M., & Hulscher, S. (2013). Modelling tidal dynamics in a mangrove creek catchment in Delft3D. *Coastal Dynamics*, 833-844.

Inman, D. (2005). Littoral Celss. *Encyclopedia of Coastal Science*, 594-599. doi:https://doi-org.ezproxy2.utwente.nl/10.1007/1-4020-3880-1_196

IPCC. (2019). *Summary for Policymakers. In: IPCC Special Report on the Ocean and Cryosphere in a Changing Climate.*

James, R., Christianen, M., van Katwijk, M., de Smit, J., Bakker, E., Herman, P., & Bouma, T. (2020). Seagrass coastal protection services reduced by invasive species expansion and megaherbivore grazing. *Journal of Ecology*, 2025-2037. doi:DOI: 10.1111/1365-2745.13411

Kalke, C., & Kats, K. (2011). *Lac Buoy Placement Project.*

Kraus, N., Larson, M., & Wise, R. (1999). Depth of closure in beach-fill design. *Proceedings of the 12th National Conderence on Beach Preservation Technology*, 271-286.

Lesser, G., Roelvink, J., van Kester, J., & Stelling, G. (2004). Development and validation of a three-dimensional. *Coastal Engineering*, 883-915.

Lott, C. (2001). *Lac Bay: Then and Now… A Historical Interpretation of Environmental Change.*

Masselink, G., & Puleo, J. (2006). Swash-zone morphodynamics. In *Continental Shelf Research, 26(5)* (pp. 661-680). doi:10.1016/j.csr.2006.01.015

Mil-Homens, J. (2016). *Longshore Sediment Transport, Bulk Formulas and Process Based Models.* PhD Thesis ISBN 978-94-6186-616-5. doi:https://doi.org/10.4233/uuid:f7703aba-2760-47b1-99c2-a076a84d9b0f

Neumann, B., Vafeidis, A., Zimmermann, J., & Nicholls, R. (2005). Future Coastal Population Growth and Exposure to Sea-Level Rise and Coastal Flooding - A global assessment. *PLOS One*. doi:doi:10.1371/journal.pone.0118571

Puleo, J., Beach, R., & Allen, J. (2000). Swash zone sediment suspension and transport and the importance of bore-generated turbulence. *Journal of Geophysical Research: Oceans*, 17021-17044. doi:https://doi.org/10.1029/2000jc900024

Reguero, B., Beck, M., Agostini, V., Kramer, P., & Hancock, B. (2018). Coral reefs for coastal protection: A new methodological approach and engineering case study in Grenada. *Journal of Environmental Management*, 146-161. doi:https://doi.org/10.1016/j.jenvman.2018.01.024

Roelvink, D. (2017). Coastline Modelling: The next generation? *Book of Abstracts NCK days*, (p. 33).

Roelvink, D., & Reniers, A. (2011). *A Guide to Modelling Coastal Morphology (vol.12).* World Scientific.

Shi, H., & Singh, A. (2003). Status and Interconnections of Selected Environmental Issues in the Global Coastal Zones. *AMBIO: A Journal of the Human Environment*, 145-152.

Shields. (1936). *Application of similarity principles and turbulance research to bed-load movement.*

Shrestha, P., & Blumberg, A. (2005). Cohesive sediment transport. *Encyclopedia of Coastal Science*, 327-330.

The Open University. (1999). *Waves, Tides and Shallow-Water Processes.* doi:https://doi.org/10.1016/B978-0-08-036372-1.X5000-4

United Nations. (2014). *World Urbanization Prospects: the 2014 revision.* New York: United Nations.

University, T. O. (1999). *Waves, Tides and Shalow Water Processes.* Oxford: Butterworth-Heinemann.

Van Rijn, L. (1993). *Principles of Sediment Transport in Rivers, Estuaries and Coastal Seas.* doi:10.1002/9781444308785

Van Rijn, L. (2007). Unified View of Sediment Transport by Currents and Waves. I: Initiation of Motion, Bed Roughness, and Bed-Load Transport. *Journal of Hydraulic*, 649-667.

Van Rooijen, A. (2011). *Modelling sediment transport in the swash zone.* TU Delft.

Wagenaar Hummelinck, P., & Roos, P. (1969). *Een natuurwetenschappelijk onderzoek gericht op het behoud van het Lac op Bonaire.*

Wagenaar, H. &. (1969). -.

WeShareBonaire. (2020). *WeShareBonaire*. Retrieved from https://www.wesharebonaire.com/

Appendix A, Delft3D numerical scheme

The system of equations used to solve the shallow-water equations in Delft3D consist of the hydrostatic pressure assumption, horizontal momentum equations, continuity equation, transport equation and one of the available turbulence closure models (Lesser, 2004).

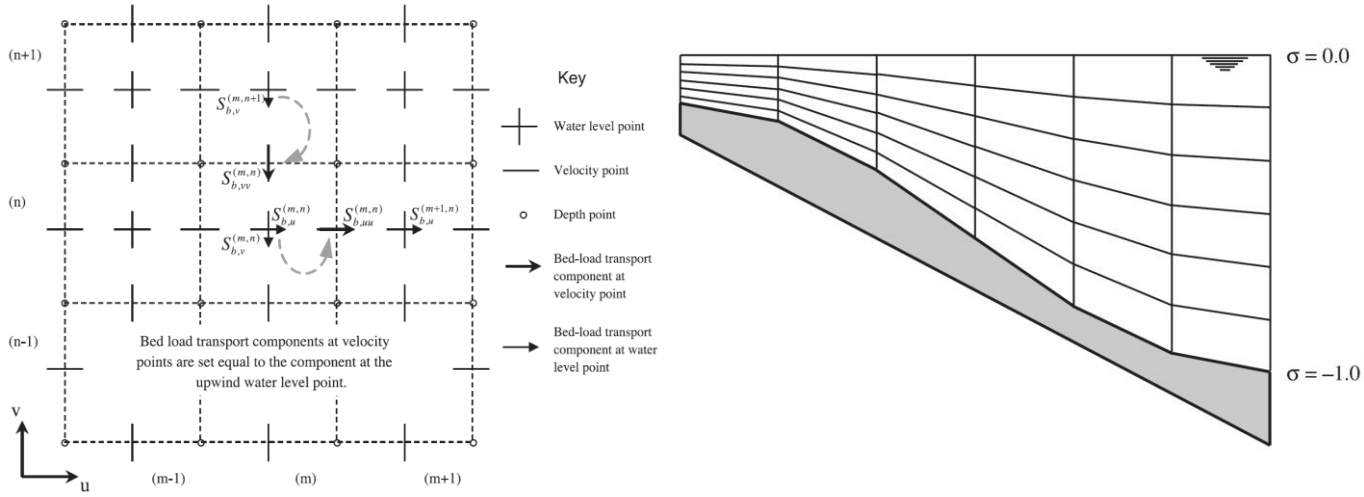

Figure 50, Staggered grid to solve transport equations as used in Delft3D-FLOW (L) and Vertical grid subdivided in σ-layers of equal thickness (R) (Deltares, 2018)

Hydrostatic pressure assumption

As shallow water is assumed, the vertical momentum equation reduces to the hydrostatic pressure equation. This excludes vertical acceleration due to buoyancy effects or variations in the bottom topography. The hydrostatic pressure equation is given by:

$$\frac{\partial P}{\partial \sigma} = -\rho g h$$

where the left term indicates the change of pressure over depth, and the right term the hydrostatic pressure at a given water depth.

Horizontal momentum equation

The horizontal momentum equations for incompressible fluids are given by:

$$\frac{\partial U}{\partial t} + U\frac{\partial U}{\partial x} + v\frac{\partial U}{\partial y} + \frac{\omega}{h}\frac{\partial U}{\partial \sigma} - fV = -\frac{1}{\rho_0}P_x + F_x + M_x + \frac{1}{h^2}\frac{\partial}{\partial \sigma}\left(v_V\frac{\partial u}{\partial \sigma}\right)$$

$$\frac{\partial V}{\partial t} + U\frac{\partial V}{\partial x} + V\frac{\partial V}{\partial y} + \frac{\omega}{h}\frac{\partial V}{\partial \sigma} - fU = -\frac{1}{\rho_0}P_y + F_y + M_y + \frac{1}{h^2}\frac{\partial}{\partial \sigma}\left(v_V\frac{\partial v}{\partial \sigma}\right)$$

Where the first four terms on the left describe the accelerations over space and time, and the fifth term the Coriolis force. The first term on the right is the horizontal pressure term given by the Boussinesq approximations, the second term the Reynold's stresses, the third term represents the contributions due to external source and sinks of momentum and the last term the turbulence closure model.

Continuity equation:

The depth-averaged continuity equation for incompressible fluids is given by:

$$\frac{\partial \zeta}{\partial t} + \frac{\partial [h\bar{U}]}{\partial x} + \frac{\partial [h\bar{V}]}{\partial y} = S$$

where $\frac{\partial \zeta}{\partial t}$ is the change of the free surface elevation relative to the undisturbed water level over time, the second and third term the flow in the x and y direction and S implies withdrawal or discharge of water, evaporation or precipitation.

Transport equations:

The advection-diffusion (mass-balance) equation calculates the suspended sediment transport above the Van Rijn's reference height.

$$\frac{\partial c^{(l)}}{\partial t} + \frac{\partial u c^{(l)}}{\partial x} + \frac{\partial v c^{(l)}}{\partial y} + \frac{\partial \left(\omega - \omega_s^{(l)}\right) c^{(l)}}{\partial \sigma} = \frac{\partial}{\partial x}\left(\varepsilon_{s,x}^{(l)} \frac{\partial c^{(l)}}{\partial x}\right) + \frac{\partial}{\partial y}\left(\varepsilon_{s,y}^{(l)} \frac{\partial c^{(l)}}{\partial y}\right) + \frac{\partial}{\partial \sigma}\left(\varepsilon_{s,\sigma}^{(l)} \frac{\partial c^{(l)}}{\partial \sigma}\right)$$

where c is the mass concentration of sediment fraction, u, v and ω flow velocity components, $\varepsilon_{s,x}$, $\varepsilon_{s,x}$ and $\varepsilon_{s,\sigma}$ the eddy diffusivities of sediment fraction and ω_s the sediment settling velocity of sediment fraction.

Turbulence closure models

There are four different turbulence closure models which can be used within Delft3D in order to determine the vertical viscosity (v_H and v_V) and diffusivity (D_H and D_V). The input of these models vary in the turbulent kinetic energy k, dissipation rate of turbulent kinetic energy ϵ and/or the mixing length L (Deltares, 2018). The four turbulence closure models are:

- Constant coefficient
- Algebraic Eddy viscosity closure model (AEM)
- k-L turbulence model
- k-ϵ turbulence closure model

Appendix B, Monthly wave roses

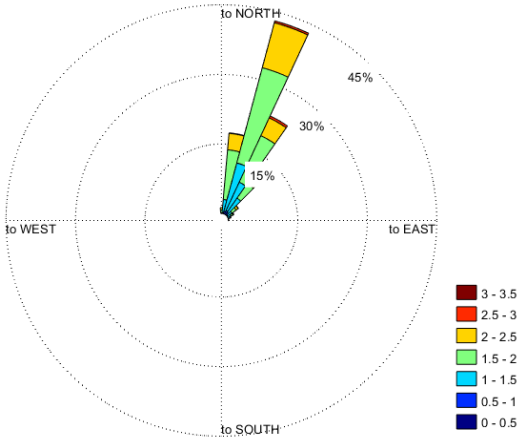

January

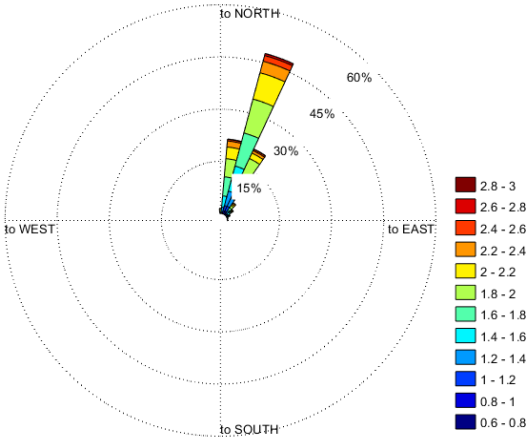

February

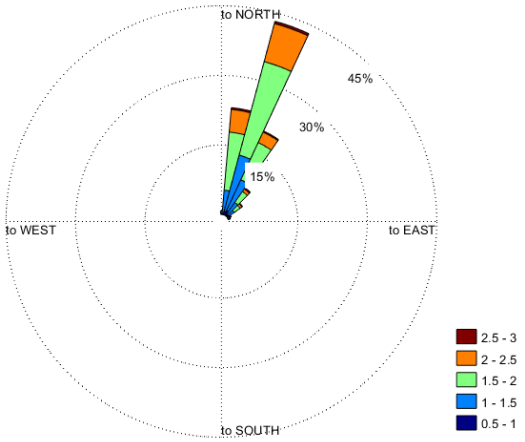

March

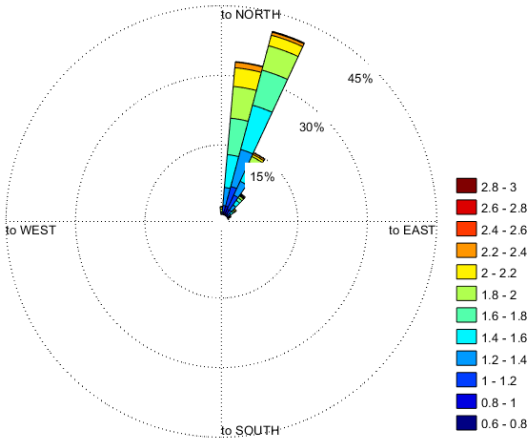

April

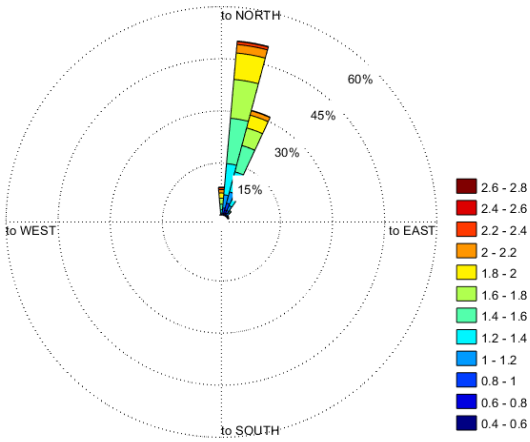

May

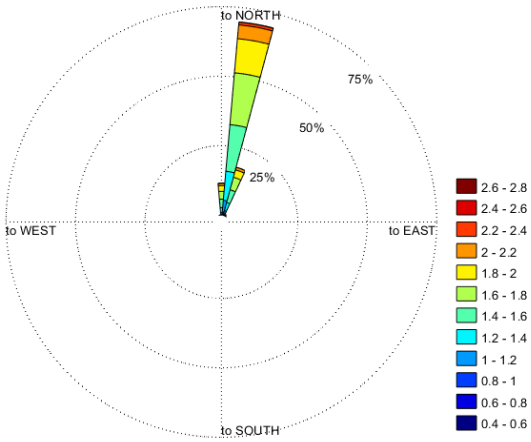

June

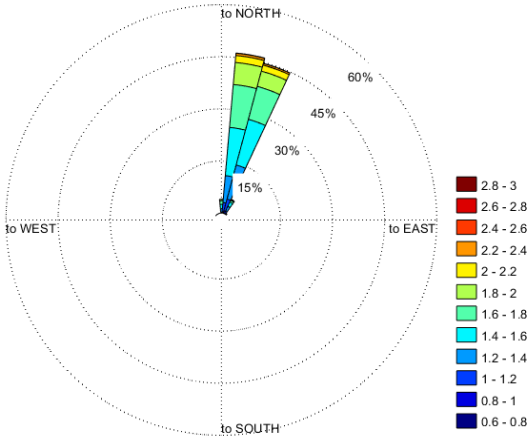

July

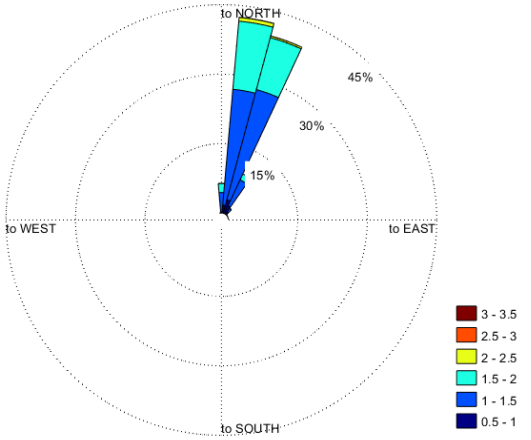

August

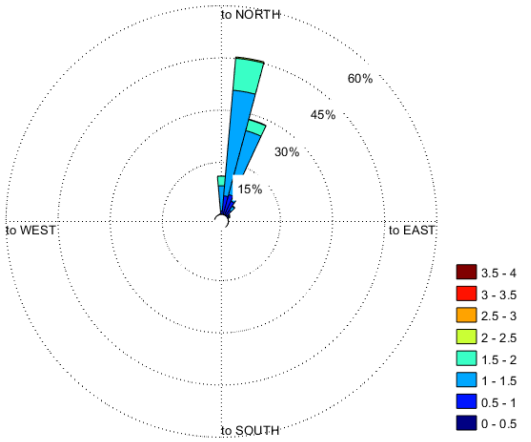

September

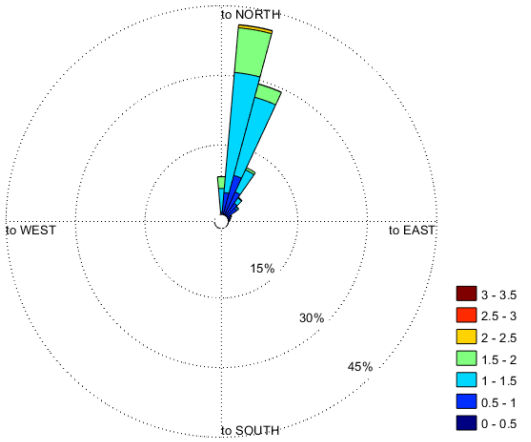

October

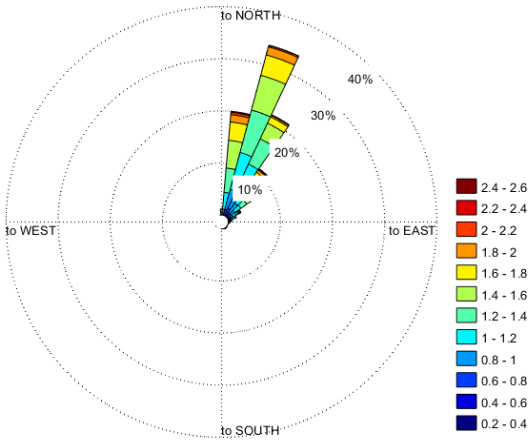

November

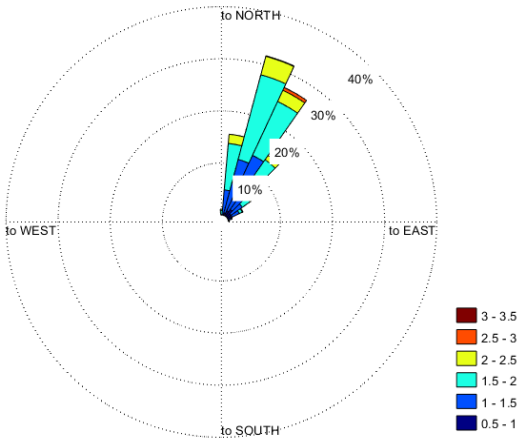

December

Appendix C, Grid properties

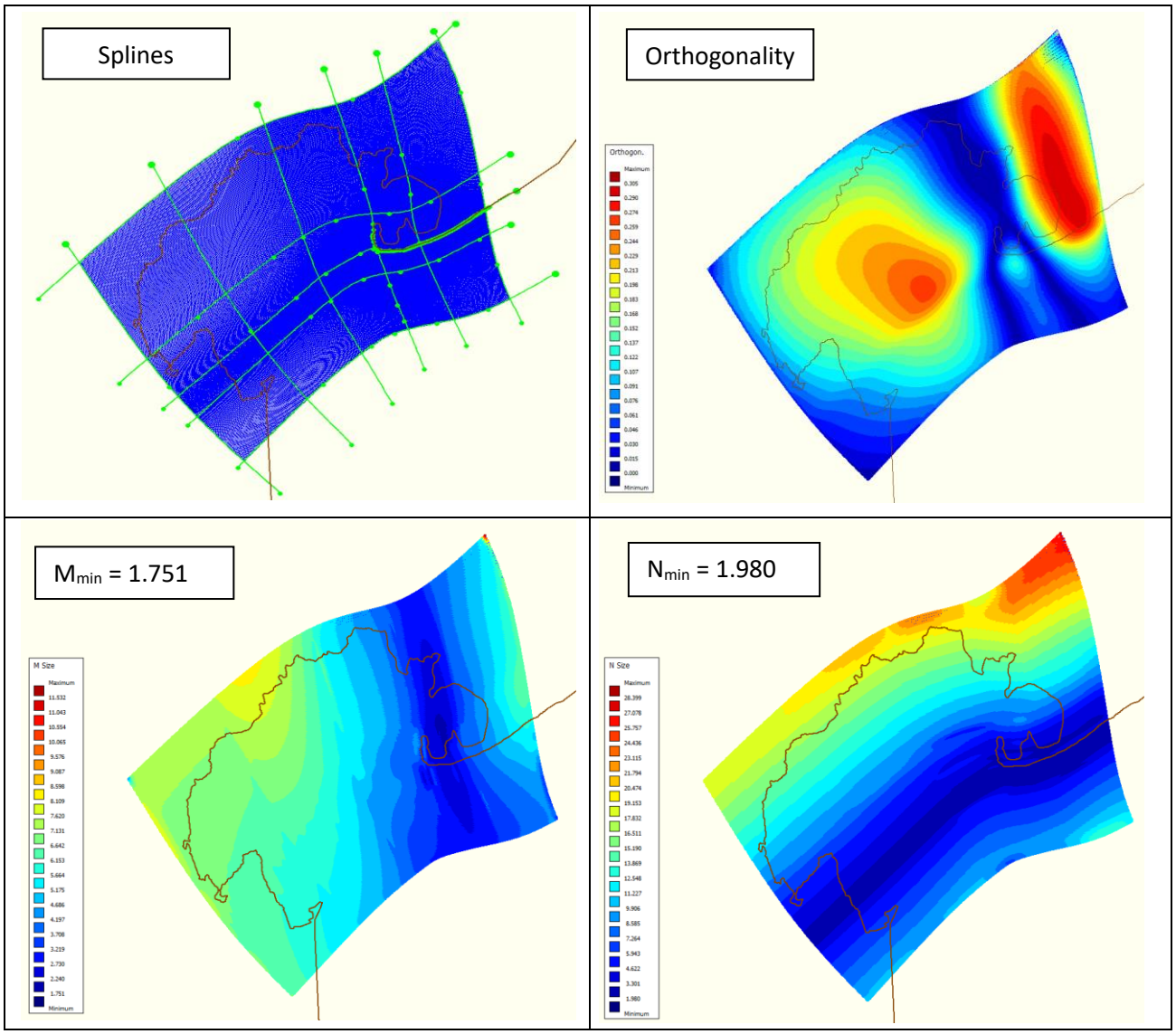

Appendix D, Alternative description and questionnaire for MCA survey

Alternative A. No measure

The first alternative which will be introduced into the MCA will be the 'zero' situation scenario. No measurements will be implemented and the erosion will continue to cause for coastal retreat. In this alternative it is likely that, over time, Lac Cai is being separated from the mainland. In order to keep Cai connected to the mainland, the building of an bridge will be necessary to connect the two parts again. An open bridge with a span of about 5 meters (see Figure 51) could be the fitting solution in case the height will be sufficient to prevent damage by a storm with a return period of 50 years and reinforced abutments.

Figure 51, Example of suggested open bridge in larger scale

Ecological: The mangrove area behind the beach ('Pariba di Cai') will be in direct connection with the open sea which changes the water balance and can have negative impacts on the environmental value of the area. (Bonaire.nu, 2019).

Cost: The time of investment will be postponed but the effective life cycle cost will be higher compared to the other alternatives. The investment cost for the building of a bridge between the mainland and Lac Cai beach together with the high maintenance demand of reinforced concrete structures in marine environments will add up.

Alternative B. Sea grass and Sand nourishment

An interesting strategic alternative might be the combination between sand nourishment and vegetation. In this scenario the coast will be partly restored and in the newly created shallow areas the vegetation can be planted. A suitable native species with wave damping characteristics is *Thalassia testudinum* (turtle grass) When the seagrass is established it will lead to wave attenuation, decrease in bed shear stresses and therefor a decrease in erosion. (James et al., 2020).

Sand nourishment on its own could be a solution but would have various drawbacks. A large deposition of a volume equal to the amount of the eroded sediment will in theory lead to the restoration of the beach in its original state. However, the actual feasibility and impact of such a major intervention is hard to predict. Furthermore, the origin of the erosion is not addressed and therefor will only function as a temporary solution. Additional nourishment will be necessary periodically to remain the coastal profile and prevent for returning into the same problematic scenario as currently is the matter.

This 'Building with Nature' solution using the establishment of sea grass in front of the beach will have wave attenuating function and cause for vegetation induced drag forces. Thereby the root system of the vegetation enhances sediment deposition rates. The establishment and survival of sea grass is an uncertain factor which should be further investigated and monitored. Crucial aspects relating to this survival are, for instance, the exposure to waves and high nutrient levels (La Nafie et al. 2012)

Figure 52 schematizes the eroded hollow area in front of the access road which covers a width of approximately 200 meters and has shown a maximum coastal retreat of nearly 30 meters. Sand nourishment to heighten the current profile by 0.5 meters will create the needed shallow areas for the establishment of the sea grass and widening of the beach. The integral of the parabolic function for this problem shows the total area of the coastal erosion covers 4000 square meters what gives a total volume of 2000m^3 sand deposition.

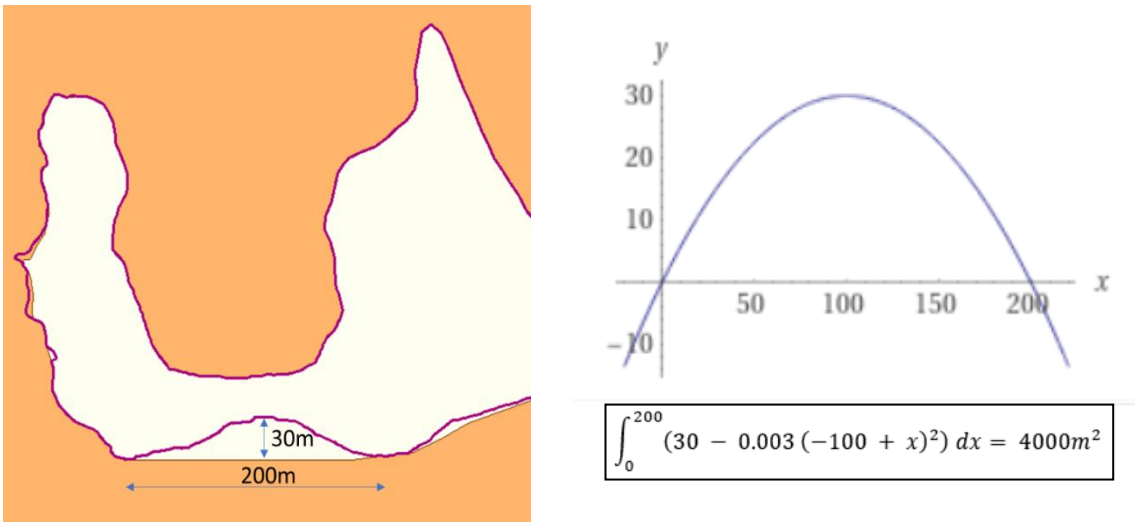

Figure 52, Compared to a straight coastline, the hollow area covers width of 200m with coastal retreat of 30m (left) which can be schematized by the parabolic function (right)

Ecological: The initial sand nourishment can cause for sedimentation and nutrient enrichment on the coral ridges which can smother and kill reef organisms and therefor lead to a decrease in ecological value. On the other hand, over time the fully grown sea grass will contribute to the environmental value of the area because this vegetation creates a vital habitat for endangered species of sea turtles, reef fish and conch (STINAPA Bonaire, 2014).

Cost: The cost for sand nourishment depends on the distance towards the nearest sediment reservoir and can increase up to 10€ per cubic metre (Schasfoort & Janssen, 2013).

Alternative C. Mangrove restoration

The impact of the loss of mangrove fringes was already investigated earlier in this thesis project and were prove was given for the correlation between mangrove loss and the erosion. From the research conducted Erdmann & Scheffers (2006) there occurred mangrove mortality between the years 1961-1996 which can be confirmed by analyzing the aerial pictures from these years and compare them with the current situation of the mangrove fringe. In this alternative, the possibility and effectiveness of the restoration of this mangrove fringe towards its original state (1961) is investigated.

Figure 53, Historical areal picture of Lac Cai showing the original state of the mangrove fringe

To create the right conditions for reconstructing mangroves, permeable structures will be used to create sheltered zones. The construction of some permeable braided walls parallel to the coast will reduce flow velocities and wave impact and due to the permeability will cause for accretion of suspended sediments (Wilms, Van Wesenbeeck & Tonneijck, 2020).

Environmental impact: the restoration of the mangrove will increase the ecological value and add to the biodiversity of the area by providing in critical nesting and feeding areas for birds, fish and crustaceans. Furthermore, these mangroves act as a water filter and cause for a decrease in the amount of pollutants effecting surrounding coral reefs.

Figure 54, Permeable structure to create favourable conditions for mangrove rehabilitation

Cost: The total direct cost of a 530 hectares mangrove rehabilitation project in Indonesia amounted to 690,000 USD for design, implementation, management and monitoring. (Wetlands International, 2016). Based on the large scale of this project it can be assumed that the investment cost are economized and therefor the rehabilitation on smaller scale will most likely be more costly per hectare.

Alternative D. Breakwater

The fourth alternative design which will be investigated is the construction of a breakwater at the North side of the beach and parallel to the coast. This alternative is based on the measure completed in June 2019, where a rock formation was dumped in front of the coast. Breakwaters act as a wave barrier, allowing the beach to grow while preventing erosion. As waves hit the breakwater, they deposit their load of sediment along it. However, any part of the coast not protected by the breakwater continues to experience erosion.

Figure 55, An overview of the current situation at Lac Cai were a pile of rocks is deposited perpendicular to the coast in the form of a breakwater (Google Earth)

Unfortunately, this measurement did not have desired result so far and therefor the effectiveness will be investigated by means of the long-term modelling. The result of the model could show opportunities for improvement of the current construction, such as expending in length or width.

Environmental impact: Hard structures are designed from the perspective focusing on the performance rather than adding to the ecological value. The impact of this breakwater construction is not considered to be harmful for the existing environment but neither contributes in a positive manner.

Cost: The breakwater is built by a local contractor with the use of local materials from the island. This resulted in a sustainable and cost-effective measure.

Figure 56, Current situation at Lac Cai were a pile of rocks is deposited perpendicular to the coast in the form of a breakwater

Alternative E. Groyne

Another hard solution which will be studied in this MCA is the construction of a groin at the southside of the beach perpendicular to the coast. Because the channel between the coral ridge and Lac Cai functions as a sediment trap, the eroded sediment is moving inside the bay. This groin will prevent the sand for flushing away and lead to accumulation of sand in front of the coast. Figure 58 shows an example of such a measure taken in Wakatiti, Hawai. Dimensions are approximately 50 meters long with a width of 10 meters.

Environmental impact: The construction of this groin will cause for a decrease in sedimentation inside the bay and therefor interfere with the current equilibrium profile. This could disturb the ecological balance. Furthermore, the construction site will reach seawards which will probably conflict with the surrounding coral reefs.

Cost: Based on the investment cost in the construction project of Wakatiti, this alternative is ought to be one of the most expensive measures. Some cost could be saved by relocating the rocks from the current breakwater and use these for the new construction.

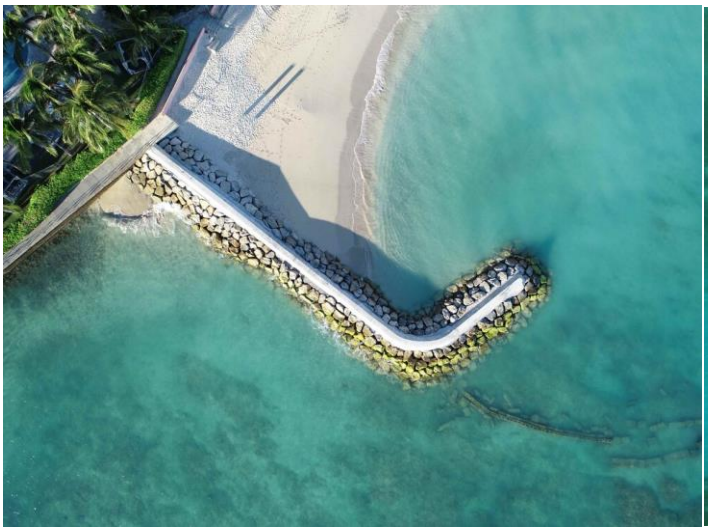

Figure 58, Example of the Royal Hawaiian in Wakatiti, Hawai (Waikīkī Beach Special Improvement District Association, 2020)

Figure 57, Schematic overview of a groin at the south side of the beach at Lac Cai (Google Earth)

Appendix E, Assessment form

Main criteria	Weight (pnt)	Specific sub-criteria / indicators	Scores of Alternative				
			A	B	C	D	E
1. Impact on hazard reduction	…	Meters coastline retreat reduction	X	X	X	X	X
2. Cost	…	Investment-, maintenance- and life cycle cost	…	…	…	…	…
3. Environmental impact	…	Positive or negative impact on existing nature	…	…	…	…	…
4. Local acceptance	…	landscape, tourism and fishing activities	…	…	…	…	…
5. Local feasibility	…		…	…	…	…	…

Appendix F, Assessed tables

Main criteria	Weight (pnt)	Specific sub-criteria / indicators	Scores of Alternative				
			A	B	C	D	E
1. Impact on hazard reduction	5	Meters coastline retreat reduction	X	X	X	X	X
2. Cost	5	Investment-, maintenance- and life cycle cost	++	-	-	--	--
3. Environmental impact	2	Positive or negative impact on existing nature	0	++	++	--	--
4. Local acceptance	3	landscape, tourism and fishing activities	--	--	+	0	0
5. Local feasibility	3		++	0	+	+	0

Alternative	1. Reduction impact in m	2. Cost in €	3: Environ. impact	4: Local Acceptability	5. Local Feasibility	**Scoring**
	5 pnt	5 pnt	2 pnt	3 pnt	3 pnt	
A. No measure	-	5	3	1	5	49
B. Sea grass + nourishment	-	2	5	1	3	32
C. Mangrove restoration	-	2	5	4	4	44
D. Breakwater	-	1	1	3	4	28
E. Groin	-	1	1	3	3	25

Position : Sr. coastal Engineer

Years of Experience : 18

Main criteria	Weight (pnt)	Specific sub-criteria / indicators	Scores of Alternative				
			A	B	C	D	E
1. Impact on hazard reduction	5	Meters coastline retreat reduction	X	X	X	X	X
2. Cost	4	Investment-, maintenance- and life cycle cost	++	--	-	--	--
3. Environmental impact	1	Positive or negative impact on existing nature	0	+	++	--	--
4. Local acceptance	2	landscape, tourism and fishing activities	-	0	++	+	+
5. Local feasibility	5		+	+	++	-	-

Alternative	1. Reduction impact in m	2. Cost in €	3: Environ. impact	4: Local Acceptability	5. Local Feasibility	**Scoring**
	5 pnt	4 pnt	1 pnt	2 pnt	5 pnt	
A. No measure	-	5	3	2	4	47
B. Sea grass + nourishment	-	1	4	3	4	34
C. Mangrove restoration	-	2	5	5	5	48
D. Breakwater	-	1	1	4	2	23
E. Groin	-	1	1	4	2	23

Position : Sr. coastal Engineer

Years of Experience : 25

Main criteria	Weight (pnt)	Specific sub-criteria / indicators	Scores of Alternative				
			A	B	C	D	E
1. Impact on hazard reduction	5	Meters coastline retreat reduction	X	X	X	X	X
2. Cost	3	Investment-, maintenance- and life cycle cost	+	--	-	--	--
3. Environmental impact	5	Positive or negative impact on existing nature	0	+	++	--	--
4. Local acceptance	5	landscape, tourism and fishing activities	-	+	++	-	-
5. Local feasibility	4		-	--	+	-	-

Alternative	1. Reduction impact in m	2. Cost in €	3: Environ. impact	4: Local Acceptability	5. Local Feasibility	**Scoring**
	5 pnt	3 pnt	5 pnt	5 pnt	4 pnt	
A. No measure	-	4	3	2	2	45
B. Sea grass + nourishment	-	1	4	4	1	47
C. Mangrove restoration	-	2	5	5	4	72
D. Breakwater	-	1	1	2	2	26
E. Groin	-	1	1	2	2	26

Position : Coastal Ecologist

Years of experience : 8

Worked in Bonaire

Main criteria	Weight (pnt)	Specific sub-criteria / indicators	Scores of Alternative				
			A	B	C	D	E
1. Impact on hazard reduction	5	Meters coastline retreat reduction	X	X	X	X	X
2. Cost	5	Investment-, maintenance- and life cycle cost	+	--	--	-	--
3. Environmental impact	3	Positive or negative impact on existing nature	0	+	++	-	-
4. Local acceptance	5	landscape, tourism and fishing activities	--	+	+	+	+
5. Local feasibility	3		0	--	--	+	+

Alternative	1. Reduction impact in m	2. Cost in €	3: Environ. impact	4: Local Acceptability	5. Local Feasibility	**Scoring**
	5 pnt	5 pnt	3 pnt	5 pnt	3 pnt	
A. No measure	-	4	3	1	3	43
B. Sea grass + nourishment	-	1	4	4	1	40
C. Mangrove restoration	-	1	5	4	1	43
D. Breakwater	-	2	2	4	4	48
E. Groin	-	1	2	4	4	43

Position : Coastal zone manager

Years of Experience : 25

Main criteria	Weight (pnt)	Specific sub-criteria / indicators	Scores of Alternative				
			A	B	C	D	E
1. Impact on hazard reduction	5	Meters coastline retreat reduction	X	X	X	X	X
2. Cost	4	Investment-, maintenance- and life cycle cost	++	-	-	--	--
3. Environmental impact	2	Positive or negative impact on existing nature	0	++	++	-	-
4. Local acceptance	2	landscape, tourism and fishing activities	0	+	++	+	+
5. Local feasibility	3						

Alternative	1. Reduction impact in m	2. Cost in €	3: Environ. impact	4: Local Acceptability	5. Local Feasibility	**Scoring**
	5 pnt	4 pnt	2 pnt	2 pnt	3 pnt	
A. No measure	-	5	3	3		32
B. Sea grass + nourishment	-	2	5	4		26
C. Mangrove restoration	-	2	5	5		28
D. Breakwater	-	1	2	4		16
E. Groin	-	1	2	4		16

Position : Coastal engineer

Years of Experience : 5

Main criteria	Weight (pnt)	Specific sub-criteria / indicators	Scores of Alternative				
			A	B	C	D	E
1. Impact on hazard reduction	5	Meters coastline retreat reduction	X	X	X	X	X
2. Cost	2	Investment-, maintenance- and life cycle cost	++	-	--	--	--
3. Environmental impact	5	Positive or negative impact on existing nature	0	++	+	--	--
4. Local acceptance	3	landscape, tourism and fishing activities	--	+	++	0	0
5. Local feasibility	3		0	-	++	++	0

Alternative	1. Reduction impact in m	2. Cost in €	3: Environ. impact	4: Local Acceptability	5. Local Feasibility	**Scoring**
	5 pnt	2 pnt	5 pnt	3 pnt	3 pnt	
A. No measure	-	5	3	1	3	37
B. Sea grass + nourishment	-	2	5	4	2	47
C. Mangrove restoration	-	1	4	5	5	52
D. Breakwater	-	1	1	3	5	31
E. Groin	-	1	1	3	3	25

Position : Marine Ecologist

Years of Experience : 25

Worked on Bonaire